An Intrabody Signal Propagation Study for Human Body Hydration

Clement Ogugua Asogwa

M.Eng (Information and Communication), B.Eng (Electrical)

College of Engineering and Science

Victoria University

SUBMITTED IN FULFILMENT OF THE

REQUIREMENTS

FOR THE DEGREE OF

DOCTOR OF PHILOSOPHY

August, 2016

DOCTOR OF PHILOSOPHY DECLARATION

"I, Clement Ogugua Asogwa, declare that the PhD thesis entitled 'An Intrabody Signal Propagation Study for Human Body Hydration' is no more than 100,000 words in length including quotes and exclusive of tables, figures, appendices and references. This thesis contains no material that has been submitted previously, in whole or in part, for the award of any other academic degree or diploma. Except where otherwise indicated, this thesis is my own work".

Clement Ogugua Asogwa

Date: 31st August, 2016

Abstract

Human body composition refers to the relative proportions of fat, bone, water, muscle and minerals in the body. Adequate proportions of these are a primary requirement for healthy living. Measurement of body composition is important for medical diagnosis and for understanding the physiological proportions of body tissues for physical fitness and exercise performance. Studies in human body hydration, as an example, provides the information necessary to understand the desired fluid levels for optimal performance of the body's physiological and metabolic processes during exercise and activities of daily living. It can help identify, or quantify issues of ill-health or wellbeing, e.g. lymphoedema and risk of heart attack. This thesis proposes a new system for assessing human body hydration which measures changes in body fluid level in real time. Hydration rates are modelled using a time constant τ which characterises individual specific metabolic function and anthropometric parameter θ which represents the muscle-fat ratio similar to Body Mass Index (BMI) of an individual. In this research, the amount of change in the volume of body fluid was predicted using the attenuation of a galvanically coupled signal passing through the body. Data from theoretical simulation showed that the rate of hydration for individuals with high θ and low τ could be as high as 1.73 dB/minute, which decreases to 0.05 dB/minute for persons with low θ and high τ. Similar to theoretical results, the empirical data measured on a variety of subjects showed the rate of hydration varying from 0.6 dB/minute for subject with BMI 22.7 kg/m^2 down to 0.04 dB/minute for 41.2 kg/m^2 BMI. The circuit model is sensitive enough to detect 1.30 dB reduction in attenuation when as little as 100 mL of water is consumed. Current techniques such as isotope dilution are complex, expensive, time consuming and more suitable for laboratory purposes. Popular methods like bioimpedance analysis use statistical estimates of tissue impedance to calculate the amount of fluid in different compartments of the body. This assumption makes the result less accurate and less sensitive. The proposed model predicts that individuals with high BMI would have higher time-dependent biological characteristic, lower metabolic rate, and lower rate of hydration. The system is suitable for integration into a wearable device to measure hydration rates in

real time with further application value in diagnosing and monitoring treatment of body fluid disorder which was demonstrated on lymphoedema affected limbs of human subjects. The results show that the amount of change in attenuation suffered by a signal propagating through a lymphoedema affected limb was half the amount measured on an unaffected limb and the flow rate measured varied from 0.15 dB/minute – 0.37 dB/minute on the affected limbs while the rate on a healthy part varied from 0.44 dB/minute to 1.83 dB/minute. Finally, it was shown that a galvanically coupled intrabody signal propagating at 900 kHz can predict changes in the volume of the body fluid which is useful for early diagnosis and monitoring of oedema and related fluid disorders.

Acknowledgements

I express the highest appreciation to God Almighty for the grace and mercy bestowed on my family and I, that has allowed me to realise my dream of undertaking and completing my doctoral research training degree. I wish to express my gratefulness for the inspirations, encouragement, support and mentoring from my family members, supervisors, friends and colleagues. To all who have supported me in my academic journey, I would like to say a thousand times over, thank you.

To my supervisor, Dr. Daniel Lai, who through patient, hard work, sound academic training, inspiration, encouragement, and guidance, mentored me. Words fail me to express my sincere appreciation. I am very grateful to Daniel. Many thanks also to Professor Stephen Collins for his coaching, administrative support, constant reviewing and prompt responses to my requests. Many thanks to Dr. Patrick McLaughlin for helping with the ethics application and clinical experiments, to Lymphoedema Association of Victoria (LAV) for participation and Lina Comologaran for providing her clinic for the tests.

My special appreciation also to all TEPS research students and friends, old and new, the likes of Seyedi, Behailu, Assefa, Kim, Rui, Joannis, Shabbir and Zibo. I am also greatly thankful to all the staff of the Graduate Research Centre for their timely assistance and the scholarship support throughout my PhD studies and to the College of Engineering and Science. I would also like to thank Suddinna for her supportive role during my experiments and to all the participants who freely volunteered their time for my experiments and my other friends like Rev. Bayo Adeniran, Rev. Sam Ajayi, Mrs. O.Aghachi, Dr. Akerejola, Isaac, Lekan, Uche and Frank, whose prayers and good will put faith and hope that is now a reality.

Looking back and forward, I would count two great hands God has used, beside my supervisors; my wife, Ebere, and children, Afoma and Faithful, who despite my unavailability, stood courageously firm and provided, above all, the moral security and peaceful home that helped me stay focused throughout the research. To my well beloved mother, and in loving memory of my late father and siblings, and all others not mentioned here, I say, may God bless you all, Amen.

List of Publications

Peer-Reviewed Journal Papers

- Asogwa, C.O., Teshome, A.K., Collins, S.F. and Lai, D.T.H., 2016. "A Circuit Model of Real Time Human Body Hydration". IEEE Transactions on Biomedical Engineering, 63(6), pp.1239-1247.

- Asogwa, C.O., Collins, S.F., Mclaughlin, P. and Lai, D.T.H., 2016. "A Galvanic Coupling Method for Assessing Hydration Rates". Electronics, 5(3), p.1-16.

- Asogwa, C.O., Johanis A. B, Patrick M., Collins, S. and Lai, D.T.H., "A Galvanic Intrabody Method for Assessing Fluid Flow in Unilateral Lymphoedema" (Submitted to MDIP Electronics)

- Asogwa, C.O., Vlad Libeson, and Lai, D.T.H., "A New Wearable Surface Electrode For Intrabody Communications Based on Conductive Textile" (Submitted to IEEE Sensor journal)

Peer-Reviewed Conference Papers

- Asogwa, C.O., Seyedi, M. and Lai, D.T.H, "A preliminary investigation of human body composition using galvanically coupled signals". In Proceedings of the 9th International Conference on Body Area Networks (pp. 346-351). ICST (Institute for Computer Sciences, Social-Informatics and Telecommunications Engineering), London, September, 2014.

- Asogwa, C.O., Lai, D.T.H and Collins, S., "An empirical measurement of body hydration using galvanic coupled signal characteristics". In Proceedings of the 9th International Conference on Body Area Networks (pp. 342-345). ICST (Institute for Computer Sciences, Social-Informatics and Telecommunications Engineering), London, September, 2014..

- Asogwa, C.O., Lai, D.T. and Collins, S.,"Effect of Changing Body Fluid Levels on Intrabody Signal Propagation". 12th International Conference on Intelligent Environments, London, 12-14th September 2016. Ebook, Ambient Intelligent and Smart Environments, vol.21, p.552-559

Contents

List of Figures

List of Tables

Abbreviations

AAMI	**A**ssociation for the **A**dvancement of **M**edical **I**nstrumentation
ADH	**A**ntidiuretic **H**ormone
ANSI	**A**merica **N**ational **S**tandard **I**nstitute
BCC	**B**ody **C**hannel **C**ommunication
BIA	**B**ioelectrical **I**mpedance **A**nalysis
BIS	**B**ioelectrical **I**mpedance **S**pectroscopy
BMI	**B**ody **M**ass **I**dex
CLM	**C**ircumferential **L**imb **M**easurement
CT	**C**omputed **T**omography
DUT	**D**evice **U**nder **T**est
ECG	**E**lectrocardiography
ECW	**E**xtracellular **W**ater
EMG	**E**lectromygrophy
EMS	**E**mergency **M**edical **S**upply
FFM	**F**at **F**ree **M**ass
FM	**F**at **M**ass
GDP	**G**ross **D**omestic **P**roduct
GIBC	**G**alvanic **I**ntrabody **C**ommunication
HBC	**H**uman **B**ody **C**ommunication

HRE	**H**uman **R**esearch **E**thics
IBC	**I**ntrabody **C**ommunication
ICNIRP	**I**nternational **C**ommission **N**onionizing **R**adiation **P**rotection
ICW	**I**ntracellular **W**ater
IEEE	**I**nstitute of **E**lectrical and **E**lectronic **E**ngineering
ISO	**I**nternational **O**rganisation for **S**tandardization
LAV	**L**ymphoedema **A**ssociation of **V**ictoria
MRI	**M**agnetic **R**esonance **I**maging
MF-BIA	**M**ulti-**F**requency **B**ioimpedance **A**nalysis
MLLB	**M**ulti-layer inelastic **L**ymphoedema **B**andaging
NFPA	**N**ational **F**ire **P**rotective **A**ssociation
PAN	**P**ersonal **A**rea **N**etwork
REE	**R**esting **E**nergy **E**xpenditure
RMR	**R**esting **M**etabolic **R**ate
SEG-BIA	**S**egmental **B**ioimpedance **A**nalysis
SPG	**S**pecific **G**ravity
SR	**S**weat **R**ate
TBW	**T**otal **B**ody **W**ater
UCA	**U**rine **C**olour **A**nalysis
UWW	**U**nder **W**ater **W**eighing
VNA	**V**ector **N**etwork **A**nalyser
WBAN	**W**ireless **B**ody **A**rea **N**etwork
WHO	**W**orld **H**ealth **O**garnization

Physical Constants

Permittivity of free space $\varepsilon_0 = 8.8541 \times 10^{-12}$ F/m

Symbols

ϵ_r	relative permittivity	
ϵ_0	permittivity of vacuum	F/m
σ^*	complex conductivity	S/m
σ_i	static ionic conductivity	S/m
z^*	complex specific impedance	Ω
α_n	distribution parameter	
ζ	relaxation time constant	
τ	time characteristic of an individual	minute
θ	muscle-fat ratio	
A_m	cross-sectional area of muscle	mm^2
A_f	cross-sectional area of fat	mm^2
s	skin	
f	fat	
m	muscle	
bc	cortical bone	
bm	bone marrow	
F_T	thickness of fluid layer	mm
F_n	thickness of fluid in the nth layer of the arm	mm
f_{BW}	bandwidth in frequency	Hz

D_b	density of the whole body	kg/m^3
D_{fat}	density of fat mass	kg/m^3
D_{ffm}	density of fat free mass	kg/m^3
R_l	load resistance	Ω
t	time	minute
t_f	time to reach water balance	minute
t_n	thickness of nth layer of the arm	mm
r	radius of arm	mm
V_i	transmit voltage	$volt$
V_0	output voltage	$volt$
V_{ib}	initial body fluid volume	mm^3
V_w	amount of fluid consumed	mm^3
V_b	volume of fluid after hydration	mm^3
W_{fat}	weight of fat mass	kg
W_{ffm}	weight of fat free mass	kg
wt	body weight	kg
wt_g	gain in weight due to fluid intake	kg
Z_A	longitudinal impedance corresponding	Ω
Z_b	diagonal impedance	Ω
Z_{ES}	contact impedance	Ω
Z_i	input impedance	Ω
$Z_F(t)$	variable impedance	Ω
Z_{f0}	impedance before hydration begins	Ω
Z_L	longitudinal impedance	Ω
Z_0	output impedance	Ω

Z_T transverse impedance Ω

Z_w impedance after fluid intake Ω

To the glory of God, in service to humanity

Chapter 1

Introduction

In the world today, one unresolved challenge to governments is how to balance the priorities between available resources to meet an increasing demand for health services and the associated costs. The 'Obamacare' quagmire in the USA is a typical case at hand. Presently, the increase in demand for health services is primarily due to global increase in population caused by increased life expectancy in some countries and natural birth, prevalence of prolonged diseases, economic growth, healthcare infrastructure improvements, and advancements in technology [1]. In fact it is estimated that global health spending will continue to rise to the tune of $9.3 trillion USD in 2018 [1]. In Australia, for example, health expenditure grows faster than the broader economy; over the recent past decade (2004-2014), nominal GDP growth rate was 6.28 % while the ratio of health expenditure to GDP is 9.12 % [2]. The huge market forecast and expenditure in health means a challenge to cut costs while improving

the quality of care without compromising regulations. One strategy to improve health care at a reduced cost is the technology for real-time healthcare monitoring system. According to MeMD the potential cost savings of using biometric devices to monitor patients with serious conditions is 88 % [3]. Similarly, a projection by Juniper Research publication 2014 reports that remote patient monitoring could save global health care systems up to USD 36 billion by 2018 [4]. Nowadays, both short-term diagnostic recording such as clinical electrocardiogram or long-term chronic recording, example cardiac monitoring, logging of physiological data, recording vital signs have been made seamless with wireless monitoring electronic devices and sensors attached on them. The sensors send continuous data through wireless connection to a remote server or medical repository or to a physician, thereby eliminating the cost of continuous hospital visits while enabling constant monitoring. In some cases, a large number of sensors are connected together to monitor the brain, organs and muscle movements simultaneously which are transmitted to a remote station or to user's device. For example monitoring Parkinson's disease requires simultaneous monitor of muscle and brain activities of the patient [5]. Similarly, monitoring the history of change in patients with gait disorder, Alzheimer disease and other chronic diseases require simultaneous monitoring of brain coordination and muscular activities of the patient [6, 7]. This applies to other diseases that affects two or more organs in the body or diseases with multiples of symptoms that affects different tissues. Monitoring in

this sense requires a baseline knowledge of a healthy human body composition such as the total amount of water in a healthy adult or the threshold for identifying health risks. For instance monitoring hydration levels is critical to health because severe dehydration can cause heart failure [8] and a loss of 10% of total body water puts one at a considerable risk of death [9]. Thus sport scientists and exercise physiologists monitor body weight changes, hydration levels and other vital signs of athletes to maintain physical fitness and improve performance especially at an elite level. Therefore it is essential to understand the appropriate proportions of body composition such as bone mass, water, muscle, tissue and body fat necessary for the body to function properly.

1.1 Body Composition Estimation

Body composition by definition refers to the relative proportions of fat, bone, water, muscle and minerals, otherwise classified as fat and fat-free mass (FFM), in the body. A good body composition means appropriate proportion of body fat and fat-free mass in normal range for healthy living. Measurement of body composition is gaining popularity because it is fundamental to the knowledge and understanding of the physiological mechanisms of the body and for both medical and physical fitness. Today, it is known that human body composition can be affected genetically or influenced by external factors that induce human body physiological adaptation changes

such as climatic conditions, exercise, disease, or even diet [10]. This means that investigations into human body composition is vital for both medical reasons and individual care. It can help identify, or quantify issues of ill-health or wellness. Body composition measurements are now a routine practice in indoor, gyms, clinics, hospitals and research laboratories [11] as a way of evaluating body fitness and health. Fluid accumulation- oedema, in the limb, ankle, and trunk which causes obvious swelling of the affected part are either a direct result of a disorder or potential sign and symptom of a disease such as heart failure [12, 13], diabetes [14, 15], and lymphoedema [16] and more, while frequent loss of fluid due to diarrhoea, vomiting, high fever and so on which causes dehydration are also a lead to other associated health risks such as malaria [17, 18].

A 2006 report by Boscoe *et al* indicates that the prevalence estimate of hyponatremia (a fluid disorder characterized by a relative excess of body water to body sodium content) is between 3.2 to 6.1 million annually in the USA and costs between \$1.6 billion and \$3.6 billion USD [19]. This is largely due to the amount of time spent in hospital for treatment and monitoring [19]. The huge cost can be lowered by reduction in inpatient setting by using sensors that monitor changes in body fluid levels and transmitting the monitored signals wirelessly to an intended device, a physician or qualified clinician for immediate follow up (Fig.1.1). Some of the most commonly used methods for body composition measurement are bioelectrical impedance analysis, dilution techniques, air displacement plethysmography, dual energy

X-ray absorptiometry [20], and magnetic resonance imaging, MRI. Recent technologies include three-dimensional photonic scanning and quantitative magnetic resonance. All of these allow for measurement of different body composition elements or tissues such as fat, fat-free mass, bone mineral content, total body water, extracellular water, total adipose tissue, skeletal muscle, select organs, and ectopic fat deposits [21].
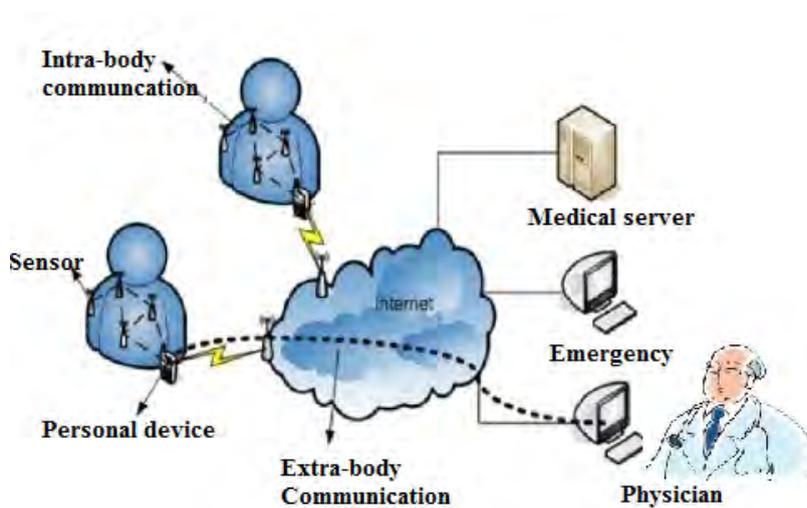
FIGURE 1.1: Intrabody communication network system [22].

Through experiments, Pace and Rathbun [23] first discovered that the total body water (TBW) on guinea pig is a constant fraction of fat-free mass (FFM). This led to several other investigations on adult human cadavers that showed that the ratio of TBW to FFM in humans is 0.737 ± 0.036 [24]. Thus, the body fat is calculated as

$$Fat = \text{ body mass - FFM}$$

$$= \text{body mass - TBW}/0.73$$

Some of the methods for calculating TBW includes deuterium, hydrogen or tritium isotope dilution which quantifies total body water by assuming a uniform dilution and distribution of tracer element over the entire body [25]. These methods involve either ingestion or injection of a given amount of the tracers and noting an equilibrium period and the sampling times [26]. This has a risk of possible overdose and correction has to be made for urinary losses of the tracers. Moreover, the experiment lasts for as much as between 3-4 hours [27] to assess an individual's water level. Bioelectrical impedance methods (BIA) on the other hand, assumes that 73% of a human body FFM is water [28]. It uses a two-compartment body model to analyse the resistance or impedance of the body due to small electrical current flow as a relation to changes in total body water (a review of current techniques of body composition is detailed more in chapter 2).

The main hypothesis of this thesis is, "can signal attenuation of a galvanic coupled intrabody signal be used to indicate body fluid levels?" This question arises because the average quantity of water consumed by a healthy person in a temperate region is between 2600–2700 mL per day [29]. This amount suggests a dynamically changing fluid level which changes the impedance of of the body. To investigate this, this thesis shall use the principles associated with the movement of electric current in wires to develop a technique that can detect changes in body fluid volume by the changing signal attenuation. This will be performed using a very small and harmless

amount of current ($<$ 1 mA) passed through the limb.

1.2 Objectives

The main objective of this thesis is to develop a new model for accessing human body hydration in a manner that will respond to real time changes in daily fluctuations of human body water levels. Presently, there exists in Institute of Electrical and Electronic Engineering (IEEE) 802.15.6 [30] a standard for intrabody communication (IBC) with an existing circuit model for communication through a human body. The objective of this thesis is to use some of the principles in IBC to design a circuit model for assessing changes in human body fluid level by observing the attenuation of a propagating signal passing through the body. Research on wireless communication including wireless body area networks (WBAN) or personal area networks (PAN) study signal attenuation in relation to air channel characteristics [31]. In IBC circuit models, the human body is modelled as a static channel (non-time varying) so that signal attenuation is constant. This thesis, seeks to incorporate dynamic changes by designing a new human body circuit model with dynamically changing impedance characteristic in response to changes in body fluid level and then use the variable changes in signal attenuation to study human body composition focusing more on the changes in body fluid levels. The variation in the signal attenuation(negative gain) is mainly due to changes in the physiological composition of the

contributing tissues. Human body tissue and fluid state dynamically changes in accordance with variations in physiological parameters such as body mass index and daily fluctuations of fluid level due to dehydration. For this reason, this research will investigate and characterise human body fluid level using a propagating galvanic coupled signal. It would be realisable because water constitutes 60-70 % of the entire body composition of an adult. Moreover, the interaction of an electrical signal passing through the human body is strongly affected by the volume of tissue fluid and its dielectric properties, afterwards validate the circuit model through comparison with empirical measurements to characterise hydration levels on volunteer subjects. This will be followed by further testing on individuals with body fluid disorder such as lymphoedema. Therefore, by coupling a low frequency electrical signal galvanically on the body, the signal passing through the tissue will vary in attenuation to the changes in the water level which will help us achieve the following as the core objective of this thesis:

a. Investigate human body composition using galvanically coupled signal propagation;

b. Investigate physiological processes that deal with fluid changes;

c. Develop a time dependent model to explain human body hydration;

d. Test the application of a galvanic coupled signal to assess human body hydration;

e. Investigate a pathological application for diagnosing issues of body fluid disorder, example patients with lymphoedema disease.

1.3   Organization of Thesis

This thesis is divided into 7 chapters. A brief summary of the chapters is presented below.

- Chapter 2 reviews current techniques for evaluating human body hydration and issues associated with their use. This thesis will also discuss the electrical properties of human body tissue as a merit for proposing a new system for assessing hydration rates.

- Chapter 3 outlines the research methodology and the materials used for the experiment. It also includes ethical requirements for the conduct of the research in regards to human safety regulations, privacy acts, safety equipment testing, protocol design and field measurements.

- Chapter 4 is the design of a real time circuit model and empirical measurements to provide a comparison with the simulation result. This chapter also highlights the effects of changing fluid levels on a propagating intrabody signal passing through the body and shows a first order process proposed for modelling hydration in a human body.

- Chapter 5 discusses the assessment of human body hydration rates using a galvanic coupled intrabody signal propagating through the body. Two main features are presented here. Firstly, determining a baseline signal attenuation over a period of 30 minutes and establishing the sensitivity of a galvanic intrabody technique in relation to the smallest amount of water consumed that will cause a detectable change in signal amplitude and a comparison with current methods of hydration assessment.

- Chapter 6 is describes for pathological application on body fluid disorder on patients diagnosed with lymphoedema as a case study.

- Chapter 7. The thesis concludes with a highlight on the potential applications and challenges of galvanic coupling signal transmission as a system for investigating human body composition and finally propose future research areas in this field.

Chapter 2

Literature Survey

Body composition evaluation refers to the estimation of the percentage proportions of human body fat and fat-free mass which are related to a persons overall state of health. Since human body parts have multifaceted geometry with complex internal geometry, direct measurement of the relative proportions of the various body components as a single entity is difficult. However, by applying fractional density theory which states that the density of a mixture containing more than one substance at different proportions and densities can be calculated as a sum of the densities of each of the constituent components, the overall density can be estimated. Thus, by subdividing the human body, for example, into subcomponents will theoretically provide a better estimate and easier-to-manage assessment of the entire body as an integral of its subcomponents. Similarly, since the goal, as stated in chapter 1, is to develop a simple method for assessing human body composition using changing signal attenuation

with some of the principles of signal attenuation in a galvanic intrabody communication (GIBC) which is broad, this research will mainly focus on changing body fluid levels as a vital component of a human body. Consequently, the review shall concentrate on the various theories and methods for assessing human body fluid level in biological sciences as well as the human body models developed in engineering for galvanic intrabody communication and signal propagation through human tissue. The information gathered from these disciplines shall be used to both formulate and verify if a galvanic signal attenuation can indicate changing body fluid levels in the proceeding chapters of this thesis. The rest of this chapter is organised as follows: section 2.1 the importance of body fluid to human body system functionality. Section 2.2 the history of human body composition assessment and its significance to medical sciences and a review of some of the methods for assessing human body hydration. Finally, section 2.3 will review relevant literature relating to human body circuit models for GIBC and the electrical properties of the human body as a signal transmission channel. At the end, summarise the chapter by highlighting relevant research gaps as an impetus for a new proposed method for assessing hydration using the effects of changing signal attenuation in relation to changing body fluid levels.

2.1 Importance of Body Fluid

Water is an important and major constituent of body cells, tissues and organs and contributes about 60 % of total body weight (TBW) of an adult [32], accounting for 73.2 % of fat free mass of the body [23]. It has strong electrical polarity which makes water a good solvent of other polar molecules. This property allows water to serve as a building block for macromolecules such as proteins and as a solvent for body minerals, vitamins, amino acids, glucose and more. It helps in digestion, absorption, transportation, and excretion of toxic substances and regulation of body temperature. Ions in the body are hydrated by the dipole nature of water making the cells to be surrounded by aqueous electrolytes which gives rise to electrolytic conductivity of the tissue [33]. The body loses water through faecal excretion, sweat production, evaporation, respiration and urination. This is compensated for through metabolic water production by oxidation of substrates that contain oxygen or nutrients that produce energy, dietary intake and absorption through the skin. Water appears in plasma and blood cells as soon as 5 minutes after intake [34] indicates how important it is to the body. Consequences of excessive fluid losses or inadequate fluid intake includes hypohydration, urinary infections, reduction in cognitive function, reduction of cellular metabolism and death if the body losses more than 10% of the total body water [9]. A recent report by Rothlingshofer *et al.* [35] showed that loss of body fluid decreases the electrical conductivity of

the body (up to 6% increase in muscle impedance). Similarly, over-consumption of water causes intoxication and hyponatreamia [9], a condition where the amount of sodium in the blood is abnormally low or a disorder in body electrolyte. Water balance in the body is achieved when the amount of water losses are compensated by the amount of intake from food and beverages as well as metabolic water production. Metabolic water production accounts for 250 to 350 mL per day of body water in a sedentary person [36] and increases with increase in physical activity. Metabolism increases with increase in human activity which also increases the average daily demand for water. Thus the relationship between metabolism and hydration. It is suggested that resting metabolic rate accounts for 65-70 % of a total 24-hour energy expenditure of human beings. The Mifflin-St. Jeor equation [37], written below, for resting metabolic rate (RMR) also known as resting energy expenditure (REE) is widely used for estimating daily energy expenditure is related to body metabolism [36].

$$REE = \ 10.52 \text{ x weight - } 12.18 \text{ x height - } 4.32 \text{ x age -} 1660$$

Dividing the REE by the square of a persons height will arrive at a relation which suggests that daily hydration is related to an individual's metabolic activity and his body mass index. This assumption shall be included and investigated the new circuit model in chapter 4.

2.2 Human Body Hydration Models

The assessment and classification of human body hydration state is important particularly due to the physiological processes of water in association with healthy living. The body needs water for metabolism, temperature regulation, circulation of food substances, blood flow and maintenance of electrolyte balance [38]. There are three classifications of water level in the body, *euhydration*, which is the state of normal water balance in the body, *hyperhydration* which occurs when there is excess amount of water in the body and *hypohydration* which is associated with excess water deficit in the body [39, 40]. Total body water is the sum of the extra cellular and intracellular waters (Fig. 2.1). In general, water in the body is grouped as existing in two compartments namely: intracellular fluid compartment, found within cells; and extracellular fluid compartment found outside cells, which also includes interstitial fluid and plasma water. Fig.2.1 shows the proportion of body fluid in the compartmentalised fluid spaces. Total body water (TBW) is the amount of fluid found in the intracellular and the extracellular tissue spaces, which is reported to contribute about 63.3% (0.6 L/kg) of body mass of an adult [41]. Fluid exchanges between the two compartments are regulated by both osmotic and hydrostatic pressure in the body.

Among the earliest theories for estimating the total amount of water in a human body began with the development of the classic two-compartment (2-C) model of the human body which was built on
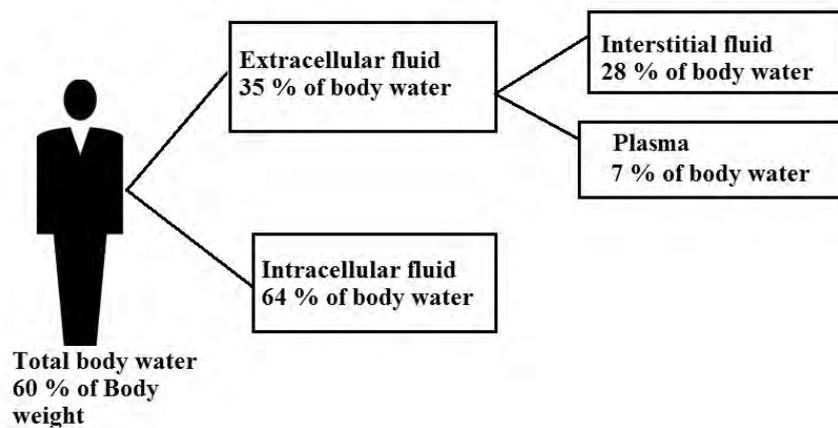
FIGURE 2.1: Distribution of total body water in a 70 kg adult from Max, L. *et al* [36] and Watson, P.E *et al* [42]

the idea of the body being made up of a fat and fat-free component [23]. This theory was used to develop a method called under water weighing (UWW) or hydrodensitometry [43]. In UWW, the subject is completely submerged in water and the volume of water displaced is combined with subject's weight to calculate the density of the whole body (D_b). The total body weight is the summation of the weight due to fat mass (W_{fat}) and weight of fat free mass (W_{ffm}). Thus,

$$\frac{1}{D_b} = \frac{W_{fat}}{D_{fat}} + \frac{W_{ffm}}{D_{ffm}} \tag{2.1}$$

where D_{fat} and D_{ffm} are the densities of the fat and the fat-free component. This assumes that the density of fat is relatively constant, an assumption that is oversimplified because the FFM is heterogeneous and varies with an individual's activity [44]. Consequently, further developments of 3-C and 4-C models emerged and most recently Wang *et al* [45] developed a comprehensive assembly of the various models, starting from the 2-C model to the whole body in

what is known as the 5-C model. Fig.2.2 is the diagram of the multi compartment model proposed by Wang and his colleagues.
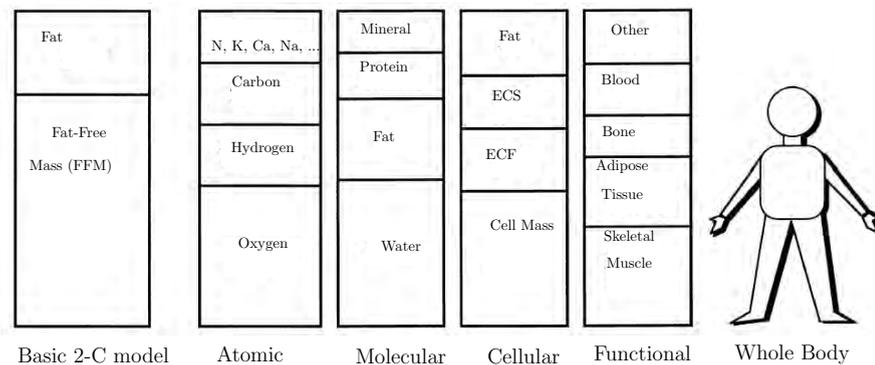
FIGURE 2.2: 5-Compartment Model of human body composition [45, 46]

This research shall examine more recent methods for estimating human body hydration from simple methods to more complex techniques. This includes assessment by urine colour observation, changes in body mass, measurement of urine specific gravity, analysis of blood sample, Bioelectrical Impedance Analysis (BIA), Bioelectrical Impedance Spectroscopy, and isotope dilution.

2.2.1 Urine Colour Observation

The mechanism used by the kidney for urine concentration is aimed at regulating water and sodium excretion in the body [47]. When the amount of water consumed is large enough to reduce the concentration of blood plasma, a urine more dilute than blood plasma is produced; on the other hand, when water intake is insufficient to dilute blood plasma concentration, a more concentrated urine than the blood plasma is produced [47]. Thus, urine concentration, physically evidenced by its colour, has been used to investigate hydration

status. Research evidence shows that urine colour has been used for determining hydration state, much like urine specific gravity, and serum osmolality [48]. In an experiment by Armstrong *et al* [48], the authors demonstrated that urine colour indices can be used to evaluate mild dehydration level; however urine color changes can be affected by illness, medications, and the use of food supplements [49] or body physiological abnormalities, interaction of food substances in the body and bacterial growth on a urine specimen [50]. The research showed that urine colour had a linear relationship with urine specific gravity method but not so with plasma osmolality, plasma sodium, or hematocrit methods [51] which has a slow response to mild loss of body fluid until a certain amount is reached [48, 52]. Thus this can be classified as the simplest method but very difficult to match exact urine colour to a certain magnitude of hydration level. Moreover, the colour changes can be affected by other pre-experimental conditions of subjects such as intake of supplements and multivitamin, which was observed on a subject in this research. Recent improvement involves the use of urine test strip or dipstick to determine pathological changes in patient's urine such as presence of proteins, glucose, blood particles, specific gravity and acid level usually to determine infection [53].

2.2.2 Urine Specific Gravity

The specific gravity of human urine increases due to increase in the concentration of chemical substances in the urine [51]. The urine

concentration is determined by the amount of urinary waste per unit volume of urine. It is measured using a refractometer. A refractometer assess hydration status based on the urine specific gravity it measured. Urine specific gravity measures the ratio of the density of urine relative to the density of pure water. A specific gravity greater than 1 means the fluid is denser than water [41]. The concentration of blood cells and plasma changes as soon as 5 minutes after water intake [34].

Urine specific gravity can increase as a result of:

a. Loss of body fluid (dehydration)

b. Diarrhoea that causes dehydration

c. Heart failure

d. Sugar (glucose) in the urine

e. Medications and the use of food supplements [49]

f. Physiological abnormalities, example a disorder that causes flow of urine with concentrated substrates [50].

The decrease in urine specific gravity can be due to:

i. Excessive fluid intake

ii. Damage to kidney tubule or kidney failure

iii. Kidneys' regulatory malfunction example, *diabetes insipidus.*

2.2.3   Body Mass Changes

The human body mass contains 60-70 % water with dynamic systems of gaining water. Short term changes in body weight can be attributed to loss or gain of body water because 1 mL of water has a mass of 1 $gram$ [54]. As a result, changes in body weight are usually used as indicator of loss or gain in body water. This method is simple but more reliable than urine colour observation. Although there is also no standard scale for quantifying a hydration or dehydration level in this technique, the changes in weight are referenced to a known baseline measurement. For instance, a 2 % loss in body mass, which is regarded as severe dehydration [40], is calculated from a predetermined weight before dehydration occurred. In sports science, this technique is often extended to measure the sweat rate by measuring post exercise body mass and subtracting it from a predetermined average body mass, usually remeasured before the start of an exercise which estimates the changes in body weight due to loss of body water. The sweat rate calculated this way is based on the assumption that changes in body mass during exercise is a result of water loss mostly through sweating. The sweat rate (SR) is thus calculated by the formula

$$\frac{\text{weight before drink - weight after drink + volume consumed - urine volume}}{\text{exercise time}} =$$

In this thesis, the initial body mass measured after fluid restriction

will be recorded as W_0, the body mass resulting from fluid intake as W_1 while the body mass after urinating as W_2. Other fluid losses through evaporation, respiration or urination leading to dehydration increases tissue impedance [35] which is represented as a time dependent variable in the circuit model developed in chapter 4.

2.2.4 Blood Sample Analysis

This method involves the collection of blood sample for analysis of the concentration of haemoglobin (protein contained in red blood cells) in one part and hematocrit, which involves the assessment of the volume of red blood cells in relation to the total blood volume (red blood cells and plasma). The concentration of blood changes with increase or decrease of water in the body. Because both the hemoglobin and hematocrit are based on the blood sample, this method is dependent on the plasma volume. Plasma or Serum Osmolality is the most popular method used in the blood sample technique of hydration assessment, but the results are affected by changes in posture, exercise, and sodium chloride balance in the body. Some researchers have suggested the analysis of blood osmolality as the most valid index of hydration assessment [55] but not for TBW estimation. Although it may be suitable for assessing a person's hydration level, it has been demonstrated that plasma osmolality does not respond quickly to loss of body fluid after exercise or during daily activities. For example, an investigation by Francesconi *et al.* [52] showed that participants who lost up to 3% of body mass through sweating did

not show any difference in haematocrit or serm osmolality immediately after. Further research evidence concluded that the volume of blood plasma does not necessarily change until a certain amount of water had been lost [48] in order to maintain cardiovascular stability [40].

2.2.5   Bioelectrical Impedance Analysis

The bioelectrical impedance analysis (BIA) method for accessing human body composition is based on a postulated relationship between the volume of a conductor, (human body) and the length of the conductor (height), the impedance of the conductor and the material it is made of. It assumes that the entire human body is a perfect cylindrical conductor and the impedance is related to the nature of the conductor, its length, the cross-sectional area and the signal frequency. By assuming the body as a homogeneous cylindrical conductor with length proportional to the height (H) of an individual, and negligible reactance component (Xc) then the equivalent body impedance is represented by the resistance (R). With these approximations, the volume of the cylindrical conductor would be proportional to H^2/R, usually measured at 50 kHz. The bioelectrical impedance analysis technique was based on a 2-C model of a human body comprising of fat and fat free mass. Thus with the estimate of TBW by BIA technique, the total body fat and fat-free mass is calculated on the assumption that 73.2% of human body fat-free mass is water [23]. The BIA method is popular because it is non-invasive, cheap and

easy to use. Measurements are performed using 4 electrodes, two at the wrist and two at the ankle. The single-frequency BIA, which usually operates at 50 kHz, is unable to distinguish the distribution of total body water into its two main components-extracellular and intracellular water because a 50 kHz current would not penetrate completely into cells due to the high resistance of the outer layer of the skin and the capacitive properties of cell membranes. The effects of capacitive behaviour of tissue membranes means that ICW can only be measured at higher frequency while ECW can be measured at low frequency. Human tissue has both resistive and reactive components and cell membrane capacitance contributes significantly to the effective impedance of electrical signals across tissues [33]. Schwan classified biological tissues into frequency-dependent electrical properties and placed them into three frequency regions (α, β and γ) [56]. Single-frequency bioelectrical impedance (SF-BIA) are affected by changes in the body fluid state. This is because SF-BIA gives an estimate of FFM and TBW but does not include ICW, and thus its value is most suitable for normally hydrated people. For example, Asselin *et al.* [57] reported that a severe dehydration of 3 % of body mass resulted in a water loss that was not properly accounted for by the prediction equations in bioimpedance analysis as compared to the observed changes in individual body mass. These constraints led to the development of an improved BIA technique that uses a multi-compartment model of the human body with multi-frequency for analysis. It uses low or intermediate frequencies

for estimating the extracellular fluid volume (ECW) and higher frequencies for estimating intracellular fluid volume (ICW), the sum of which gives an improved estimate of the overall body water, FFM, ICW and ECW.

2.2.6 Bioelectrical Impedance Spectroscopy (BIS)

BIS was proposed to distinguish between the ECW and ICW fluid volumes which accounts for the presence of non-conducting elements by dividing the human body into extracellular resistance R_e, intracellular resistance R_i and capacitance of cell membrane C_m; as shown in the equivalent circuit, Fig.2.3, in combination with Hanai's mixture conductivity theory [58]. In Figs.2.1 and 2.2 the various fluid spaces and the compartmentalised human body consisting of extracellular space being made up of plasma and interstitial fluid and intracellular fluid space (ICF) containing ionic elements which depend on the type of cell are illustrated.

Because of the capacitive behaviour of the cell membranes, the extracellular water resistance R_e is measured at low frequencies while the combined ICW and ECW are measured at higher frequencies. There is no exact range specified in the literature, which could be due to the overlap in the frequency-dependent dispersive regions of biological tissues discussed in section 2.2.1 and illustrated in Fig 2.7. However, Nyboer has suggested that at frequencies below 1 kHz, current mostly passes through the extracellular fluids while, between 500-
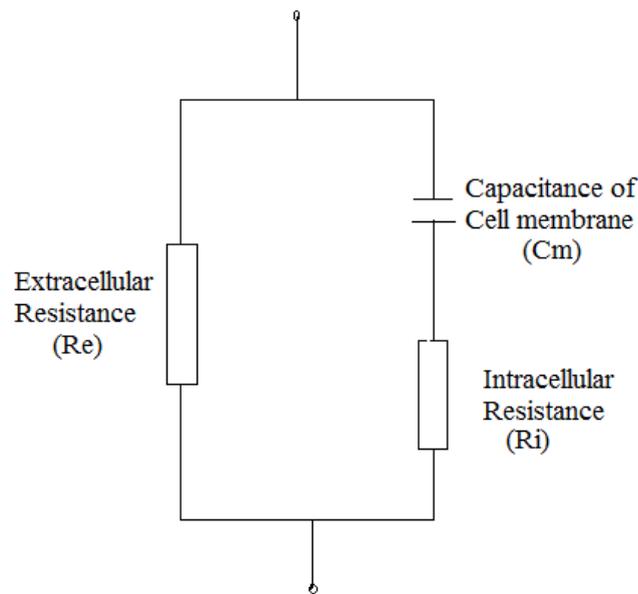
FIGURE 2.3: Equivalent circuit of tissues with parallel resistances

800 kHz, it penetrates both the extracellular and intracellular fluids [59, 60]. Consequently, BIS allows resistance and reactance measurements over a wide range of frequencies. Measurements of total body water with the BIS technique has been validated by Van Loan *et al.* (1993) [61] and Wabel *et al.* in 2009 [62] and has strong correlation with isotope dilution methods. The impedance locus, Fig.2.4 is used to illustrate the effects of variation of impedance with frequency. Resistances are extrapolated at zero and infinite frequencies representing measurements of extracellular and intracellular fluids. A typical instrument based on this model is Xitron, San Diego, CA. The frequency at which the maximum value of the reactance occurs is called the characteristic frequency (Fc) which is assumed to occur at 50 kHz in a single frequency BIA method. In recent times, other applications involves phase angle measurements which are used to

provide information about cell functionality to establish some clinical parameters such as the body immune deficiency, existence or likelihood of cancer disease and hemodialysis [63, 64].
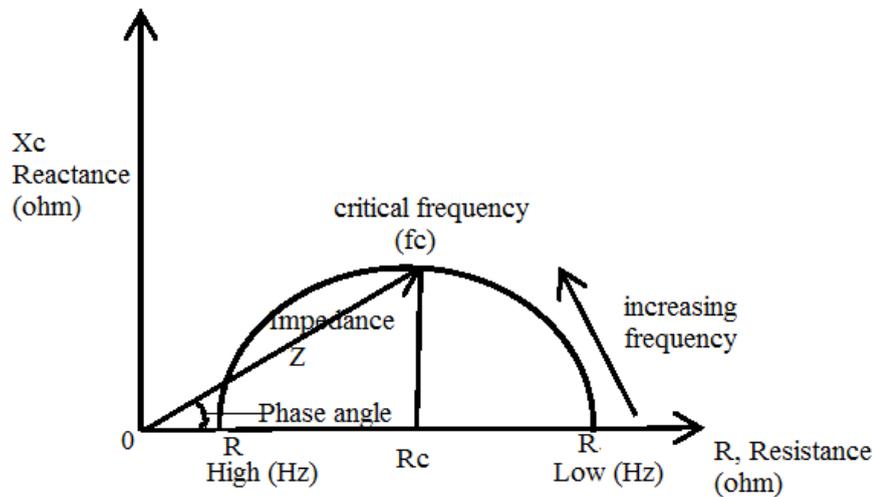
FIGURE 2.4: Reactance versus resistance as a function of frequency adapted from Jaffrin *et al* [65]

2.2.7 Segmental Bioelectrical Impedance Method (SEG-BIA)

Segmental bioelectrical impedance is based on the principles of the total body bioelectrical impedance method to measure the specific resistance of an arm, leg or trunk. SEG-BIA is mostly used for the evaluation of diseases that affect body fluids. In a BIA measurement, surface electrodes are usually placed on the hand and foot (Fig.2.5); however, some instruments allow foot-foot or hand-hand placement of electrodes in which the subject is allowed to stand erect. There are also instances where BIA measurements use four electrodes with two electrodes placed on the dorsal region of the hand, and two on the dorsal region of the foot on the same side of the body, Fig.2.5.
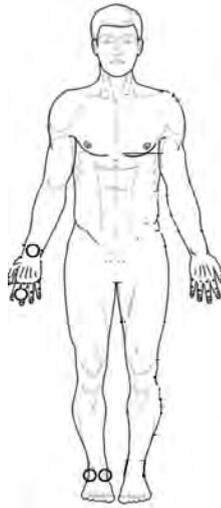
FIGURE 2.5: BIA measurement-electrode placement

In SEG-BIA, additional electrodes are attached to the wrist and to the foot on the opposite side, thereby creating a segmented measurement of body impedance as desired, Fig.2.6.
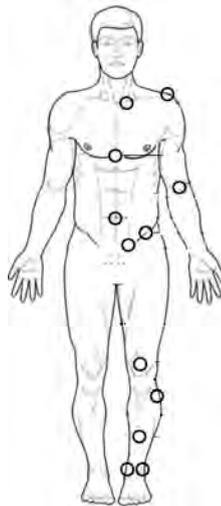
FIGURE 2.6: Segmented Bioipedance measurement

2.2.8 Isotope Dilution Technique

Isotope dilution technique is the most complex and expensive method for assessing human body hydration. It involves the use of stable

non-radioactive isotopes such as deuterium, tritium, oxygen-18, and radioactive potassium as a tracer to track the body's distribution of water. The calculation is based on the assumption that if the quantity of the tracer substance is known, and the starting and equilibrium concentrations are measured, then the volume of the space into which the tracer was diluted can be calculated. Although this laboratory method is considered more accurate than others, and are usually used as the 'gold standard', it assumes that the tracer substance circulates uniformly throughout the area under investigation so that

$$\frac{\text{Amount of tracer used}}{\text{Concentration}} = Volume$$

The important considerations for this technique includes:

a. A tracer must be nontoxic to the body;

b. Tissue specific. This means that it must be able to circulate rapidly and uniformly only in the targeted tissue spaces. For example radioactive potassium, $^4 0K$ is usually used to determine intracellular tissue volume;

c. A tracer must not undergo changes due to body metabolism, otherwise the volume estimate would be inaccurate;

d. Tracer element must not be excreted before it is uniformly distributed (although a technique has been developed to correct for excretion);

e. The amount of tracer used and its concentration must be easy to measure;

f. Lastly, the presence of a tracer element must not in anyway affect body fluid distribution in any part of the body.

If any of the requirements (b) to (e) are violated the ratio of the amount of tracer used to the concentration would be incorrect unless otherwise accounted for in the design. Conditions (a) and (f) may not affect accuracy of the result but may affect individual health. Isotope dilution result is considered the reference or baseline value for comparison with other techniques, however it takes several hours for the tracer to equilibrate, especially when the body is unsettled due to routine exercise or daily activities. Also it requires the collection of blood, urine or saliva samples which increases further the time it takes to assess an individual's fluid level and the process can not be repeated quickly. Moreover, the technique requires expertise skills, and complex equipment like positron emission tomography tracer (PET- Tracer) which is very expensive, therefore it is not suitable for field measurements. Besides, the result is not totally accurate [46], and its ability to distribute uniformly in all tissue spaces is still debated. Amstrong *et al* [27] argued that there is not yet a tracer technique to directly assess and measure accurately the intracellular and interstitial fluid volume which is also noted in unpublished on line body fluid physiology posts.

Table 2.1 summarises the different methods for assessing the amount of fluid in the a human body.

TABLE 2.1: Summary of body fluid assessment techniques

Method	Strength	Weakness	Comment
Urine Colour Analysis (UCA)	Very simple No speciality skill is required	Subjective Limited accuracy	1.No standard colour code 2. Affected by dietary intakes, drugs and supplements[49]
Urine Specific Gravity	More reliable than UCA 3. Inexpensive	Result can be altered by medication	1. Limited accuracy
Densitometry	Easy to perform	Measures TBW only	over simplified result
Body mass measurement	Self-administered Simple and inexpensive	Limited accuracy Measures TBW only	1. Accuracy depends on sensitivity of scale
SF- BIA	Good for TBW	1.Cannot differentiate ECF from ICF 2. It is based on a 2-C model of human body	2. Over simplified 1. No standardised calibration 2. Subject to uncertainties 3. Does not respond quickly to acute changes in body fluid levels [66] 4 .Measures only extra-cellular fluid [67]
MF-BIA	Measures ECW and ICW, Good for whole body fluid measurement in healthy normal-weight people	2. Does not respond to acute changes in fluid level from overhydration or dehydration	1.Different devices used for different body parts 2.Not suitable as a wearable device
BIS	Measures ECW, ICW, FFM, FM,TBW 2.Wider frequency range(5 - 1000 kHz) 5. Segmental BIS calculates body composition segment by segment 7. Bulky, not suitable as a wearable device	3. Needs further refinement particularly for populations with abnormal body geometry (e.g. very high BMI) Assumes a constant specific resistivity of the fluid compartment measured 6. Did not include the effects of temperature and metabolism [68] on the assumptions	1. Theoretically differentiates ECW from ICF 2. Quantifies body cell mass 3. Impedance data in the frequency spectrum is fit into Cole's model [65] 4. Uses statistical modelling equations based on Hanai mixture theory to calculate resistances at different frequencies
Analysis of Blood Sample	Higher accuracy than previous methods	1.Result is affected by postural changes and exercise 2. Complicated and risky	Measures the concentration of electrolyte substance in the blood and comparison with a reference

Table 2.1 – continued from previous page

Method	Strength	Weakness	Comment
		3. Does not evaluate the amount of water by tissue compartment [55] 4. Does not respond quickly to mild reduction of water [52]	
Isotope Dilution	High accuracy, 1. Tracks the distribution of water in the body Suitable for laboratory research	1. Complicated and expensive 2. Requires different isotopes for different tissue compartments 3. Large time consuming 4. Can be affected by metabolism 5.Insensitive to 1 kg loss in TBW [46]	Assumes uniform circulation of tracers and risks overdose

Fig.2.7 is summary of the different methods of body fluid assessment by accuracy and complexity

2.3 Modelling the Human Body as a Transmission Channel

In 2012, the IEEE 802.15.6 was standardised for data communication in and around the human body [30]. Under this, a wireless, non-RF based protocol called intrabody communication (IBC) emerged which uses living tissues as the communication channel. In order to implement this, a tissue model is required to investigate the characteristic behaviour of a propagating electrical signal either in a galvanic or capacitive coupling. The different methods which have been used for IBC study include: electrical circuit model [69, 70], finite element model [71, 72], finite element time domain models [73] and quasistatic dielectric principle [74]. But the first use of human
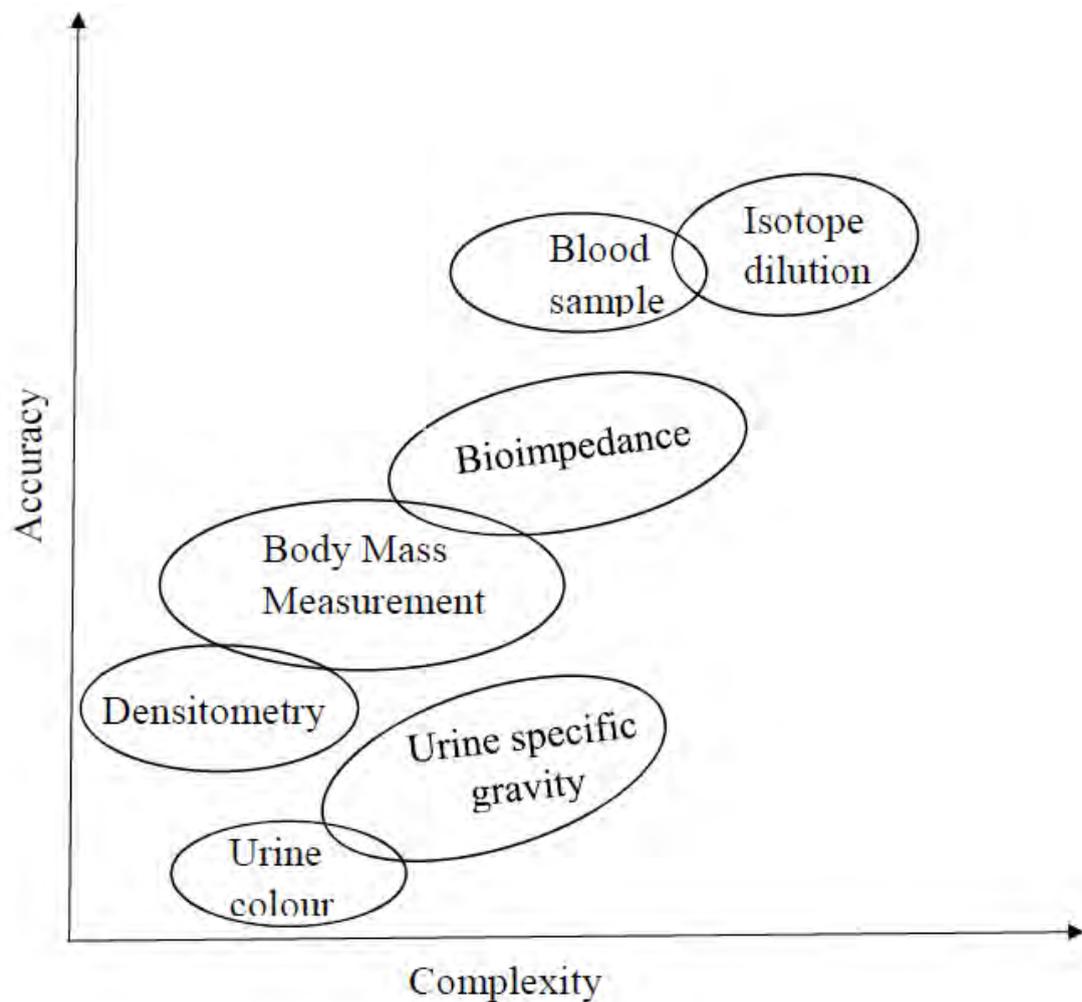
FIGURE 2.7: Comparison of body fluid assessment techniques by accuracy and complexity

body for data communication was proposed as a Personal Area Network (PAN) by Zimmerman [75]. This technique uses near field and electrostatic coupling of signals; consequently, low frequency communication without electromagnetic radiation can be achieved that has the advantage of low power consumption. This assures safety and could further provide significant insight into human body composition since the signal amplitude change is dependent on the changes in the medium through which the signal propagate, the materials and method through which it was connected.

2.3.1 Electrical Property of Human Tissues

Firstly, the flow of electrical current through a material, including biological tissue, is largely dependent on two main properties: relative permittivity (ϵ_r) (the ability to trap or store charges) and conductivity (σ) (ability to move charges). Schwan [56] measured the specific resistance of tissues to current flow and provided a discussion of the fundamental processes underlying the electrical property of biological tissues. He found that tissues display some properties of both insulators and conductors because they contain dipoles which can inhibit current flow as well as charges which can cause current flow. Tissue response to current flow is dependent on parameters such as the nature of cells and its distribution in the tissue, tissue anisotropic property, operating frequency of the input signal as well as time varying changes in body fluid level. Schwan's work [56] grouped biological tissues into frequency dependent electrical properties that could classify them into three frequency regions α, β and γ. Further research published by Gabriel *et al* [76] provided a comprehensive overview of human body electrical properties spanning a frequency range from 10 Hz to 20 GHz. This result is widely accepted, although it assumed homogenised tissue layers in the body. However, it was Schwan [56] who characterized biological tissues into three dispersive regions in a way still relevant to current studies as:

- The low frequency region called α dispersion is associated with ionic diffusion on the cellular membrane and occurs in the 1 Hz

to 100 kHz frequency range.

- β dispersion or mid-frequency region is associated with the polarization of the cellular structure of membranes between the intracellular and the extracellular tissue and lies between 100 kHz to 10 MHz.

- γ dispersion operates primarily at frequencies in the gigarhertz range which is associated with higher radiation and human body antenna effects.

2.3.2 Signal Propagation Through Human Tissue

Electrical signal propagation across tissues are influenced by frequency-dependent dielectric properties of tissues. Fig.2.7 shows the classification of human tissue by dielectric property by frequency dependent dispersive regions.
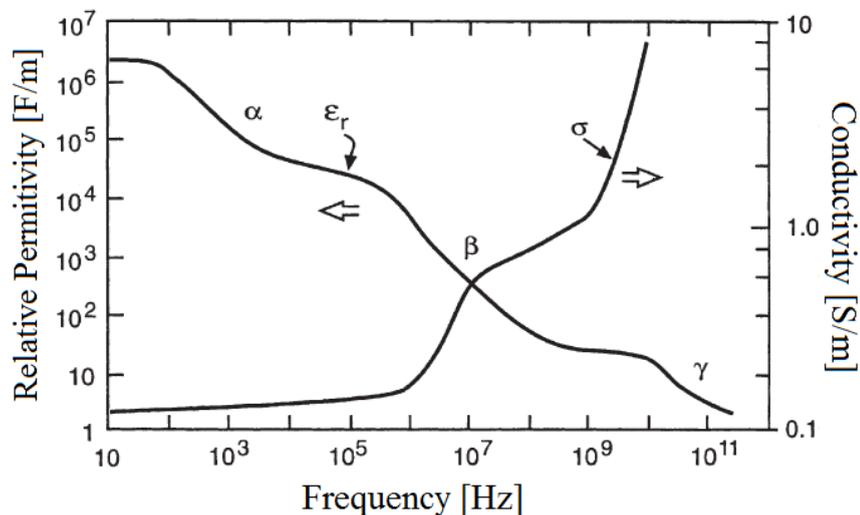
FIGURE 2.8: Classification of human tissue dielectric properties using frequency-dependent dispersive regions adopted from Miklavcic, D *et al*[77]

The conditions of human tissue vary over time, which in turn means variations in its dielectric properties. The Cole-Cole equation [78] is used to approximate the changes in the dielectric properties of various tissues over a wide range of frequencies.

$$\epsilon^*(\omega) = \epsilon_\infty + \frac{\Delta\epsilon_n}{1 + (j\omega\zeta_n)^{(1-\alpha_n)}} \qquad (2.2)$$

where $\epsilon^*(\omega)$ is the complex dielectric constant at angular frequency ω, and $\Delta\epsilon_n$ is the degree of the dispersion calculated from the difference between permittivity at an infinite frequency above the dispersion ϵ_∞ and permittivity below the dispersion ϵ_s; ζ is the relaxation time constant and α_n is the distribution parameter.

The summation of the frequency-dependent permittivity is expressed in equation 2.3. The nature of the material causes the different changes in dispersion in the three separate regions.

$$\epsilon^*(\omega) = \epsilon_\infty + \sum_n \frac{\Delta\epsilon_n}{1 + (j\omega\zeta_n)^{(1-\alpha_n)}} + \frac{\sigma_i}{j\omega\epsilon_0} \qquad (2.3)$$

The complex conductivity σ^* and the complex specific impedance z^* of the tissue are given by

$$\sigma^* = j\omega\epsilon_0\epsilon^* \qquad (2.4)$$

$$\sigma^* z^* = 1 \qquad (2.5)$$

σ_i is the static ionic conductivity.

Figs.2.8 - Fig.2.10 depict the dielectric relationship of human tissues with frequency. The high relative permittivity at lower frequencies implies that signal propagation across human tissues have higher attenuation at low frequencies. Since relative permittivity of tissue is higher at low frequencies (Fig.2.9), this research proposes observing signal attenuation on tissues at low frequencies to measure variabilities in human body hydration with respect to time. In addition high frequencies are affected by external factors such as the human body antenna effect and possible radiation. The frequency range for this study lies between 800 kHz to 1.5 MHz which lies within the β dispersion region, as shown in Fig.2.7, and which is related to the cellular structure of biological materials [33] reaching into the intracellular fluid spaces. At very high frequencies, dipolar reorientation of proteins and organelles can occur which is not favourable. Moreover, signal penetration decreases at frequencies far into the γ dispersive region (Fig.2.10).
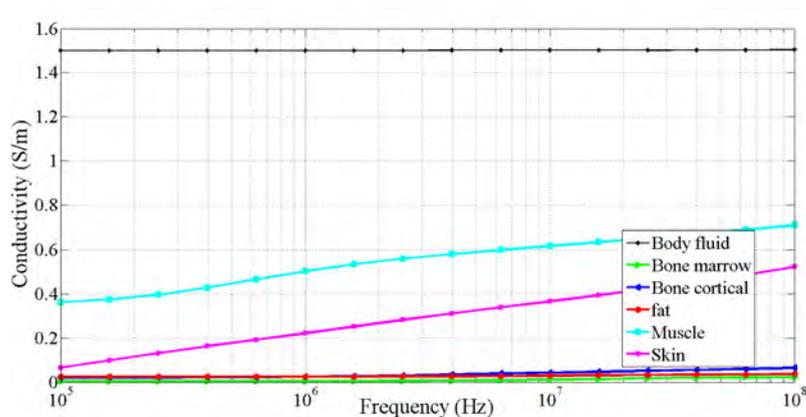
FIGURE 2.9: Conductivity (S/m) of tissues at different frequencies. Data source [79]

This research postulates that since the body fluid consists mainly of
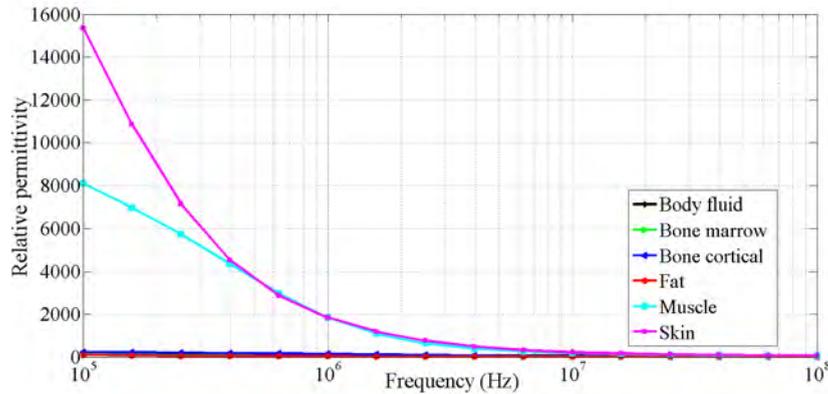
FIGURE 2.10: Relative permittivity of tissues at different frequencies. Data source [79]
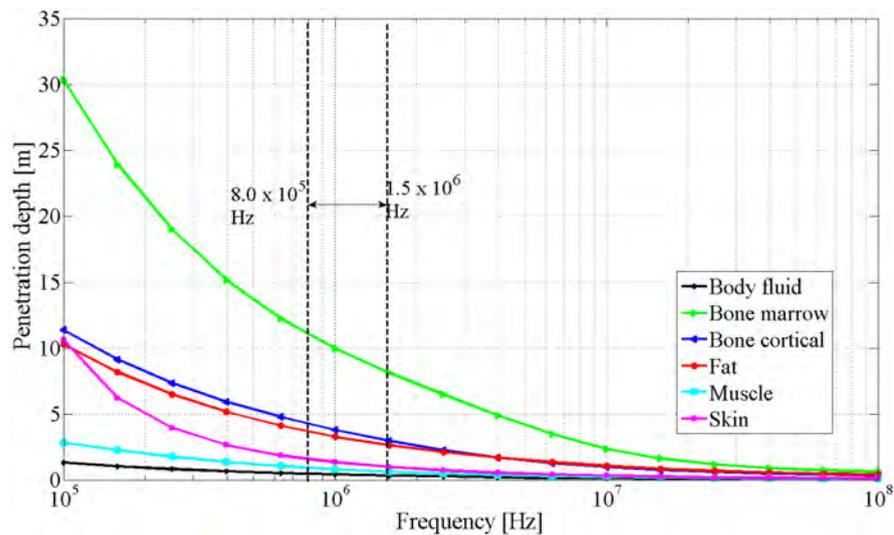
FIGURE 2.11: Penetration depth of some tissues at different frequencies. Data source [79]

aqueous solutions of ions and cations which influences signal propagation across tissues (see Fig.2.8). Water constitutes about 60% of total body mass of an adult [32] and human body needs an average of two litres of water per day to replace lost fluid [80]. These dynamic changes in body fluid levels, which also changes the impedance of the body, can be observed by observing the changes in signal attenuation propagating across tissues. In 2011, Lisa *et al* reported that dehydration can cause up to 6% increase in muscle impedance [35].

The increase in tissue impedance as the fluid losses increases can be observed in real time by observing the characteristic changes in the propagating signal amplitude across the affected tissues as the loss occurs. This study will do this using some of the principles used in intrabody signal transmission.

2.4   Human Body Circuit Model

The first use of a human body as an electric circuit model for signal transmission started with the pioneering work of Zimmerman [75] whose circuit consisted of four transverse and longitudinal impedances between the transmit and receive electrodes connected through the arm. This model was used in capacitive coupling in which the dominant signal transmission path is through the environment surrounding the body. In subsequent studies Wegmueller *et al* [72] proposed a similar four terminal electrode model with five body tissue impedances and included the effect of the inter-electrode impedances which was omitted in the original model of Zimmerman. The improvement enhanced its application in galvanic coupling instead of Zimmermna's capacitive model. In later years, Song *et al* [69] reconstructed the human geometry of Wegmueller circuit and approximated it to a homogeneous solid volume with an output impedance from the transmitter and input resistance from the receiver (Fig.2.11) in which Z_{ES} is the impedance of the contact interface to the body at the transmitter and the receiver nodes,
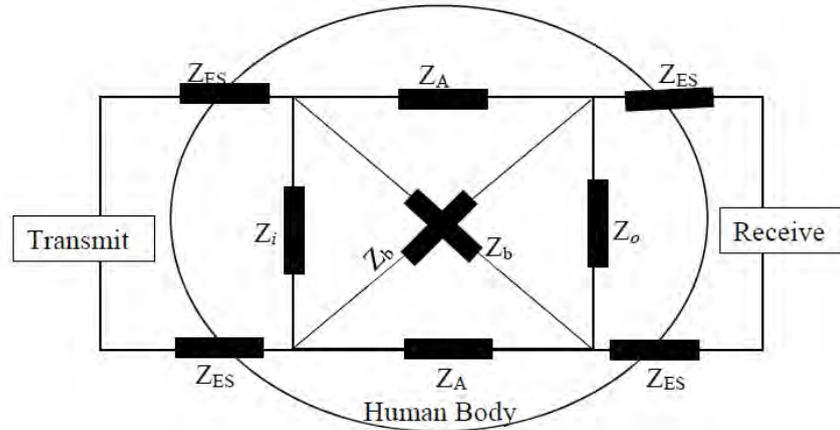
FIGURE 2.12: Simplified four terminal galvanically coupled IBC circuit showing approximations of the impedance components by Song *et al* [69]

Z_i and Z_0 are the input and output impedances. Z_A is the longitudinal impedance of the transmission path. This model was later improved by Behailu *et al* [70] in which the diagonal impedances were eliminated and Z_A consisted of the skin, fat, muscle, and bone. Each of these models follow a consistent assumption of a static impedance property of the conducting tissues which is one of the major issues in galvanic coupling that this thesis will address and to propose a model that is adaptable to day to day living.

Figs.2.13 and 2.14 are the pilot test on this frequency range which showed the effects of changing body fluid level on intrabody signal propagating between 900 kHz and 1.5 MHz with subjects S1–S6. Subjects were given water to drink and attenuation (negative gain) were measured 5 minutes after intake for 30 minutes. The result shows that maximum gain occurred between 900 kHz and 1.1 MHz within 20 minutes after intake. Therefore, the frequency range for this study will be between 800 kHz – 1.2 MHz.
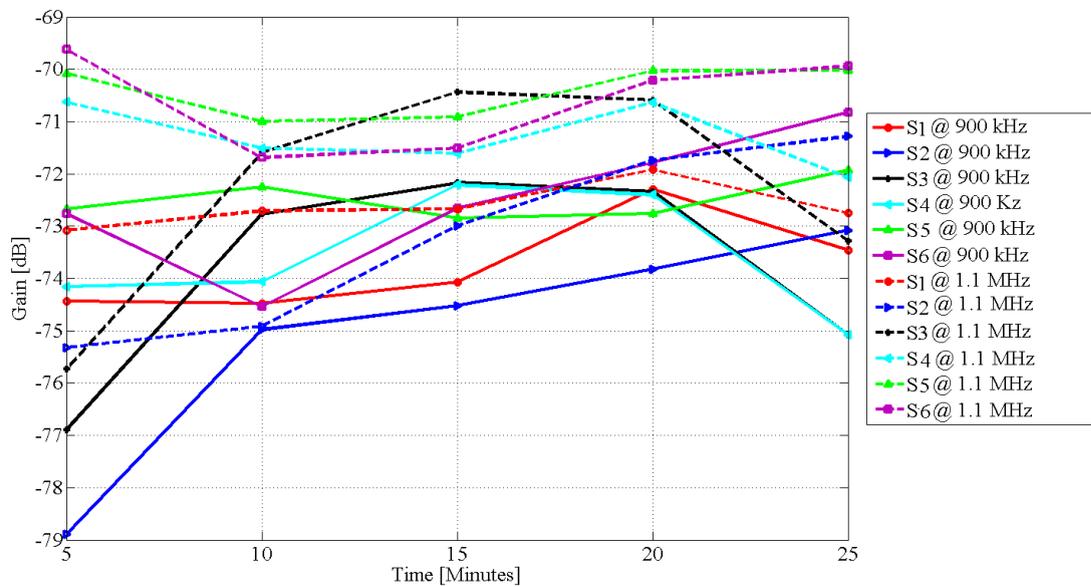
FIGURE 2.13: Effect of changing body fluid level on intrabody signal propagating at 900 kHz and 1.1 MHz on 6 subjects
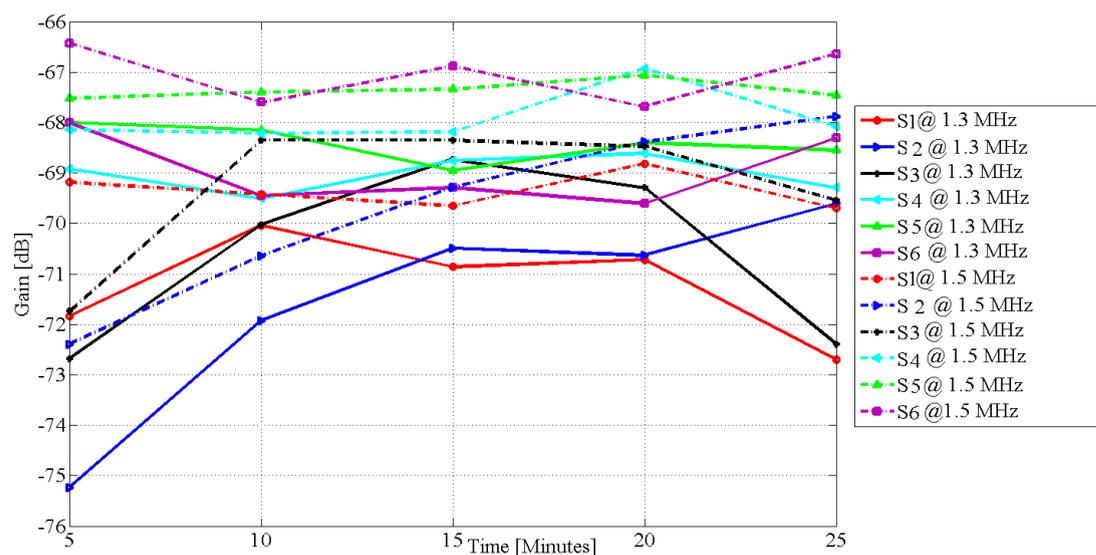
FIGURE 2.14: Effect of changing body fluid level on intrabody signal propagating at 1.3 MHz and 1.5 MHz on 6 subjects

2.5   Research Gap

This chapter has reviewed different methods used for estimating the amount of water in the body and various other techniques for assessing hydration levels. In general, the most popular method of body fluid assessment involves the use of electrical current passing through tissues, which, depending on the frequency can be used for assessing either the total body water or the amount of water in the extracellular fluid space of the tissues or those that exist in intracellular tissues partitioned from external fluid spaces by cell membranes known to behave like capacitors. With current passing through tissue spaces, the impedance can be measured which is used to estimate the amount of water present in those spaces. However, most BIA methods are not validated for patients with a hyper or hypo hydration fluid state [81]. BIA is easily altered by changes in hydration status. Therefore a real time measurement of hydration using the changing tissue impedance due to changes in hydration status would give better monitoring result. Consequently, this study reviewed as well the electrical properties of tissues and how a propagating electrical signal can yet be used to characterise the tissue behaviour in terms of the changing body impedance due to changes in hydration status. This work also considered the appropriate frequency considering that high frequencies are associated with human body antenna effects and radiation, and very low frequency will have issues relating to the capacitive behaviour of cell membranes. The choice for operating frequency was gained from high relative permittivity of

biological tissues at low or intermediate frequencies and the cellular structure of biological materials in the β dispersive region Fig.2.7. The region lying between 800 kHz and 1.5 MHz provided a suitable penetration depth (Fig.2.10) and maximum gain was measured between 900 kHz and 1.1 MHz which further strengthened the choice for the frequency band selected for this study. Using the recently defined IEEE 802.15.6 protocol standard for human body communication [30], a galvanic coupled intrabody signal can therefore be applied and the propagating signal used for characterising tissue properties by changing fluid levels in real time which has potential application in medicine and clinical monitoring of fluid disorders and personal fitness.

In order to incorporate the effects of changing fluid levels which occurs in a human body on daily basis, this research will begin with the development of a new circuit model which would have, instead of static tissue impedance, a variable impedance that changes with changing human body hydration levels in chapter 4, test it in chapter 5 and examine its biomedical application for possible diagnosis of early development of body fluid disorder such as oedema in chapter 6. The next page is chapter 3, which will examine the materials and methods required to successfully achieve this goal.

Chapter 3

Measurements, Materials and Methods

In order to establish the use of galvanic coupling for assessing body fluid changes, experimental measurements are required. These measurements shall confirm simulation results regarding time varying changes in electrical signal transmitted across the human tissue. This study, assumes that a predominant cause for changes in galvanic coupling signal attenuation passed through the tissue is dynamic changes in body fluid level. The measurement set-up shall therefore, incorporate materials and methods for evaluating time varying changes in body fluid levels. To verify these assumptions, this thesis will design and simulate a circuit model that describes the proposed idea and then follow it up with feasibility, sensitivity and control tests on human subjects which entails clearly defined ethical guidelines (in line with both local and international research regulations

including the Australian Code for the Responsible Conduct of Research [82] and the guidelines of the International Commission on NonIonizing Radiation Protection (ICNIRP) [83] for radiation exposure and use of electric current on the body). The evidence is the approval by the Victoria University Human Research Ethics Committee with approval identification number: HRE-14-122 (Appendix A.2), to conduct this research.
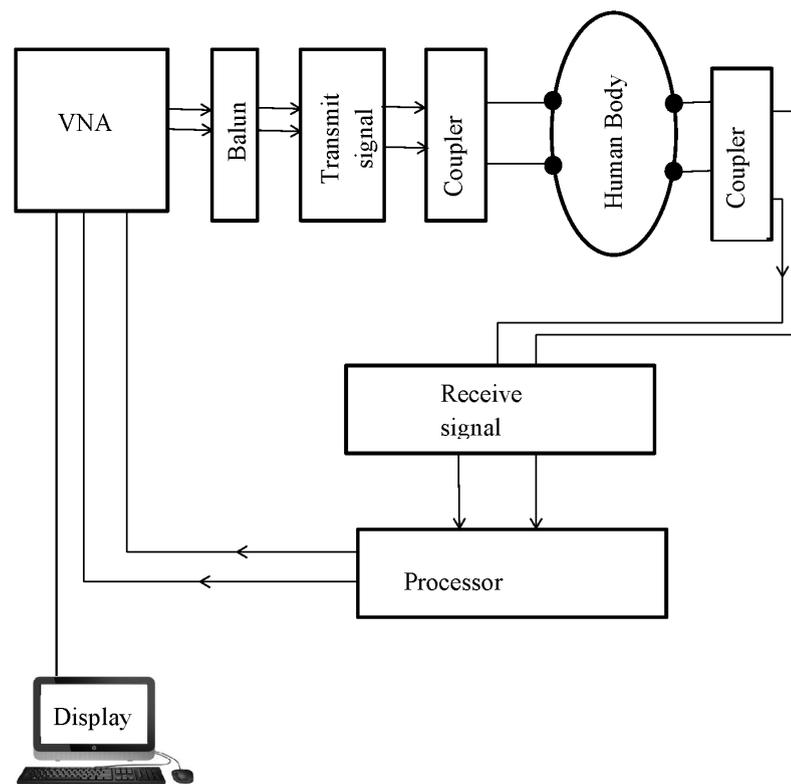
FIGURE 3.1: Block diagram of the devices used for measurement

The devices used in this experiment consisted of electronic and non-electronic gadgets. Fig.3.1 is a block diagram illustrating the use of the equipments in a typical set up. The configuration and design of the experimental procedures, including the specific use of each piece of equipment are explained in details in the succeeding sections. This

chapter is organized as follows; Section 3.1 discusses the safety and ethical requirements to perform the experiment. Section 3.2 will present the protocol designed to empirically measure human body hydration and dehydration rates. Section 3.3 explains the materials and the equipments use for this experiment.

3.1 Safety and Ethical Requirements

Strict ethical and safety requirements have to be fulfilled for these experiments because they require human subjects for experiment which involves transmission of electric current through the body ($< 1mA$), use of medical electrodes on subjects, temporary fluid abstinence and testing on subjects' urine and information about subjects' health status. To this end, several risk factors were identified:

- Risk of electric shock

- Risk associated with the use of medical electrodes, including perception, irritation and safety

- Health risk from fluid abstinence

- Health risk from urine

- Management and handling of private data or health information of participants

- Health and safety risk of participants, researchers and others.

To safeguard against these risks, the following considerations were designed and incorporated into the research in order to prevent as much as possible, or minimize chances of risk occurring and provide a management procedure in case of any unforeseen hazard.

- First, throughout the experiment the VNA was connected through a USB cable to a battery powered laptop with power save mode to avoid any risk of electric shock or power hazard from the external mains supply. The VNA was constantly set to operate at 0 dBm $< 1mA$ output power which is well within the safety guidelines (ICNIRP, 1998) [83].

- The pre-gelled self-adhesive Ag/AgCl electrodes used are biocompatible, single use and disposable as recommended in the ethical guidelines for electromyography measurements [84]. The experiments are conducted safely and with the risk management procedures medical devices on human body ANSI/AAM/ISO 109931 part 1 [85].

- Throughout the experiment, investigators will avoid direct skin contact with the participants by wearing single use medical examination gloves.

- The duration of the fluid abstinence is from 10 pm in the night to 10 am the following morning, which is considered safe and similar to, but less than, the duration usually recommended during periods of medical treatment and health diagnosis [86].

▸ All data collection and analysis in the experiment would follow the guidelines approved under section 95A of the Australian Privacy Act 1988 [87]. Subject data are de-identified and stored safely with the investigator team

3.2   Experimental Protocol

Two protocols are defined in this research, baseline measurements and measurements on healthy and unhealthy participants (participants that have been pathologically diagnosed with lymphoedema disease). Each of these protocols involves two models where there were intake and where there were no intake of fluid.

Protocol 1: Baseline measurements with and without fluid restriction.

In this protocol, participants are measured thrice. First, without fluid restriction, thereafter they are requested on another day, to abstain from fluid from after supper (10 pm) till 10.00 am, in which they will be required to provide a urine sample. They are similarly requested to refrain from any vigorous exercise; e.g. do not go to the gym. On the second, (after fluid restriction) the first measurement on both arms will be completed 30 minutes after the urine sample. The body hydration state will be ascertained by a urine specific gravity test with refractometer and will serve as control. All participants BMI are to fall within the range of 20 - 45. Measurements from

the healthy group of similar BMI will be compared against measurements with unhealthy groups of similar BMI to eliminate the effects of BMI on the measurements. Again, the duration of the fluid fast is considered safe and similar to, but less than, the duration usually recommended during periods of medical treatment and health diagnosis [86]. After this, participants are asked to drink water, measurements will be taken to detect changes in the signal as a result of the fluid intake. Participants were to remain seated during the measurement procedures to avoid measurement errors from motion artefacts. Participants were again measured after urination and the volume of urine and the elapsed time to urinate were recorded.

Protocol 2: Pathological and healthy participants.

Protocol 2.1: Pathological participants

These volunteers will have been pathologically diagnosed with unilateral lymphoedema previously. Lymphoedema disease is a fluid disorder in which some part of the body may be swollen or appear to be swollen with fluid [88]. Secondly, because of the increasing cases of lymphoedema disease in Australia. A review of research evidence suggests that more than 8000 new cases per year of secondary Lymphoedema occur in Australia [89]. This rate highlights the urgency for improved intervention mechanisms rooted in body fluid level assessment as an assistive method for early diagnosis. The fluid assessment technique should be able to indicate when excess water is removed from the body [90] e.g. during treatment, when

it is necessary to determine the volume of fluid in any part of the body [91], and as a symptom for detecting early or critical accumulation of excess fluid or low volume of fluid in any part of the body. Both measurements are essential for diagnosis and management of Lymphoedema. Further history of lymphoedema will be discussed in chapter 6

In order to clinically test this protocol for a developing or swollen area caused by fluid blockage in some part of the body, a primary choice was to target fluid associated problems in the arm. This is because the arm was used when developing the circuit model and preliminary tests conducted on healthy subjects were on the arm. Therefore, it is imperative to continue testing on the arm. Measurements were carried out at Therapist Support Laboratory Clinic (TSL). TSL is a Lymphoedema clinic in Abbotsford, Melbourne which offered the use of her office space for the clinical part of this study. It was chosen because participants would be familiar with the environment and probably used to some of the clinicians. Moreover, testing in a familiar environment would help reduce psychosocial feelings and make the subjects feel comfortable and relaxed while participating in the study. Participants were encouraged to report any discomfort with the experimental procedures and were able to withdraw if they felt uncomfortable with the experimental procedures at any time without consequences.

Protocol 2.2: Healthy participants -without lymphoedema disease

The healthy participants would have had no previous diagnosis of lymphoedema and from observation had no swollen limb. The limbs will be checked with circumferential limb measurements (CLM). A similar protocol would be adopted as with the pathologically lymphoedema diagnosed subjects. The first measurement will be without fluid restriction which be followed by fluid restriction as explained in protocol 1.

A small harmless electrical current $< 1mA$ is transmitted into the arm via a pair of the surface electrodes (transmitter electrodes) and received 20 cm at the receiver end as shown in Fig.3.10. In the first trial baseline experiment in chapter 4, six healthy volunteers participated. First, the subjects were asked to abstain from fluid after supper to 10.00 am. The subjects were given 500 mL of water and measured separately after fluid intake. The amount of water varied depending on the nature of experiment. For instance in chapter 5, to determine the sensitivity of the proposed model, different amount of water were given starting from 100 mL to 350 mL. All of the participants sat on a plastic chair and were instructed not to move as much as practically possible to avoid external physical contact. The measured arm rested on a wooden table or chair insulated to ensure no current leakage to ground. Interference and background noise was minimised by switching off electronic devices and wireless systems around the vicinity. Communication cables were isolated away from power packs and the laptop operated in battery mode. Since individual metabolism is different at different times of the day, the

experimental protocol was designed to ensure that all measurements were done at 10.00 am and that the average room temperature was maintained at 25 $\pm 0.1^0 C$. Repeated measurements were taken after abstinence from fluid and at 5 minutes interval following fluid intake of 500 mL of water. The average of 3 readings per 5 minutes interval was used to minimise measurement uncertainties. All measurements started 5 minutes after consuming a given amount of water since it was known that ingested water appears in plasma and blood cells approximately after 5 minutes after intake [34].

All protocols and measurements followed the approved procedures of the Victoria University Human Research Ethics Committee approval number HRE 14-122.

3.3 Equipment

The experimental system consisted of human body channel and electronic devices which includes vector network analyser, balun, laptop, Noraxon MultiTester, electrodes, connecting leads, refractometer, electronic floor scale, calibrated plastic cylinders, and digital thermometer. The first design of the experimental procedures are as explained in section 3.2, while further modifications were mentioned depending on the particular test being examined.

3.3.1 Measurement Equipment

Since the research aims at using the attenuation of an electric current passing through a human body to characterise changes in a person's body composition, human body is required for the passage of the signal and to relate the observed signal attenuations to changes in a person's body fluid changes. Already there exists an electrical circuit model for signal transmission through a human body in IBC, this research will carefully examine the features of the IBC circuit as a human body channel for communication different from the traditional use of coaxial cables and radio frequency micro wave systems. Thereafter, extract the important aspects of these features that is related to the proposed idea of this study in a manner that will assist the design of a new circuit model for assessing changes in human body fluid level by observing the attenuation of the signal as it passes through a body. Generally, the human body is dynamic consisting of non-homogeneous proportions of tissues and cell membranes. This means that signals transmitted across the body will vary in power depending on (a) whether the individual is still or in motion, (b) homogeneous or non homogeneous distribution of the tissue structure and fluid volume in the area used for signal transmission. To study the signal propagation across this type of medium, with focus on direct application for body composition, a suitable technique that would analyze the impact of the various tissue components to the signal flow is by measuring the scattering parameters (S-parameters)

which describes the operation of a 2-port network, in this case, comprising transmitter electrodes, human body channel, the area of the body where the electrodes are applied, which is the device under test (DUT), and receiver electrodes as shown in Fig.3.2
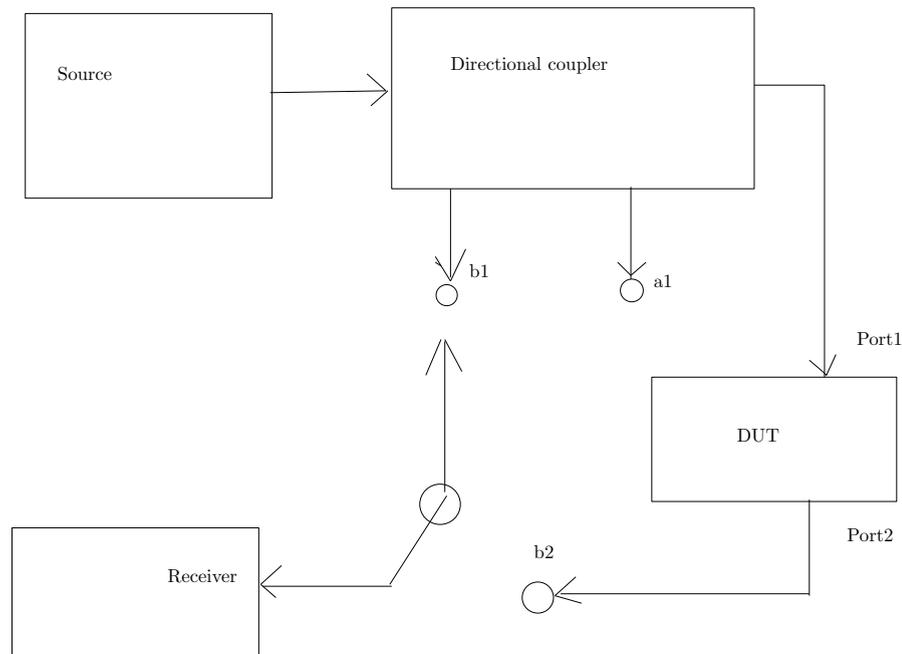
FIGURE 3.2: Schematic diagram for measuring the scattering parameters of the using a two port network model
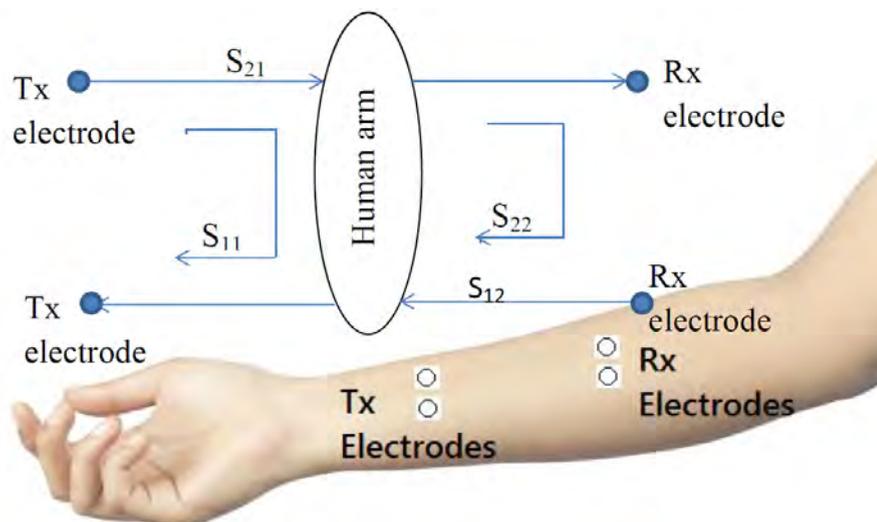
FIGURE 3.3: Human body arm showing the measurement of scattering parameters in a galvanic coupled signal transmitted from Tx and received at Rx

S_{11} is the reflected signal power measured in dB while S_{21} refers to the transmission coefficient, also measured in dB.

The incident and reflected signals can be measured with a series of directional couplers as shown in Fig.3.2 The scattering matrix relates the output signals b_1, b_2 to the input signals a_1, a_2 that are incident on the two port.

$$\begin{bmatrix} b_1 \\ b_2 \end{bmatrix} = \begin{bmatrix} S_{11} & S_{12} \\ S_{21} & S_{22} \end{bmatrix} \begin{bmatrix} a_1 \\ a_2 \end{bmatrix}$$

$$S_{11} = \frac{b_1}{a_1}|(a_2 = 0) \tag{3.1}$$

$$S_{21} = \frac{b_2}{a_1}|(a_2 = 0) \tag{3.2}$$

The transmission and refection loss coefficients shall be obtained in dB using the relation

$$S_{21} = -20log_{10}(\frac{V_{output-at-port2}}{V_{input-at-port1}}) \tag{3.3}$$

$$S_{11} = -20log_{10}(\frac{V_{reflected-at-port1}}{V_{input-at-port1}}) \tag{3.4}$$

Thus a signal transmitted through the human tissue can be characterised using a vector network analyser coupled to the body using electrodes and connecting leads.

3.3.2 Vector Network Analyser and Baluns

This study shall use a two port vector network analyzer to measure the S-parameters as shown in Fig.3.2. The VNA measures the magnitude and phase of an incident and reflected signal independently by performing continuous frequency sweeps across a calibrated range at the various ports of the device under test (DUT). Measurement with vector network analyzers are often accurate with wider dynamic range and better capability to reject broadband noise than scalar network analyzers [92]. The transmission and reflection coefficients are outputed in dB using the relation in equation 3.3 and 3.4.

During the experiment, a battery-powered MiniVNA Pro manufactured by Mini Radio Solution Inc. Poland, was connected to a balun as described in section 3.4. The VNA was calibrated using the reference load in short and open circuit available in the manual calibration kit. The calibration kits contain calibration standards which was used to verify the performance of the VNA. The calibration is repeated every six months to ensure good performance and safety. Throughout, the output power was set to 0 dB (< 1.0 mW) which is well below the recommendations of the international commission on non-ionization radiation protection (ICNIRP) which is 37 dBm ($= 5$

W) on a person weighing 65 kg [92]. In order to electrically isolate the two ports of the VNA to ensure the return current does not pass through the common earth ground, the two baluns were connected to the VNA ports as shown in section 3.4. This is to suppress undesired signal reflection at the VNA ports; however, they also transform unbalanced signal input into the galvanic coupling circuit to a balanced signal output. Fig.3.4 is a snapshot of the balun. The balun (manufactured by Mini-circuits, Brooklyn, NY, USA), is a coaxial RF transformer, FTB-1-1+, has turns ratio of one and frequency range 0.2-500 MHz. Baluns are used to electrically isolate the two ports of the VNA to ensure the return current does not make a loop through the common ground of the two ports by making the two ports equal and opposite. This means that the output has 180 degrees phase shift as shown in Fig.3.5.

3.3.3 Electrode Types

In order to characterise the signal transmitting through the body, electrodes are used to provide the communication interface between the measuring devices and the human body. A single use silver/silver chloride (Ag/AgCl) medical electrodes made by Noraxon Inc., Scottsdale, AZ, USA and single use silver-silver chloride Ambu White-Sensor 4500M, ECG electrodes made in India for Ambu Inc. Glen Burnie, MD, USA were used. Fig.3.6 depicts the two electrodes used in this research.

FIGURE 3.4: Balun model number FTB-1-1+ impedance ratio 1, and frequency range 0.2-500 MHz
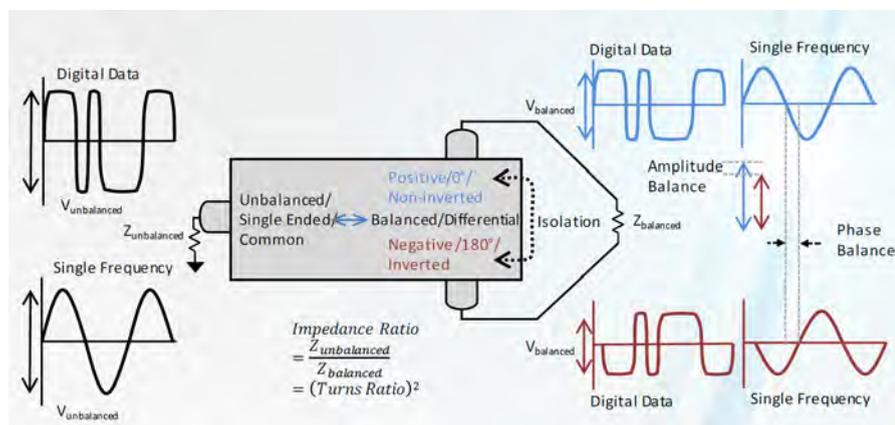
FIGURE 3.5: Function of a balun,[93]

FIGURE 3.6: Round pre-gelled medical electrodes. Left is Noraxon self-adhesive, single use, EMG electrode, product code: 270 and Right is Ambu WhiteSensor single use self-adhesive ECG electrode, product code: 4500M
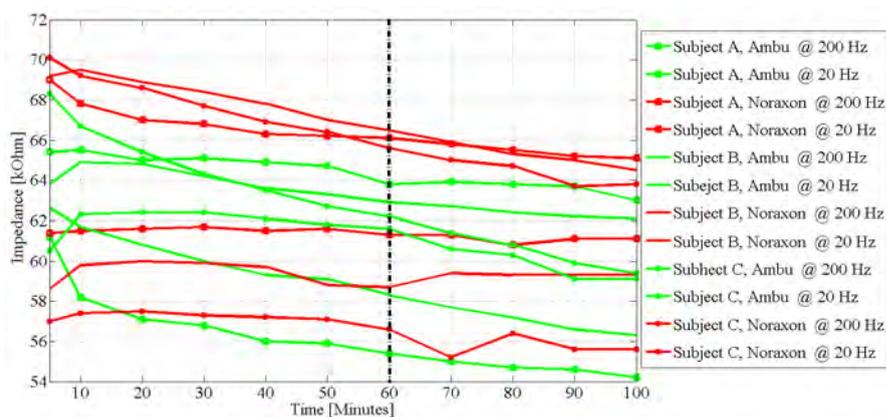
FIGURE 3.7: Comparison of skin-electrode impedance of Noraxon EMG electrode and Ambu WhiteSensor 4500M, ECG electrode on 3 subjects at 200 Hz and 20 Hz.
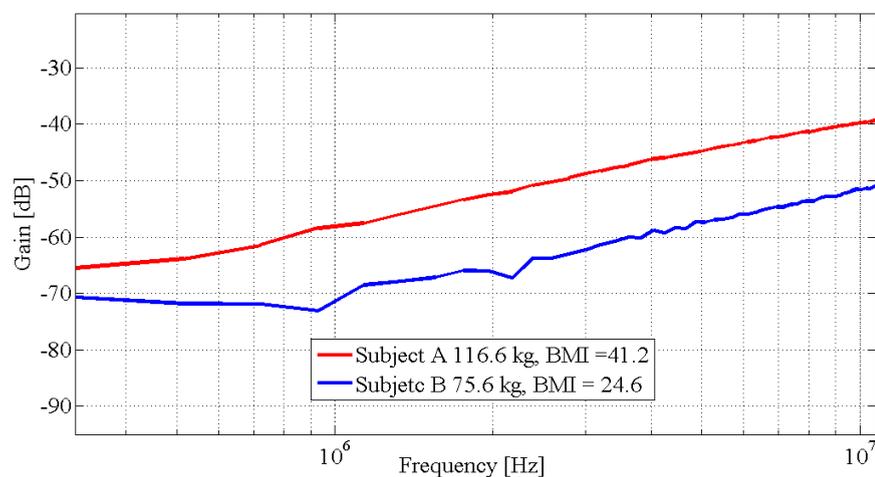
FIGURE 3.8: Gain versus frequency for high and low BMI at 10 cm distance between transmit and receive electrodes

TABLE 3.1: Change in electrode-skin impedance on 3 subjects after an hour of monitoring at 20 Hz and 200 Hz

Subject	Electrode Type	Percentage change	
		20 Hz	200 Hz
A	Ambu	9.47%	2.46%
	Noraxon	4.20%	0.16%
B	Ambu	6.86%	1.41%
	Noraxon	3.9 %	1.16%
C	Ambu	8.9%	2.72%
	Noraxon	5.27%	3.83%
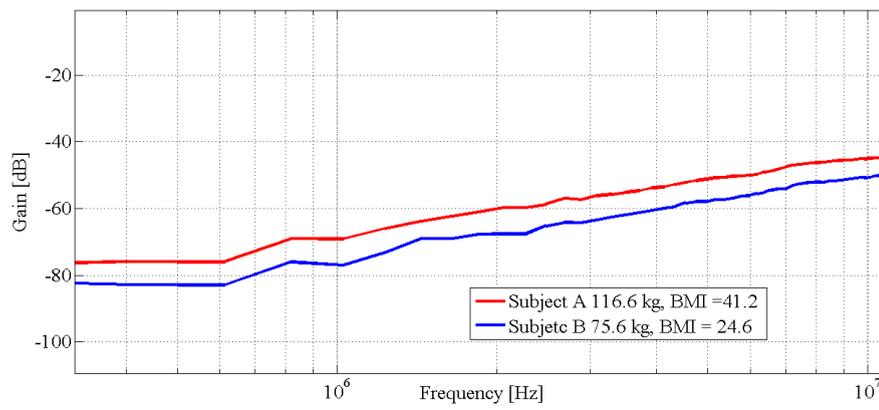
FIGURE 3.9: Gain versus frequency for high and low BMI at 20 cm distance between transmit and receive electrodes

To verify the effects of electrodes in this study, the electrode-skin impedance of the Ambu and Noraxon electrodes were measured. The result is shown in Fig.3.7. The graph depicts a decreasing value in the impedance of the electrodes. The percentage decrease between the two electrodes after one hour of monitoring is shown in table 3.1. The large decrease in the magnitude of the skin-electrode impedance depicted in Fig.3.7 has an effect on the amplitude of the received signal. However, consistency in skin-electrode impedance is critical in order to ensure that measurements relate to determining changes in body fluid levels. To ensure balance in impedance measurements, similar site and position were maintained on each subject. Table 3.1

lists the electrode skin-impedance on 3 subjects after an hour of measurement with Noraxon and Ambu electrodes. Since this research focuses on the use of galvanic coupling intrabody signal propagation for studying changes in human body composition, a further test with motion artefacts would determine how electrodes might affect measurements.

In order to determine the appropriate transmission distance for this experiment, the gain (negative attenuation) at 10 cm and 20 cm were measured at inter-electrode separation of 4 cm on two subjects with different body mass indices. The reduction in transmission distance between the transmitting and the receiving electrodes by 10 cm resulted in 3 dB gain in attenuation for low BMI and 8 dB gains for high BMI (Fig.3.8 and Fig.3.9). Therefore 20 cm transmission distance was chosen on all subjects with inter-electrode separation of 4 cm since the focus is on using the observed changes in signal attenuation for assessment of human body fluid changes. The 20 cm transmission distance extends from the lateral side of the elbow to the anterior arm between the elbow and the wrist. Signal changes due to the effects of limbs around joints [94] were minimised by avoiding measurement on joint areas.

3.3.3.1 Effects of motion artefacts on intabody signal propagation

The transmit and reflection coefficients with and without body movements using Ambu WhiteSensor electrode (model number 4500M)

and Noraxon electrode (model number 270) were measured as following. Participants were asked to bounce a hand ball on the ground every second while the measurements were taken. The processes were repeated and the transmit and reflection coefficients measured when the body was as still and when body movement was allowed by the swing of hands up and down as the bounces. The VNA outputs the scattering matrix relating to the out going signals b_1, b_2 to the incoming signals a_1, a_2 incident on the two ports and calculates the transmission and reflection coefficients in dB using equations 3.3 and 3.4.
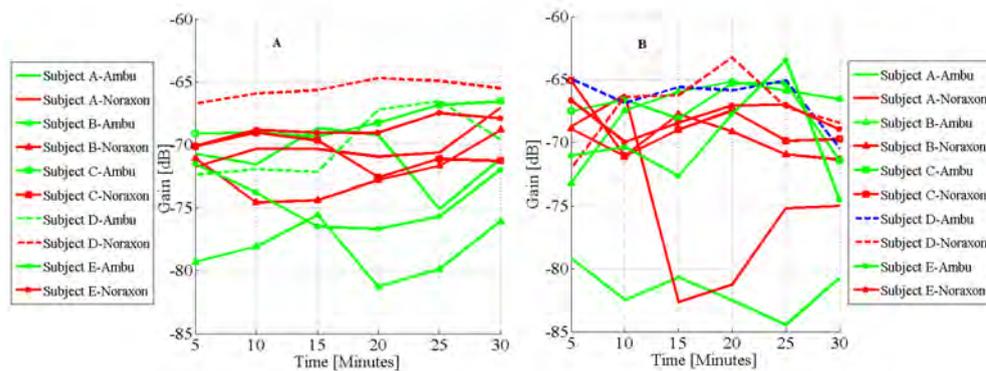
FIGURE 3.10: Transmission coefficient "A" without body movement and "B" with body movement
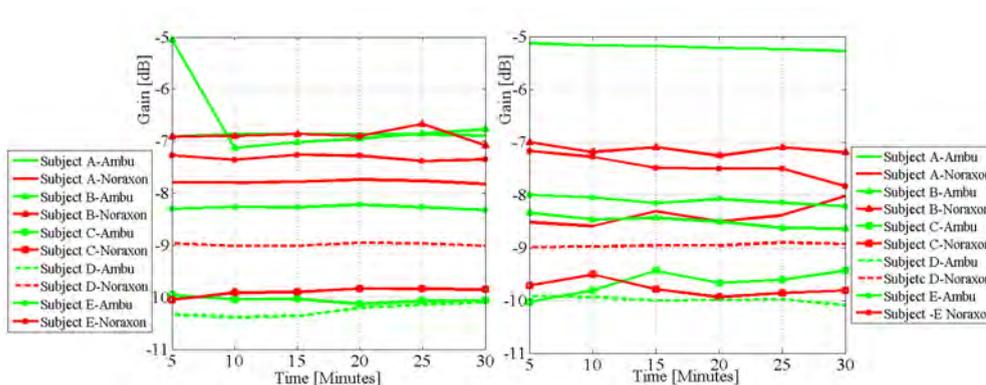
FIGURE 3.11: Reflection coefficient "A" without body movement and "B" with body movement

TABLE 3.2: Impact of electrodes to movement artefact on the transmission loss of a galvanic coupled electric signal

Subject	AmbuWhite Sensor (dB)	Noraxon 270 (dB)
A	9.0	4.0
B	6.0	2.0
C	2.0	5.0
D	8.0	6.0
E	0.5	3.0

TABLE 3.3: Impact of electrodes to movement artefact on the reflection loss of a galvanic coupled electric signal

Subject	AmbuWhite Sensor (dB)	Noraxon 270 (dB)
A	1.78	0.40
B	3.29	0.09
C	0.07	0.33
D	0.42	0.03
E	0.30	0.12

Fig.3.10 is the graph of the s-parameters showing the transmission coefficients A, without body movement and B with body movements while Fig.3.11 depicts the result of the reflection coefficient A, without body movement and B with body movement. Table 3.2 summarises the impact of body movement using the two electrodes which necessitated the choice of Noraxon electrode but emphasises the fact that an electrode with consistent skin-electrode impedance and high resistance to motion artefact would be most appropriate.

3.3.4 Noraxon Multitester

A 50 microamp, Noraxon Multitester, shown in Fig.3.11 was used to measure the contact impedance between the skin and the electrode. Again the test current is within the safety guideline on the recommendations of the (ICNIRP) [83]. Three different frequencies are

available with the Nooraxon Multitester; 20 Hz, 100 Hz and 200 Hz. They are selected using the Mode Control Selector. The values of the skin-electrode impedances on the subjects were used to characterize the performance of the electrodes.
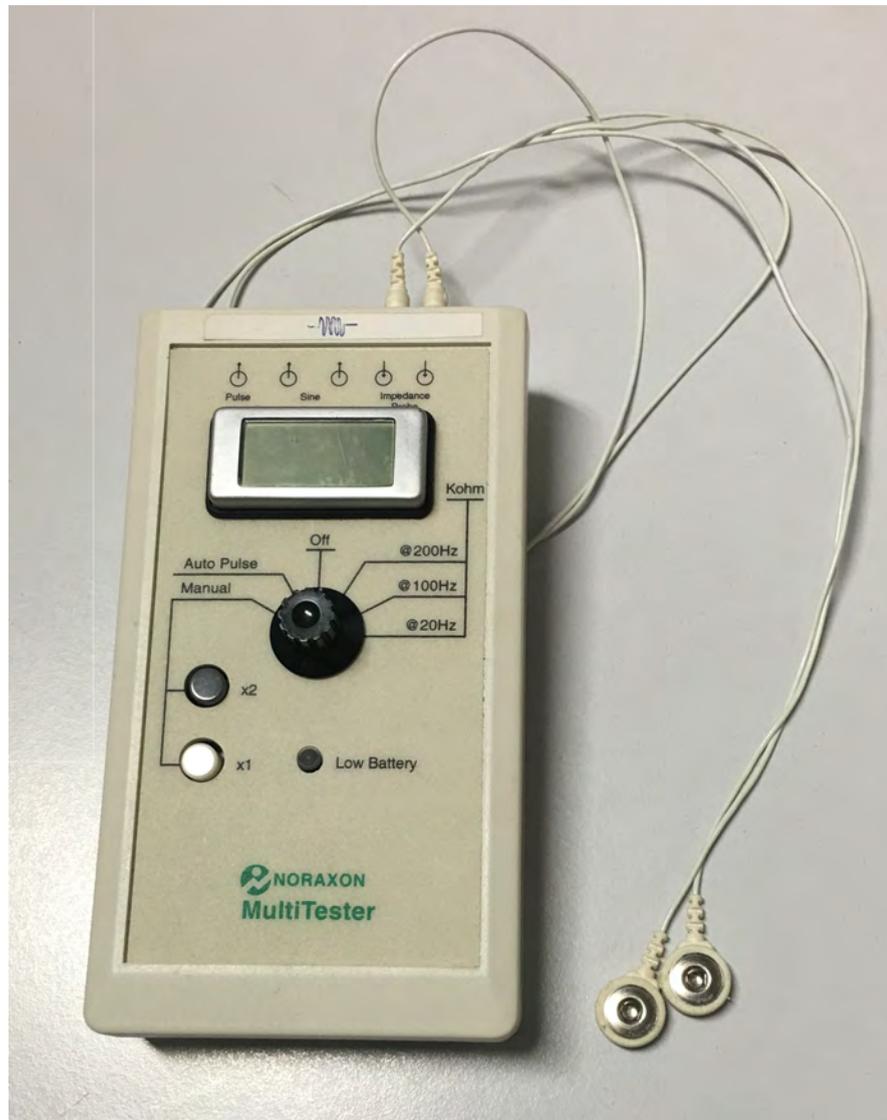
FIGURE 3.12: Noraxon Multitester for testing skin-electrode impedance

3.3.5 Sterilized Hand gloves

Medical gloves are used to prevent cross-contamination of diseases between users and participants by avoiding direct skin contact. Nitrile medical examination gloves, N-DEX, REF 7705PFTM, made in USA by Best Glove, Inc. Melno were used because they are powder-free, non-sterile and are single use, therefore are not expected to have any allergic reaction on subjects. Secondly, because it meets the single-use emergency medical examination glove requirements of National Fire Protective Association, NFPA-1999, which specifies the requirements for EMS protective clothing to protect personnel performing patient care during emergency medical operations from contact with blood and body fluid-borne pathogens, standards on protective clothing for emergency medical operations, 2008 edition [95].

3.3.6 Refractometer

A hand held refractometer, URICON-NE, 106 Cat. No. 2722 with measurement uncertainty of 0.001 from ATAGO Co., Ltd., Itabashi-ku, Tokyo, Japan was used to measure the urine specific gravity of the urine samples provided by the participants. Urine specific gravity (SPG) measures the ratio of the density of urine relative to the density of pure water. The manufactures recommend measurement of urine specific gravity at 20.0^oC. A specific gravity greater than 1

means the fluid is denser than water [41]. Urine specific gravity measurements usually range from 1.002 to 1.030. Minimal dehydration ranges from 1.010 to 1.020 with increasing severity of dehydration from 1.020 and upwards. A specific gravity of 1.030 and upwards is regarded as highly severe and values below 1.010 is classified as hyperhydration [41, 48, 51].

3.3.7 Weighing Scale

An off-the-shelf electronic WeightWatchers weight tracking & body composition monitor model number WW125A, with measurement uncertainty $\pm 50g$ was used to measure changes in body mass of the subjects. Subjects wore light clothing and were bare footed. Subject height was measured to the nearest 0.5 *cm* measured against the wall bare footed and heels together with buttocks, shoulders, and head touching the vertical wall surface and clear horizontal marking sighted.

3.4 Measurement Setup

The measurement set-up is shown in Fig.3.12. A mini ProVNA, baluns and electrodes were fixed to the body as shown in Fig.3.12. The set up follow the approved ethics recommendation and the standard safety limit set by International Commission on Non-Ionizing Radiation Protection (ICNIRP) [83] and World Health Organization

(WHO, 1993) [96]. The distance between the transmit and receive electrodes were determined experimentally as shown in Figs 3.8 and 3.9. Subject height was measured to the nearest 0.5 cm measured against the wall bare footed and heels together with buttocks, shoulders, and head touching the vertical wall surface and clear horizontal marking sighted. Their body mass were measured with the electronic weight tracking and body composition monitor.

3.5 Summary

This chapter outlines the equipments and measurement protocols used for this study. Protocol 1 will be used in chapter 4 and 5 while protocol 2 will be used in chapter 6. This chapter also verified the impact of skin-electrode impedance and motion artefacts on the electrode which provided useful insight that assisted in the choice of the electrodes.
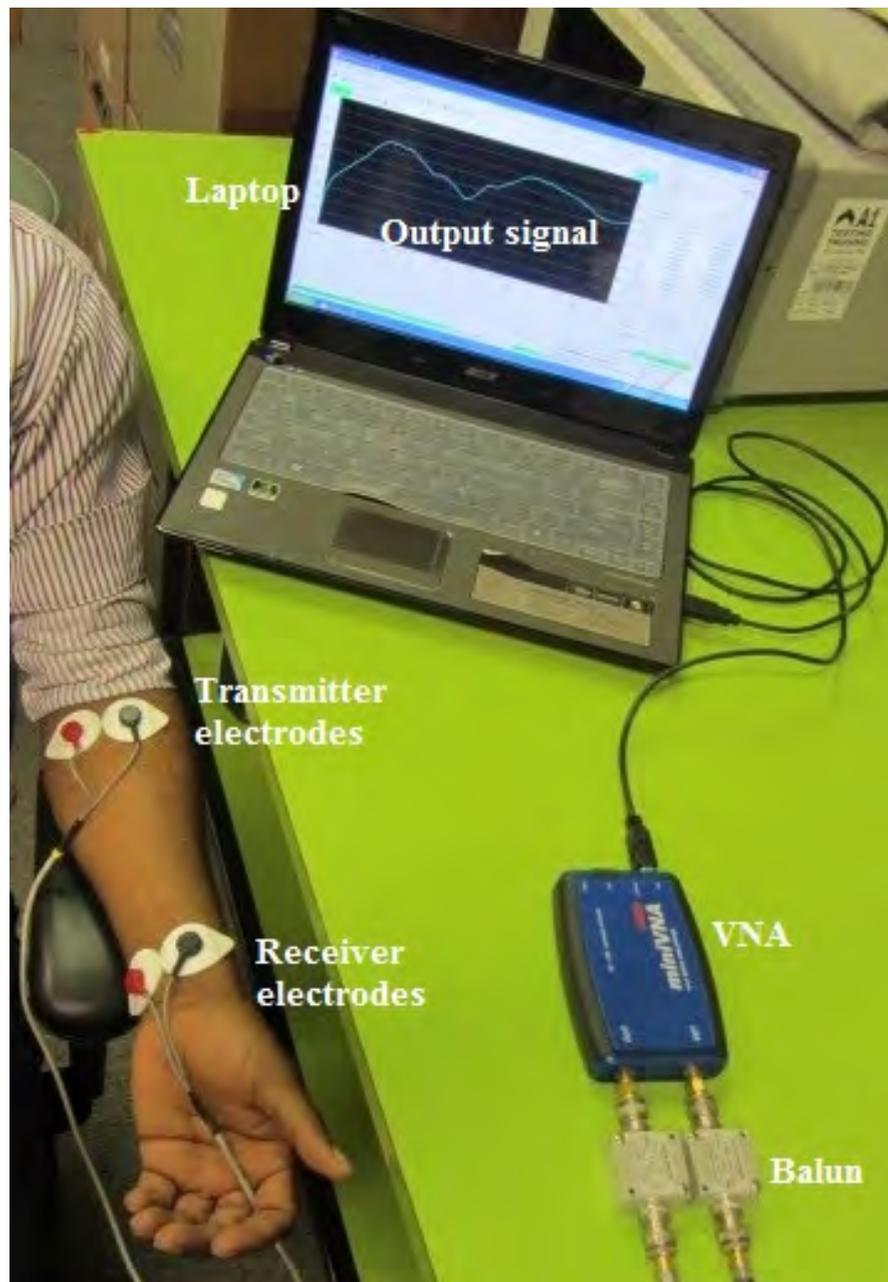
FIGURE 3.13: Galvanic-coupling circuit on the lower left arm, the four terminal silver-silver chloride Noraxon electrodes are attached to the body and connected to the VNA via a balun. The output signal shows on the laptop screen fitted with the VNA software

Chapter 4

A New Circuit Model of Real Time Human Body Hydration

Changes in human body hydration leading to excess fluid losses or overload affects the body fluid's ability to provide the necessary support for healthy living [32]. Conditions leading to excess fluid losses in the body usually result in problems such as dehydration, while fluid overload can lead to heart failure and death in some cases [9, 97]. In chapter 2, hydration was referred to as the process of gaining tissue water and the rate of hydration as the amount of change in the level of tissue water with respect to time. It is also a symptom for diseases associated with excess fluid or low level fluid in a human body [98]. Two most common techniques for measuring body hydration are bioelectrical impedance analysis [99] and urine specific gravity [40, 100]. These techniques assume a constant hydration factor and are not easily applied on a specific area of the body, except in the case of segmented BIA which has been discussed in chapter 2. For instance,

the bioelectrical impedance analysis is based on a hypothetical relationship between impedance and the electrical volume. It assumes that the entire human body is a cylindrical conductor and tissues are electrically isotropic with no reactive component. However, it has been shown that human tissue should be modelled as having both resistive and reactive components, since cell membrane capacitance contributes significantly to the effective impedance of electrical signals across tissues [33]. Schwan [56] further showed that biological tissues have frequency dependent electrical properties that could classify them into three frequency regions (α, β and γ). Current treatment of body fluid disorders such as lymphoedema are mostly monitored by changes in body weight, circumferential limb measurements, limb volume measurements, and water displacement methods which have issues with hygiene and problems with tracking sequential changes in weight and limb circumference [101]. Therefore, a new method is required to measure body fluid levels effectively

This thesis will adopt the approach of modelling the human body as a transmission channel, and propose a new time dependent component to model fluid changes. This will facilitate tracking of hydration in real time by predicting the attenuation of a propagating electrical signal. The resulting circuit model has the varying component that models body impedance changes due to fluid level changes. The validation of this model is through measurement of signal attenuation when a known signal is transmitted. The attenuation can be

measured making it possible to quantify hydration effects empirically and hygienically while tracking changes in the fluid volume on a specific area of the body. The rest of this chapter is organised as follows: Section 4.1 is the variable tissue impedance on IBC signal propagation. Section 4.2 is the hydration model with subsections 4.2.1 highlighting discussions on previous circuit models followed by the proposed hydration model as a time-dependent circuit in section 4.2.2, estimation of the fluid component in the arm in section 4.2.3 and a first order model of the changes in human body impedance due to hydration in section 4.2.4. Section 4.3 will discuss the effects of changing body fluid levels on intrabody signal propagation while section 4.3.1 is the simulation results and 4.3.2 is the empirical measurements. Finally, the chapter concludes with a discussion and summary in section 4.4

4.1 Variable Tissue Impedance on IBC Signal Propagation

An electrical signal passing through the human body is strongly affected by the dynamic changes in the volume of tissue containing fluid and its dielectric properties. Tissues have high ability to store electrical energy in an electric field at low frequency. High frequencies are affected by human body antenna effects and possible radiation. Therefore this study shall concentrate more on frequency range

lying between 800 kHz to 1.2 MHz which lies within the β dispersion region. Frequencies in the β dispersive region is also related to the cellular structure of biological materials [56, 77] (section 2.1.1). Fig.2.9 and Fig.2.10 depict the dielectric relationship with frequency of common human tissues and Fig.2.11 the penetration depth across frequency of the same tissues. Since relative permittivity of tissue is higher at low frequencies (Fig.2.10), this study shall observe signal attenuation on tissues at low frequencies (800 – 1.2 MHz) to measure variabilities in human body hydration with respect to time. An electrical signal propagating through tissues changes in proportion to changing tissue impedance. Dehydration increases the impedance of tissues [35] and hydration, conversely, does the opposite. Consequently, this thesis will use the observed signal attenuation on tissues at low frequencies to measure variabilities in human body hydration with respect to time. In literature, previous models of signal propagation across human tissue, either by finite-element method [71, 72], finite difference time-domain methods [73], equivalent electric circuit [69, 70] and quasi-static dielectric principles [74] are all based on the assumption of static tissue impedance. This assumption is contestable considering that the average quantity of water required by a normal person to replace lost fluid in a temperate environment is between 2600 - 2700 mL per day [29]. These dynamic changes in the body fluid level, which also changes the impedance of the body, and the high relative permittivity at low frequencies, is the motivation for a real-time human body circuit model to describe human

body hydration.

4.2 Hydration and Dehydration Models

The electrical conduction at low frequency is affected by the amount of water solute available in the tissue. Thus, by coupling a low frequency electrical signal galvanically on the body, the signal passing through the tissue will vary in attenuation in response to changes in the water level. Consequently, the attenuation (negative gain) of the signal amplitude will depend on the composition of the tissue in terms of the amount of water present at the time, the tissue muscle-fat ratio and the input signal frequency. Other external factors such as the type of electrode and, the distance between the connecting electrodes and environmental conditions, affect the measurements but can be experimentally controlled. Similarly, the observation by Seyedi *et al* [94] that an intrabody signal changes due to the effects of limbs around joints can be minimised by avoiding measurement on joint areas.

4.2.1 Previous Circuit Model of the Human Body

In IBC circuit model discussed previously in chapter 2, Wegmueller *et al* [72] developed a circuit model with five body tissue impedances (Fig.2.11), which was later improved by Song *et al* [69] and most

recently by Behailu *et al* [70]. This later model included Z_{ES} representing the impedance of the contact interface to the body at the transmitter and the receiver nodes, and Z_i and Z_0, are the input and output impedances and Z_A is the longitudinal impedance of the transmission path similar to that shown in Fig.2.11. However, the longitudinal impedance, represented as Z_L has four layers consisting of the skin, fat, muscle, and bone. This study extended the investigation to six layers by including a body fluid layer, which is key to this research, and also separated the bone into cortical bone and bone marrow. This was necessary because the cortical bone and bone marrow have different dielectric properties [79].

4.2.2 Proposed Model of Hydration as a Time Dependent Circuit
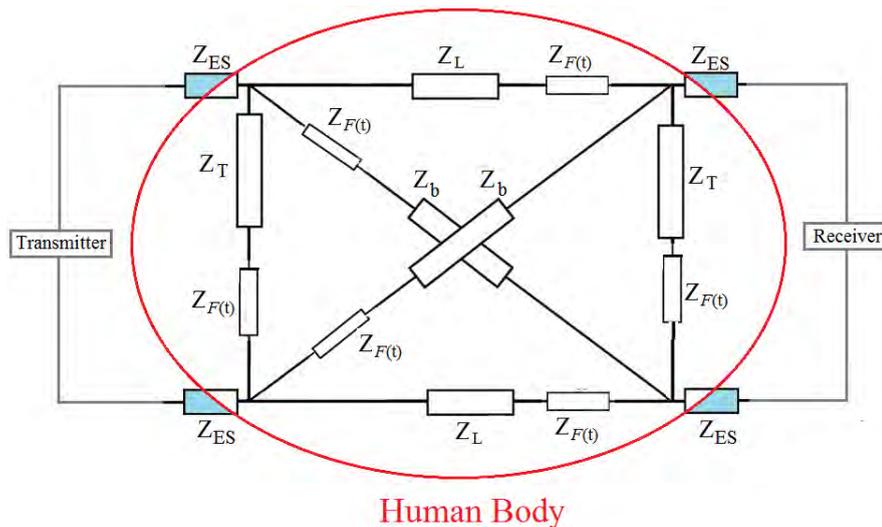
FIGURE 4.1: Improved circuit with variable impedance component from dynamic changes in human body fluid level

Thus, Fig.4.1 is the proposed circuit with a variable impedance component $Z_F(t)$ that changes with change in the volume of body fluid

and for ease of nomenclature, the transverse impedance is represented as Z_T, while the diagonal impedance remains as Z_b. The body fluid increases or decreases primarily by hydration or dehydration. Therefore assuming an average arm radius of 50 mm, the corresponding tissues consist of 3% skin, 17% fat, 55% muscle, 12% cortical bone, and 13% bone marrow [72, 102]. Using these to calculate the tissue anthropometric parameters (the thickness of the tissue layers at different arm radii), then, by optimization, calculate the corresponding size of the thickness of the body fluid layer. However, although body parts have multifaceted geometry with complex internal structures, this research assumes a homogeneous concentration of these proportions including a fluid layer over the entire arm and calculated the impedance of the six body tissue components in this model using the formula in [69].

By postulating that the changes in the amount of water in the body directly changes the resultant impedance of the body tissues, this will result in an increase or decrease in the received signal attenuation. The body fluid consists mainly of aqueous solutions of ions and cations which influence the signal propagation [33]. Moreover it has been stated that tissue impedance increases with increase in dehydration [35].

4.2.3   Estimation of the Fluid Component of the Arm

The effects of hydration changes have not been taken into account
in human body circuit models. To introduce the variable fluid com-
ponent, an approximation of a separate fluid layer among the tissues
is required which is achievable using Fig.4.2, Fig.4.3 and table 4.2.
Water contributes up to 60% of total body weight (TBW) of an adult
[32]. The dipole nature of water results in ions which contribute to
electrolytic conductivity [33]. Table 4.1 shows some of the human
body electrolytes.

TABLE 4.1: Example of body electrolytes [33]

Cations	Anions
Na^+	Cl^-
K^+	HCO_{3-}
Ca^{2+}	$Protein^-$
Mg^{2+}	PO_4^{2-}
H^+	$S0_4^{2-}$

Both the intracellular and the extracellular electrolytes support elec-
trolytic conductivity which causes potential differences that influence
current flow. The conductivity is related to the movement of the
electrolytes; adipose tissues contain relatively less water than mus-
cle tissues causing conductivity to be less in fat than in muscle and
skin [33]. Assuming a non-homogeneous lower arm with a homoge-
neous distribution of body fluid.

Let F_n denote the thickness of fluid in the nth layer of the arm,
consisting of the skin s, fat f, muscle m, cortical bone bc and bone
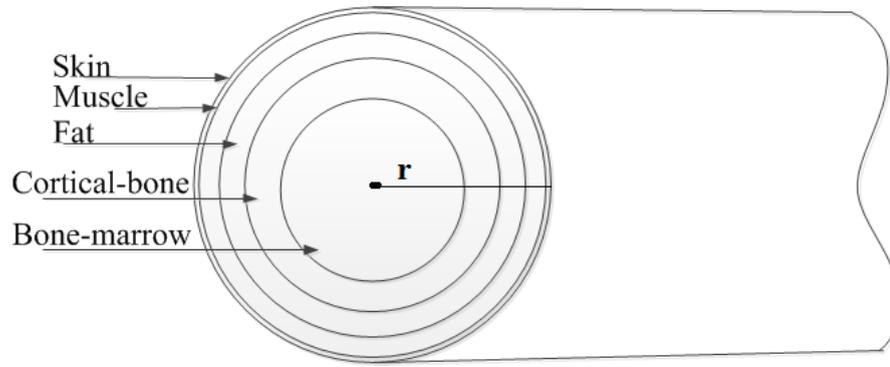
FIGURE 4.2: A cross section of the arm with radius r, showing the different tissue layers used in this experiment
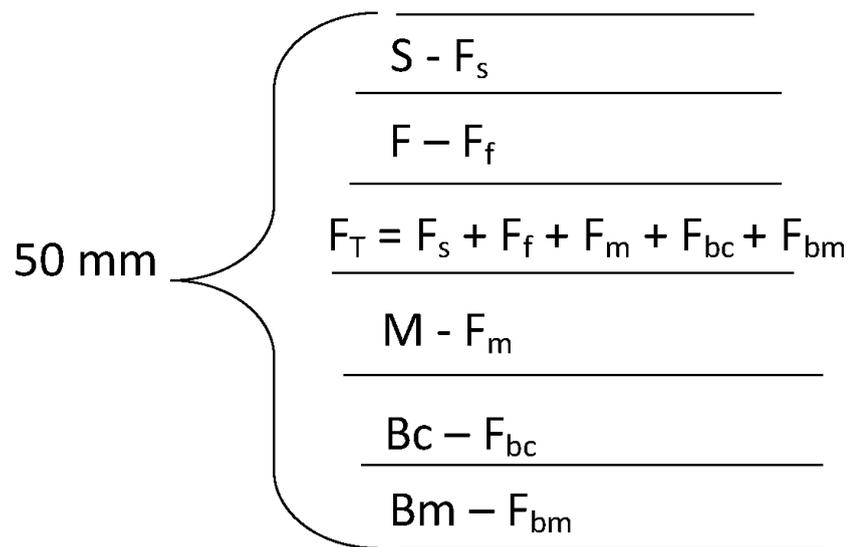
FIGURE 4.3: Approximating the fluid layer by optimization

marrow bm; therefore, the thickness of the fluid layer, F_T would be

$$F_T = F_s + F_f + F_m + F_{bc} + F_{bm} \qquad (4.1)$$

As depicted in Fig 4.3, each layer includes a fluid layer F with subscript as shown in equation 1. Similarly, if r is radius of the arm [18] and t_n the thickness of the nth layer of the arm from skin, fat, muscle, body fluid, bone cortical and bone marrow, the cross sectional area of first layer with arm radius $r = 50mm$ would be

$$\pi(r^2 - (50 - t_1)^2) \tag{4.2}$$

while the other layers would be

$$\pi((50 - t_{n-1})^2 - (50 - t_{n-1} - t_n)^2) \tag{4.3}$$

TABLE 4.2: Percentage of water on body tissues [32, 103]

Tissue Type	Percentage of Water	Thickness on arm radius (50 mm)
Skin	44	3
Fat	10	17
Muscle	70	55
Bone	22	a) Cortical bone 12
		b) Bone Marrow 13

From table 4.2 and Fig.4.3 and computing with equations 1-3, the total thickness of the fluid layer F_T is approximately 23 mm.

4.2.4 First-Order Model of The Changes in Human Body Impedance due to Hydration

Based on Fig.4.1 the transfer function can be derived. Since the circuit is symmetrical, the new circuit would have a variable impedance component $Z_F(t)$ in both the transverse and longitudinal sides, Z_T and Z_L respectively. V_i is the transmit voltage while V_0 is the output voltage at the receiver end with load R_l. Therefore, it can be inferred that any dynamic change in the impedance caused by a change in the human body hydration state would result in a change of the impedance of Z_T, Z_L, and Z_b as following:

$$\acute{Z}_T = Z_T + Z_F(t) \tag{4.4}$$

$$\acute{Z}_L = Z_L + Z_F(t) \tag{4.5}$$

$$\acute{Z}_b = Z_b + Z_F(t) \tag{4.6}$$

$$V_0 = I_0 R_l = \frac{V_i R_l \sigma_5}{\sigma_2} \tag{4.7}$$

Hence, from Figure A.1 (Appendix A)

$$\frac{V_0}{V_i} = \frac{-R_l \sigma_5}{\sigma_2} = \frac{-2 R_l \acute{Z}_T^2 (\acute{Z}_b + \acute{Z}_L)}{\sigma_2} \tag{4.8}$$

where $\sigma_2 =$

$8Z_{ES}^2(\acute{Z}_L^2 + \acute{Z}_L\acute{Z}_T + \acute{Z}_b\acute{Z}_L + \acute{Z}_b\acute{Z}_T) + 4Z_{ES}\acute{Z}_L^2(\acute{Z}_L + \acute{Z}_T + \acute{Z}_b) + 4Z_{ES}\acute{Z}_T(\acute{Z}_L\acute{Z}_T + \acute{Z}_b\acute{Z}_L + \acute{Z}_b\acute{Z}_T) + 2\acute{Z}_L^2\acute{Z}_T(\acute{Z}_L + \acute{Z}_b)$;

and $\sigma_5 = 2\acute{Z}_b\acute{Z}_T^2 + 2\acute{Z}_L\acute{Z}_T^2$;

The details of the derivation can be found in Appendix A.

If a measurable change in the amount of body fluid results in a change in the time-dependent impedance element $Z_F(t)$ for time a t after fluid intake and hydration occurs. It implies that the transfer

function (equation 4.8) is also time-dependent, i.e

$$\frac{V_0}{V_i} = g(t) \tag{4.9}$$

And the signal gain

$$G = 20log|\frac{V_0}{V_i}| \tag{4.10}$$

also varies proportionally with the time-varying changes in the impedance of the body as a result of the changes in the body fluid volume.

After fluid intake, as hydration occurs, the impedance of the body fluid $Z_F(t)$ decreases. This causes a decrease in the signal attenuation of the electrical signal passing through the tissues. If the initial state of the impedance at $t = 0$ just before hydration is Z_{f0}, and as the body fluid increases, the time-dependent impedance of the body fluid decreases in the form of a first order process given by

$$Z_F(t) = Z_{f0} - Z_w(1 - e^{-\frac{t}{\tau}}) \tag{4.11}$$

where t is the time for the change in impedance to occur, Z_{f0} is the impedance at time $t = 0$ just before hydration begins, t_f is time to reach the state of water balance, Z_w is the impedance resulting from the water consumed and the ratio $\frac{t}{\tau}$ is a characteristic that predicts the rate of hydration. τ is the time constant that characterises a particular individual. Therefore, assuming an initial fluid volume

V_{ib} before hydration, V_w is the amount of fluid consumed then the body will hydrate to a fluid volume V_b given as

$$V_b = V_{ib} + V_w(1 - e^{-\frac{t}{\tau}}); t = 0; V_b = V_{ib} \qquad (4.12)$$

Thus this research proposes equation (4.12) as the formula for estimating human body hydration at time t after fluid intake. V_w is the amount of water consumed by the subject, t is the time to absorb $V_w e^{\frac{t}{\tau}}$ amount of water. Fig.4.4 shows the effects of τ on the rate of hydration.
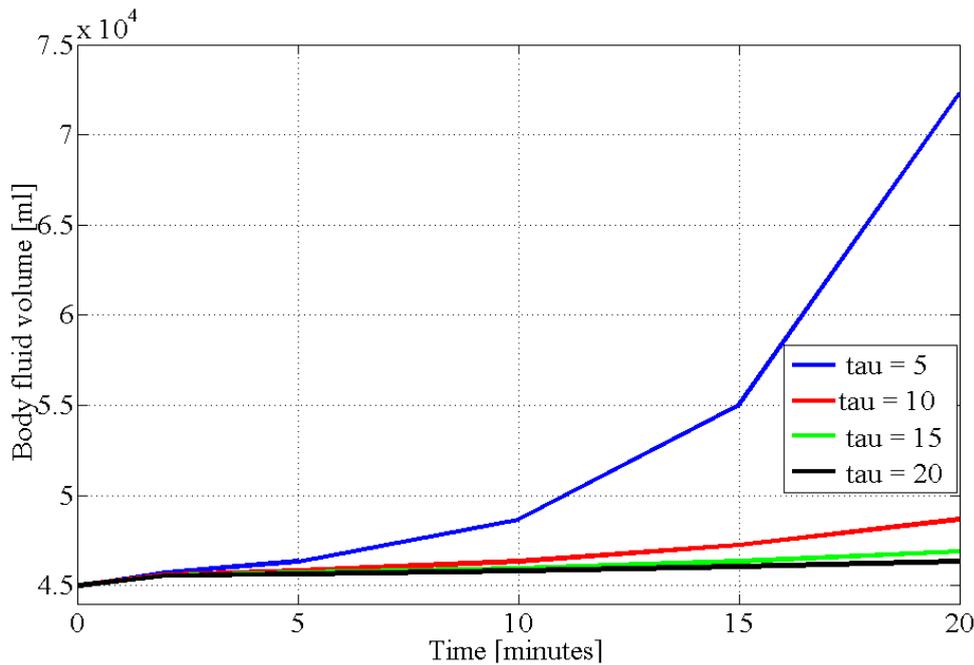
FIGURE 4.4: The effect of τ on the rate of hydration with initial body fluid volume set at 45,000 ml and 500 ml water intake.

To verify the effects of the anthropometric measurements, let θ denote the muscle-fat ratio which is a surrogate measure of body fat, similar in definition to the body mass index, BMI measured in (kg/m^2) [104]. By setting the dimensions of the tissues contributing to the

longitudinal impedance to the distance between the transmitter and receiver electrode pairs, the cross-sectional area of the contact interface of the muscle and fat can be used to calculate θ as

$$\theta = \frac{A_m}{A_f} \tag{4.13}$$

$$= \frac{\pi(r^2 - (50 - (t_1 + t_2 + t_3 + t_4))^2)}{\pi(r^2 - (50 - (t_1 + t_2))^2)} \tag{4.14}$$

A_m is the cross-sectional area of muscle to the distance between the transmitting and receiving electrodes and A_f the cross-sectional area of fat to the same distance between the transmitting and receiving electrode pairs. $t_1 - t_4$ is the thickness of the tissue layers in the arm corresponding to the skin, fat, fluid and muscle layers respectively (Fig.4.4). Table 4.3 is the classification of the anthropometric measurements to represent different indices of the proportion of body fat, by varying the proportions of A_m and f_m in equation 4.14, where for the purposes of simulation $0 < \theta < 1$. By definition the anthropometric ratio implies that high θ corresponds to low fat index or low BMI and low θ corresponds to high fat index or high BMI.

TABLE 4.3: Anthropometric measurement index, muscle-fat ratio

Index	Ratio
θ_1	0.9
θ_2	0.6
θ_3	0.3
θ_4	0.2

Based on the discussions above, a new expression for signal attenuation (G), in a galvanic coupled human body circuit can be defined

as $G(f, t, \tau, \theta)$, where f is the input signal frequency, t is the real time of observation, τ is specific to time varying characteristic of the subject, and θ is the anthropometric measurements of the body. The changes in attenuation (negative gain) can be calculated from equation 4.15 below:

$$G(f, t, \tau, \theta) = 20log(\frac{-2R_l\acute{Z}_T^2(\acute{Z}_b + \acute{Z}_L)}{\sigma_2}) \qquad (4.15)$$

where τ is found by equating the measured attenuation to the transfer function equation (4.15). Fig.4.8 depicts the effect of different values of τ on the rate of hydration at constant θ while Fig.4.9 shows the graph corresponding to different proportions of τ and θ that represent different combinations of the individual biological characteristic τ and the anthropometric ratio θ. Again show in Fig.4.10 the converse combination of the individual biological characteristic τ and anthropometric ratio θ. Fig.4.10 is the simulated graph of gain against frequency of an individual with physiological combination of τ and θ.

4.3 Effects of changing Body Fluid Levels on Intrabody Signal Propagation

Water is an important and major constituent of body cells, tissues, and organs and contributes about 60 % of total body weight (TBW) of an adult [32]. It has strong electrical polarity which makes it easy

to dissolve other polar molecules. Ions in the body are hydrated by the dipole nature of water making the cells to be surrounded by aqueous electrolytes, which causes electrolytic conductivity as shown in table 4.1. Excess or inadequate water intakes are corrected by sudden hormonal changes in the body, which are activated to prevent the effects of abnormal conditions (Fig.4.6). These include hormones such as antidiuretic hormones (ADH) in response to the feeling of thirst to top up the body water requirement and, in cases of excess fluid, the kidneys modify the body osmotic pressure with a suppression of ADH secretion in response to excess water in the body leading to urine formation and excretion Fig.4.7.

After ingestion, the water inside the body is ideally distributed proportionally into the extracellular and intracellular tissue spaces by the cardiovascular system. If the osmolality of the extracellular space is high, water is drawn from the intracellular space to the extracellular to maintain equiosmolality [8]. If sufficient water was not found to restore this imbalance, the body experiences dehydration and if water was found by ingestion, say, the balance is restored by hydration, Figs 4.6 and 4.7 show the mechanisms of dehydration with minimal ingestion and normal hydration respectively, as it relates to intracellular and extracellular fluid exchanges. Further explanation on the physiology of thirst, hydration and dysfunction can be found in Simon's work [8].

In general, a normal hydration state is the condition of water balance in the body [32]. In the empirical tests, measurements of hydration
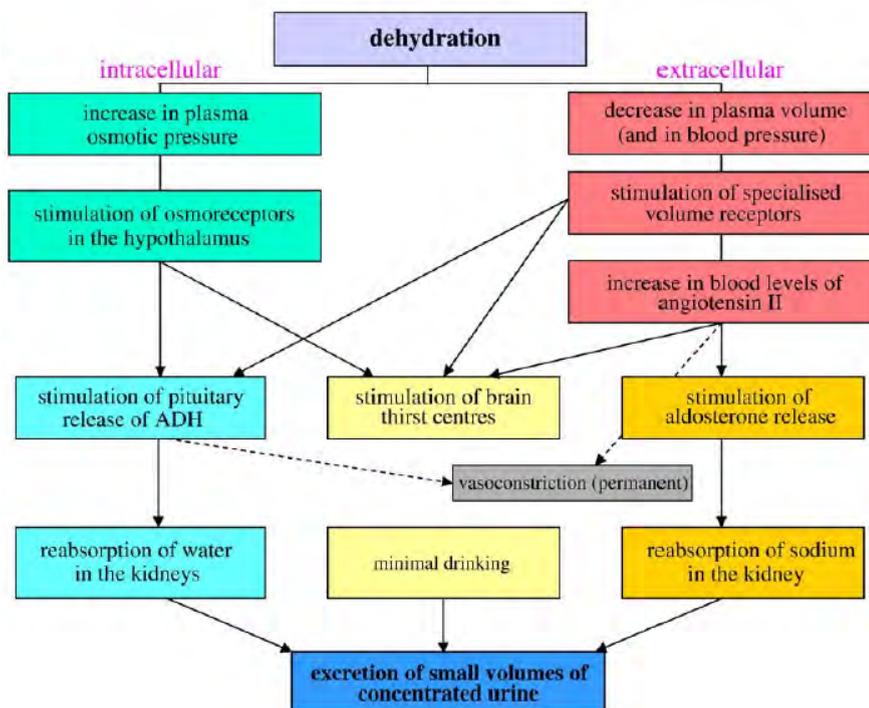
FIGURE 4.5: Physiological mechanism of dehydration [8]
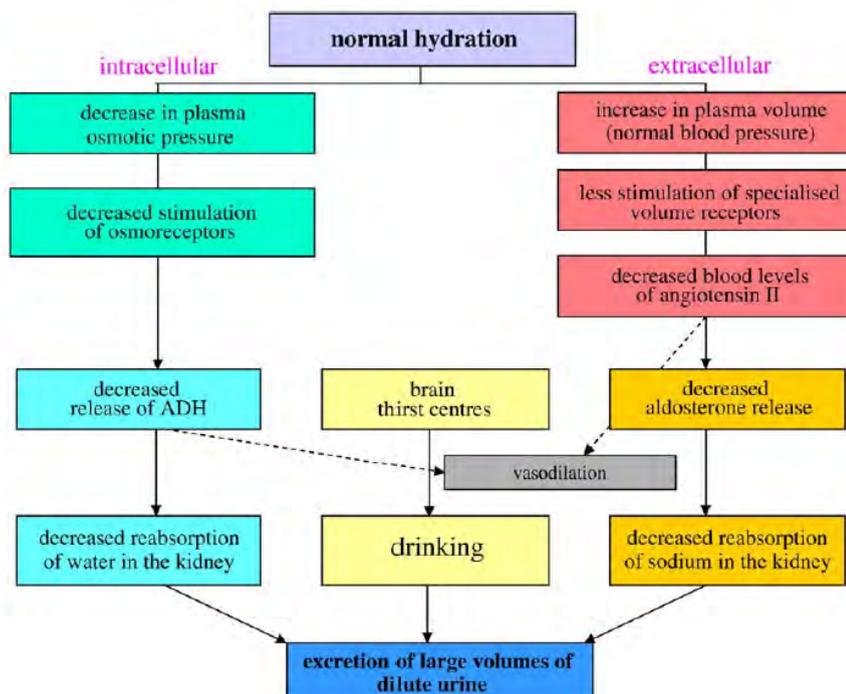
FIGURE 4.6: Physiological mechanism of normal hydration [8]

before water intake was set as the base line and then after intake at the end of fluid restriction to assess hydration. Measurements after urinating was also carried out to assess dehydration. The measurement set up is shown in Fig.3.8. Six healthy volunteers participated in the experiment. First the subjects were asked to abstain from fluid after supper to 10.00 am. Then subjects were given 500 mL of water and measured separately after fluid intake. All the subjects sat on a plastic chair with arms by their side to ensure the current was confined within the arm and avoiding external physical contact. Since an individual's metabolism is different at different times of the day, the experimental protocol was designed to ensure that all measurements were done at 10.00 am and that the average room temperature was maintained at 25 $\pm$0.1 ^oC. Repeated measurements were taken after abstinence from fluid and at 5 minutes interval following fluid intake of 500 ml of water and the average used to minimise measurement uncertainties.

4.4 Results

The theoretical graphs show different rates of hydration as a result of time-varying changes in the impedance of the body and the effects of the changes in τ. Based on this model, this research is proposing to measure the rate of hydration by changes in signal attenuation in dB/minute. From Fig.4.8, the rate of hydration is 1.73 dB/minute when τ is 5 and 0.05 dB/minute when τ is 150. The graph shows

that low τ is associated with a high rate of hydration and high τ with a low rate of hydration. Fig.4.9 is the model prediction of attenuation as hydration occurs at 800 kHz and 1 MHz. At state 0, just before hydration begins, signal gain at 800 kHz for $\theta = 0.2$ and $\tau = 150$ is -78.0 dB. This is about 6 dB difference compared with subject A, BMI 20.1 at 800 kHz and about 8.0 dB difference with subject F, BMI 41.2. Similar observation was also made at 1 MHz. The combinations of θ and τ is based on the earlier definition of θ as being related to BMI and τ as related to specific individual metabolic processes and since small values of τ resulted in higher rates of hydration, therefore can relate high θ to low τ and low θ to high τ as shown in Figs.4.8–4.9. This means that individuals with low anthropometric ratios θ are predicted to have low hydration rates while high θ would have higher rate of hydration. Fig.4.8 shows the converse combination of τ as proportional to θ which does not match empirical results at both 800 kHz and 1 MHz.

Fig.4.11 shows that attenuation is affected by time across each frequency. Further comparison of the empirical graphs (Figs.4.12-4.13) with the theoretical simulations show that in both cases, all the subjects showed that signal attenuation decreases as the body hydrates, in line with the theoretical prediction in Fig.4.10. This means that the human body impedance varies with time as the fluid level changes. Again, the six subjects have different anthropometric ratios defined by their BMI which contributed to the individual rate of hydration. Subjects A, B and C have higher rates of hydration and
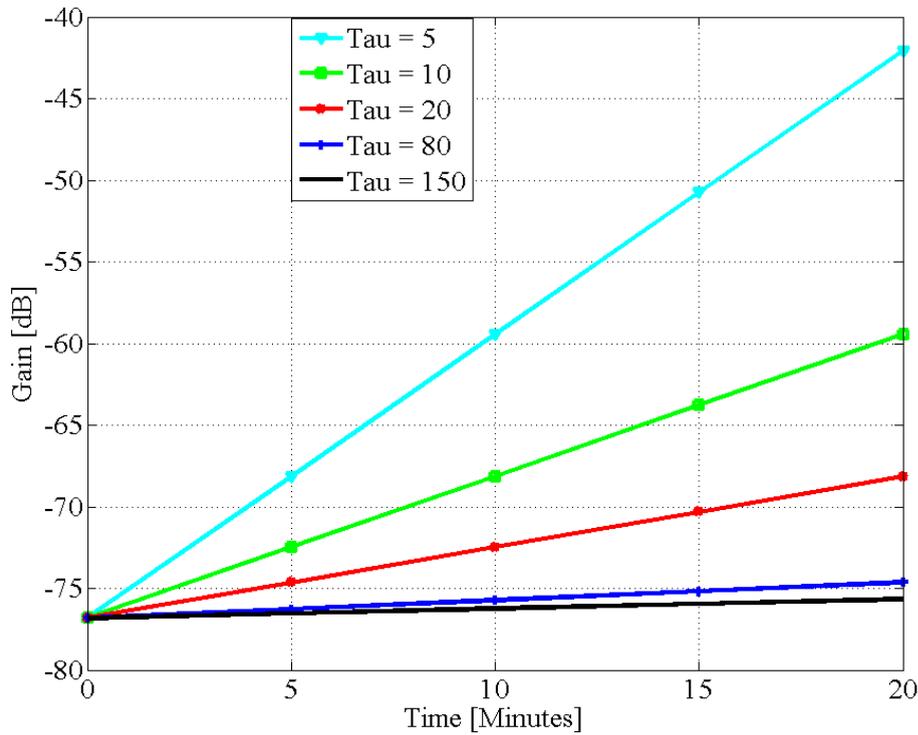
FIGURE 4.7: Graph of attenuation versus time at 800 kHz, showing the effect of changes in τ, at $\theta = 0.9$.

lower BMI ranges. For example, subject B (BMI 22.7) has average rate of hydration as 0.6 dB/minute and 0.7 dB/minute at 800 kHz and 1 MHz respectively. Similarly, subjects with high BMI (D, E and F) have almost a flat rate of hydration corresponding to their low anthropometric values as predicted in the theoretical definition. The decrease in attenuation is across all the subjects and at different rates, characterised by their differences in τ and θ, and was predicted in the simulation results. A comparison of the theoretical anthropometric parameters and the BMI ratios of the body show high BMI
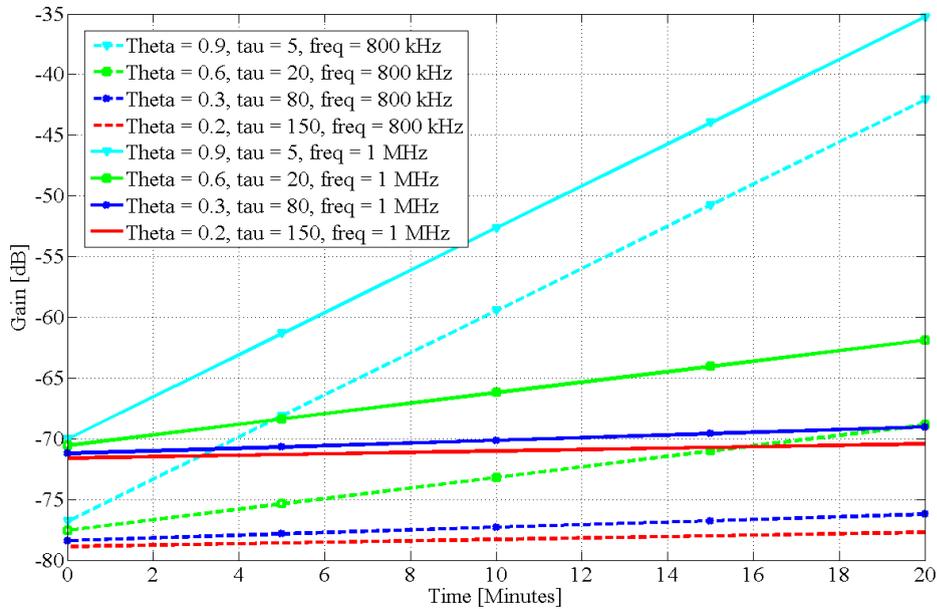
FIGURE 4.8: Model predictions of attenuation for simulated hydration at 800 kHz and 1 MHz when τ is inversely proportional to θ. This indicates low BMI equals lower time-dependent metabolic rate [105], higher rate of hydration [24] and more body of water [106]
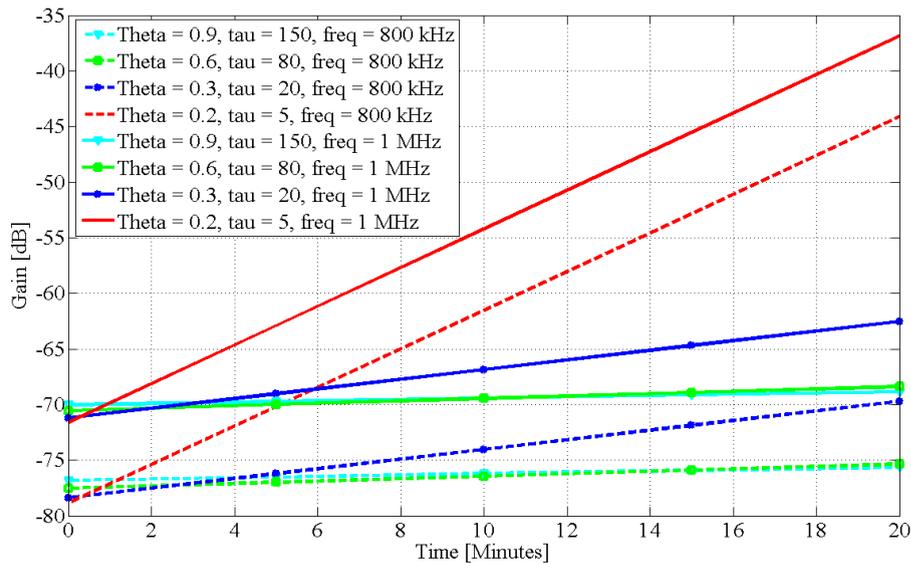
FIGURE 4.9: Model predictions of attenuation for simulated hydration at 800 kHz and 1 MHz where τ is proportional to θ. The result shows high BMI has high hydration rate and low time-dependent metabolic rate. This is not supported by empirical results and is not explained physiologically
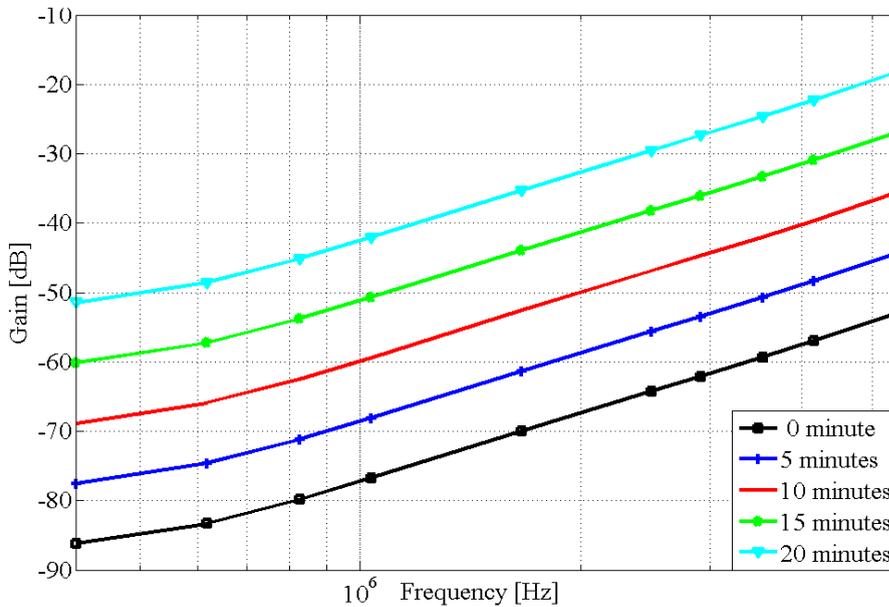
FIGURE 4.10: Attenuation against frequency as hydration occurs with $\tau = 5$
and $\theta = 0.9$.

corresponding to low θ and longer time-dependent characteristic fac-
tor τ, while low BMI corresponds to high θ with a corresponding low
τ.

4.5 Discussion

In this chapter a time-dependent circuit model for real-time human
body hydration is proposed and the experimental results show that
similar to theoretical predictions, the attenuation of an electrical
signal passing through the body tissues changes as the fluid level
changes. This change is affected by external factors such as changes
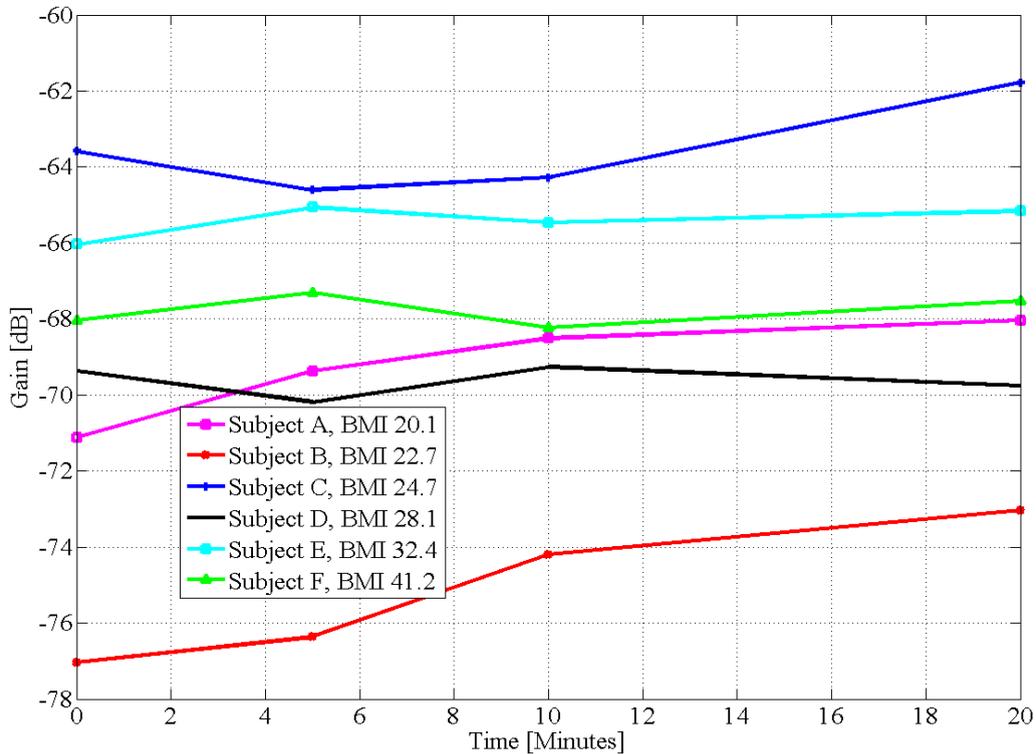
FIGURE 4.11: Changes in signal gain at 800 kHz as hydration occurs on 6 subjects after fluid intake

in atmospheric temperature, which affects perspiration, as well as individual anthropometric ratio and metabolic rates. The human body regulates the movement of water between the intracellular and the extracellular tissue spaces to maintain effective osmolarity of solutes within each compartment and to maintain a state of water balance. These dynamic variations underline a constant and varying change in the body impedance as the fluid level changes. A further water intake above obligatory water loss, in a healthy person, is usually excreted in dilute urine [107]. Hence, fluid intake after the state of water balance is reached does not cause hydration. Also fluid absorption rates vary per individual and peak rates are reached at different times.
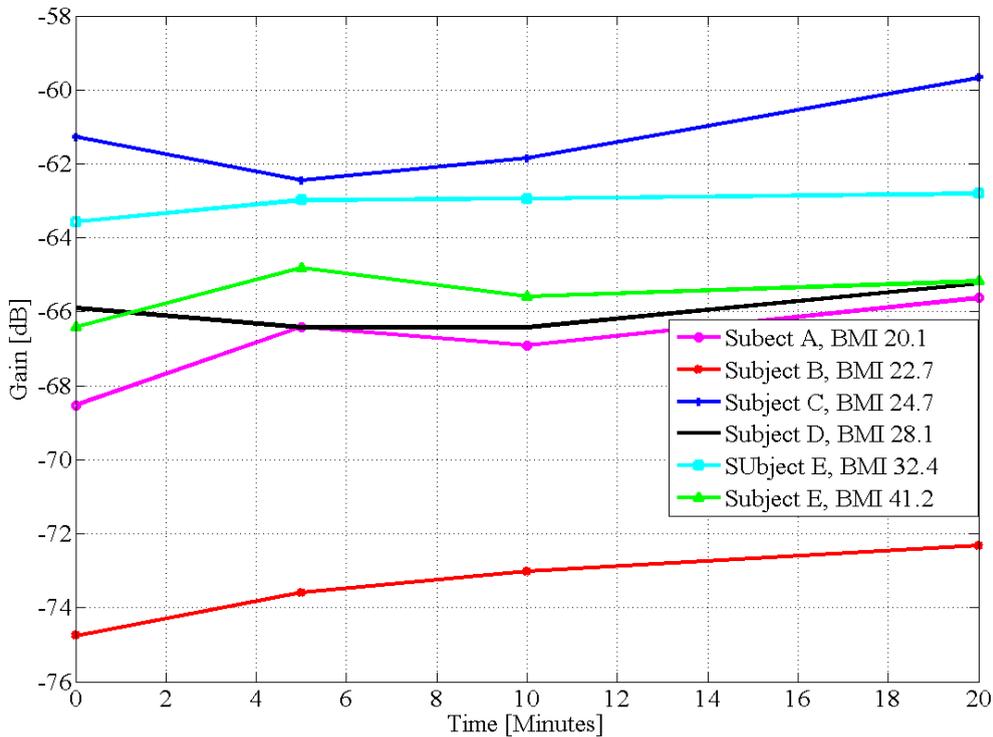
FIGURE 4.12: Changes in signal gain at 1 MHz as hydration occurs on 6 subjects after fluid intake

This chapter presents a model for evaluating human body hydration by measuring the changes in electrical signal attenuation as it propagates across tissues. This was modelled a time-dependent circuit of the body tissues that captures the fluid changes resulting from hydration and proposed a time constant τ which represented the dynamic metabolic activities of an individual that affects the body hydration rate. The study showed that smaller values of τ are associated with higher rates of hydration and larger values of τ with lower rates of hydration (Fig. 4.8). Since τ is representative of the time for complex processes of an individual metabolism, the observation on τ (Fig.4.8) coincides with Webb's findings [105] that subjects with

lower fat-free mass have higher time-dependent metabolic characteristic. This is exhibited in Fig.4.9 for example where τ is inversely proportional to θ and attenuation increases if the proportion of fat increases and decreases if the proportion of fat decreases. It also investigated the rate of change in attenuation at two separate frequencies 800 kHz and 1 MHz (Fig.4.9) which showed that when θ is 0.9 and τ is 5 the rate of hydration denoted by the rate of change in attenuation is 1.7 dB/minute and when θ is 0.6 and τ is 20 the rate of hydration is 0.5 dB/minute. At $\theta = 0.2$ and $\tau = 150$, the rate of hydration is slower. This matches physiological expectations where lower fat has a higher rate of hydration [24]. Fig.4.10 is the converse prediction of attenuation when τ is proportional to θ. At both 800 kHz and 1 MHz the result is not supported by empirical graphs (Figs.4.12-4.13) and not explained physiologically. Therefore, the parameter θ is related to BMI and BMI is known to be related to metabolic rate. For example, the Mifflin-St. Jeor equation [37] for resting metabolic rate (RMR) shows that metabolic rate is highly proportional to BMI. This means that θ and τ are interrelated.

The empirical measurements confirm this conjecture and follows the trend predicted in the theoretical model in Fig. 4.9 where τ is inversely related to muscle-fat ratio, θ. Since θ is BMI-related, then τ is related to RMR. Indeed, empirical results show subjects with higher BMI (low θ) having lower hydration rates (high τ) and lower BMI (high θ) having higher rate of hydration (low τ). This also

matches physiological expectations that high BMI (low θ) is associated with a higher proportion of fat and smaller body of water [106]. Thus the theoretical hydration patterns of people with different body mass indices in this model (Fig.4.9 and Fig.4.11) are supported by the empirical measurements (Figs.4.12–4.13). This means that under similar conditions and healthy states, individuals with high BMI would have longer time-dependent metabolic process τ, and lower rate of hydration than persons with low BMI. While θ is a measure of the muscle-fat ratio, τ is a complicated mixture of human body metabolic processes which affects hydration.

4.6 Summary

This chapter presented a new method of measuring the rate of hydration in real time by measuring the changes in the amplitude of a galvanically coupled signal passing through body tissue. It shows that real-time changes in signal attenuation can be predicted by a circuit model which incorporates the rate of hydration τ, and human anthropometric measures. This model will potentially assist in the development of new body fluid monitoring technologies which are essential for diagnosing fluid disorders and a tool for studying fluid requirements in the body. The next chapter will use this model to test hydration on a larger number of subjects as well as verify the sensitivity of a galvanic coupling circuit when used for assessing hydration levels.

Chapter 5

A Galvanic Coupled Intrabody Method for Assessing Hydration Rates

Assessment of human body composition is fundamental to the understanding of body physiological and metabolic processes. The body fluid is a dominant contributor to a person's weight, accounting for 60% of the total body mass of an adult. The body's fluid state is affected by both endogenous processes, such as body metabolism, and exogenous factors such as climatic changes, exercise, disease, and diet. Investigations into the hydration levels of the body are required because they help identify, or quantify ill-health and understanding poor exercise performance. It also includes the dangers of excessive fluid losses or inadequate intake which is associated with poor urinary function, cognitive ability and cellular metabolism [100]. The body fluid shifts between the intracellular and the extracellular tissues. This movement follows an osmotic gradient purposefully, to

maintain optimal concentrations of electrolytes and non-electrolytes in the cells, tissues and blood plasma. Two adverse conditions can be identified: hyperhydration in which there is excess water in the body and hypohydration or dehydration, when there is less than the normal amount of water to meet the body's requirement [100]. Accurate and easy estimates of hydration levels with cost effective technology are essential to assist policy makers in setting public health priorities [108], for doctors and clinicians to classify body fluid and cell mass conditions of healthy persons and patients with certain diseases [109] and for individuals, especially the elderly who are at higher risk of dehydration [9, 109]. Further research evidence on the elderly showed that older people who were dehydrated at admission were more likely to die than their counterparts [110].

An electrical signal passing through the human body is strongly affected by the size of the tissue, available fluid and its dielectric properties. It has been stated in chapter 2 that a characteristic of living tissue is its ability to store electrical energy [56]. At high frequencies, an electrical signal passing through the body becomes more difficult to manage as much of the energy radiates out. The frequency range for this research lies between 800 kHz to 1.5 MHz which lies within the β dispersion region which is related to the cellular structure of biological materials [56, 77] and can penetrate into the extracellular and intracellular tissue spaces. This also falls within the frequency range (5–1000 kHz) usually used for whole-body fluid analysis using bioimpedance spectroscopy [62]. As stated earlier, the electrical

conduction at this frequency is affected by the amount of water solute available in tissue spaces. Thus, by coupling a low frequency electrical signal galvanically on the body, the signal passing through the tissue will vary in attenuation to the changes in the water level. Consequently, the attenuation (negative gain) of the signal amplitude will depend on the composition of the tissue in terms of the amount of water present at the time, the tissue muscle-fat ratio and the input signal frequency. This research assumes that external factors, such as the type of electrode, the distance between the connecting electrodes and environmental conditions that may affect the measurements have been experimentally controlled following the steps outlined in the protocol design in chapter 3. Again, tests around joint areas were avoided due to the impact of limbs around joint areas when an electrical signal propagates through it [94].

In this research, the techniques for assessing hydration are classified as either intrusive or non-intrusive method. The intrusive method requires intravenous access to the body and is usually performed by trained personnels such as technicians, doctors or nurses. This system requires *in vivo* access and testing of the blood and is regarded as a later indicator of dehydration rather than a warning system that informs a quick preventative measure [111]. Physical signs such as urine colour observation, urine specific gravity test, and body weight changes are some examples of non-intrusive methods for assessing human body hydration [112]. This method gives oversimplified results

and poor sensitivity to changes in dehydration [113]. Wearable electronics that measure perspiration metabolites [114] can only estimate the physiological state of an individual's body fluid level under sweat and not without sweat secretion. Moreover, these techniques can not be used to target fluid disorder in a specific part of the body. However, following on the circuit model in chapter 4, this study will now verify experimentally the use of a galvanic coupled circuit as a simple method for assessing hydration rates as an easier wearable alternative. This shall be done by undertaking a composite testing of this proposed system alongside known urinary markers of dehydration. The rest of the chapter is organised as follows: Section 5.1 is the protocol designed particularly for the investigation in this chapter. Section 5.2 is a modification on the previous circuit model. Section 5.3 is a comparison of hydration measurement techniques and the intrabody signal propagation method. Section 5.4 is the result of the experiments and the summary in section 5.5.

5.1 Protocol Design

5.1.1 Experiment I: Hydration Testing

Twenty subjects, consisting of 12 males and 8 females aged between 23 and 45 years participated in this experiment. The baseline protocol in section 3 was divided into two sub protocols. Firstly, was

the hydration measurement protocol which is preceded by fluid abstinence after supper (latest 10.00 pm) till 10.00 am to induce dehydration as narrated in section 3.2. The level of dehydration on each subject was then measured by testing the specific gravity of a urine sample 1 collected prior to the start of the experiment. Because in this chapter, it was essential at this point to observe and quantify distinctive cases of tissue hydration as much as possible from the protocol the amount of water given to the subjects was increased from 500 mL in chapter 4 to 600 mL. Hydration was measured 5 min after intake because water appears in plasma and blood cells within 5 minutes after consumption [34]. In the second sub-protocol, the rate of dehydration was measured after the subjects had urinated following the consumption of 600 mL of water. It was assumed that other sources of water loss such as evaporation and metabolism contributed to the dehydration. The elapsed time to produce urine by each subject was also recorded and both measurements established the pre- and post-hydration states of each subject by the test of individual urine specific gravity of both urine samples 1, before fluid ingestion, and 2, after ingestion, with the hand held refractometer. The urine colour changes and body mass differences were recorded. The body mass of each participant was measured as W_0 before drink, W_1 immediately after drink and W_2 after urinating. A graduated cylinder was used to measure the volume of urine samples produced after the 600 mL of water intake. Both the hydration and dehydration measurements were measured by taking 5 measurements of

signal attenuation at 5 minute intervals, and the average was used. The change in post-drink weight and post-urination body mass was observed and recorded against the refractometer readings and the changes in signal attenuation. Subjects were not permitted to do rigorous exercises throughout the period of the experiment and all measurements were done at 10.00 *am* with average room temperature of $25 \pm 0.1^{o}C$ throughout to minimize the effect of temperature on body metabolism and evaporation.

5.1.2 Experiment II: Sensitivity Test By Empirical Measurement

Three subjects consented to participate further in this experiment. The experiment was performed on three random days and completed in three weeks. The control for the sensitivity test was set as the average value of the signal attenuation measured for a given period of time before fluid intake. In this study, sensitivity shall be defined as the smallest amount of water consumed that would cause the gain of a galvanic coupled intrabody signal propagating through the body to rise above the gain measured after fluid restriction and before fluid intake. Both the control and the sensitivity test were performed one after the other on the same day and under the same condition. To measure this, This time the pre-drink, post drink and the measurements after urinating was extended to 30 minutes. This is because in experiment I it was observed that, while many subjects indicated hydration within twenty minutes, it is important to observe if there

is any evidence of hydration occurring after 20 minutes in any subject. The 30 minute pre-drink measurement served as a baseline or control. The sensitivity test followed the process described in experiment I, with a variation in the amount of water consumed by the subjects ranging from 100 mL, 250 mL to 300 mL on each day of the experiment. The result is reported in section 5.4 for both hydration and dehydration stages.

5.2   Modification of the Circuit Model

Based on the proposed circuit model chapter 4, Fig. 4.1, equation 4.11 shows a variable fluid impedance given as

$$Z_F(t) = Z_{f0} - Z_w(1 - e^{-\frac{t}{\tau}}) \tag{5.1}$$

where t is the time for the change in impedance to occur, Z_{f0} is the impedance at time $t = 0$ just before hydration begins, t_f is time to reach the state of water balance, Z_w is the impedance resulting from the water consumed and the ratio $\frac{t}{\tau}$ is a characteristic that predicts the rate of hydration. τ is the time constant that characterises a particular individual. Given an initial fluid volume V_{ib} before hydration and V_w amount of fluid consumed, then the body will hydrate to a fluid volume V_b given as

$$V_b = V_{ib} + V_w(1 - e^{-\frac{t}{\tau}}); t = 0; V_b = V_{ib} \tag{5.2}$$

Therefore, It can be propose further, as a corollary, that the increase in the volume of body fluid, due to ingestion, will result in a gain in body mass by an amount equivalent to

$$wt_g = V_w e^{\frac{t}{\tau}} \tag{5.3}$$

where wt_g is gain in mass, since short term changes in body mass can be attributed to loss or gain of body water and $1mL$ of water has a mass of 1 $gram$ [54]. Again, by setting the anthropometric parameter contributing to the longitudinal impedance between the transmitter and the receiver electrode pairs as dependent on the cross-sectional area of the muscle-to fat ratio θ as given as section 4.2.4

$$\theta = \frac{A_m}{A_f} \tag{5.4}$$

where A_m and A_f are the cross-sectional areas of muscle and fat respectively to the distance between the transmitter and receiver electrode pairs. Let $0 < \theta < 1$, and high θ corresponds to low fat index (low BMI) and low θ corresponds to high fat index (high BMI) [115]. Now, BMI by definition is body mass (wt) divided by the square of the height (h^2), unit is (kg/m^2)

$$BMI = \frac{wt}{h^2} \tag{5.5}$$

Assuming no change in height, since all experimental protocols and measurements completed within 14 hours for each participating adult, then,

$$wt \propto BMI \tag{5.6}$$

and a change in wt due to hydration or dehydration will also result in a change in BMI,

$$\Delta wt \propto \Delta BMI \tag{5.7}$$

Therefore θ can be defined in terms of the changes in real body weight. It has been stated by Shirreffs [40] and Kavouras [116] that short term changes in body mass are associated with changes in human body hydration state. Since θ is inversely proportional to BMI [115], by these definitions

$$\Delta wt \propto \frac{1}{\Delta \theta} \tag{5.8}$$

or

$$\Delta wt\theta = k \tag{5.9}$$

Similarly,

$$\Delta wt \propto \Delta G \tag{5.10}$$

where ΔG is the change in gain (negative attenuation) of the electrical signal as a result of the change in the body hydration state, measured in dB/minute [115]. Δwt is related to θ by a proportionality constant k. If Δwt and θ are biological constants, then the

constant of proportionality k which affects the biological behaviour of the body under hydration is also biological and from equations 5.9 and 5.10, k is a metabolic process equivalent to τ defined in [115] which by the Mifflin-St. Jeor equation [37] is related to resting metabolic rate (RMR). Thus, the signal attenuation G in a galvanic circuit coupled through the human body can be expressed in terms of frequency f, time t, change in body weight wt, and a time-dependent constant τ [115] related to RMR.

$$G(f, t, wt, \tau) \tag{5.11}$$

This is similar to the transfer function, equation 4. 15 which indicated that individuals with high BMI will on average have lower hydration rates, will retain water longer in the body, and hence take longer to urinate. This relationship shall be used to empirically determine the attenuation per unit volume of water consumed.

5.2.1   Comparison with Simulation Prediction

Experiment II showed the minimum amount of water to be detected as 100 mL. This is calculated theoretically using the circuit model Fig.4.1 with the same parameters for the anthropometric measurements of the arm as in [102] in which a 50 mm arm radius has the thickness of body fluid layer as 23 mm estimated from [32, 103]. After consuming 100 mL of water, the maximum gain will occur when all the water consumed is retained within the 20 cm channel length.

This will increase the fluid layer thickness to 26 mm, so that for a 100 mL fluid in intake, $wt_g = 0.1\ kg$. Using the transfer function in equation 4.15, Fig. 5.7 is the simulation prediction of the sensitivity after consumption of 100 mL of water maximum signal gain occurring when the 100 mL of fluid is absorbed within the 20 cm transmission distance.

5.3   Results

Table 5.1 shows the effect of hydration on body mass and urine specific gravity from twenty subjects. Firstly, the weighing scale measurements differed slightly from expected results after 600 ml of fluid intake, i.e. $W_1 - W_0 \neq 600g\pm$ (uncertainty in measurement), in some cases. However, the changes in body mass after urinating, W_2, corresponded to the volume of urine produced for most of the subjects. Similarly, urine specific gravity (SPG) decreased from SPG1, measurement after fasting, to SPG2, measurement after fluid intake, as expected. This means that the fluid intake produced rehydration and lowering of the urine density. In a healthy person, the kidney regulates water balance by conserving water or getting rid of excess water relative to the requirement for a healthy water balance [8, 32]. When the amount of water consumed is large enough to reduce the concentration of blood plasma, a urine more dilute than blood plasma is produced; on the other hand, when the available water is too small to dilute the blood plasma concentration, a more concentrated urine

TABLE 5.1: Effect of Hydration on Body Mass and Urine Specific gravity (SPG) on 20 subjects

Subject	BMI (kg/m^2)	W_0 (kg)	W_1 (kg)	W_2 (kg)	Vol.of urine (mL)	Elapsed Time (mins)	SPG1	SPG2
A	29.3	87.60	88.15	88.10	75	118	1.021	1.018
B	20.8	56.70	57.30	57.10	190	61	1.030	1.007
C	24.2	72.55	73.10	72.60	250	56	1.025	1.010
D	31.4	83.15	83.55	83.15	340	76	1.016	1.010
E	33.1	93.40	93.90	93.50	305	111	1.017	1.008
F	28.5	75.65	76.15	75.30	360	95	1.020	1.005
G	23.5	62.80	63.20	62.80	330	60	1.016	1.010
H	31.4	101.00	101.60	101.40	150	70	1.020	1.015
I	26.4	81.65	82.10	81.85	220	99	1.023	1.014
J	36.5	104.25	104.75	104.35	325	125	1.021	1.016
K	22.9	76.00	76.55	76.30	100	70	1.019	1.016
L	23.7	73.50	74.20	73.80	300	51	1.020	1.007
M	25.6	95.30	95.70	95.50	200	60	1.031	1.007
N	25.9	78.60	79.10	78.80	175	86	1.024	1.010
O	42.5	122.8	123.30	122.25	400	155	1.011	1.010
P	24.4	64.00	64.50	63.90	250	77	1.021	1.005
Q	21.9	60.30	60.75	60.50	125	78	1.017	1.014
R	23.7	66.20	66.80	66.40	350	93	1.017	1.004
S	24.0	67.70	68.30	68.00	250	62	1.023	1.006
T	26.1	92.35	92.60	92.50	175	47	1.020	1.008

than blood plasma is produced [47]. Higher urine specific gravity values indicates higher dehydration. These instances are reflected in these results. Therefore changes in the urine specific gravity of the subjects can be matched with the differences in their body mass W_2 and W_0, and the measured attenuation after an intrabody signal is transmitted galvanically, as explained in the experiment procedure, for purpose of analysis. The average observation on the elapsed time between fluid intake and urination increases with increase in body mass index.

Subject specific cases were observed based on the assumption that

the water consumed was retained or excreted due to the body hydration state and the need to maintain homeostatic water balance [8, 32]. Case 1 Fig.5.1, $W_2 < W_0$ = Hyper hydration (example, subjects F and O). Subjects weighed less than the base line body mass after urinating and initial specific gravity is low. Subjects produced largest volume of urine after the specified drink. This suggests excess water in the subjects before the 600 mL intake,and thus $W_2 < W_0$. Absorption was observed after subjects had urinated. Case 2 Fig.5.2, $W_2 = W_0$ = optimal hydration (example, subjects D and G). Here the baseline body mass of the subjects were same as the mass after urinating and the subjects produced a large amount of urine. The fluid intake after the state of water balance was reached did not cause immediate hydration [115], therefore tissue absorption and de-absorption was not continuous and water intake did not cause significant change in signal attenuation. Fluid abstinence before $10.00am$ did not make these group of subjects dehydrate.

In case 3, $W_2 > W_0$ (a) Fig.5.3 Severe dehydration (subjects B and M). Subjects had urine specific gravity that reflected extreme water loss and the time taken to urinate was high compared to individual BMI. After urinating, dehydration occurred and was observed at different times.

The rest of the subjects were grouped as case 4 Fig.5.4, $W_2 > W_0$, mild dehydration, based on the urine specific gravity reading SPG1 measured before fluid intake. Among this group, the maximum rate of hydration was 0.44 dB/minute occurring in subject N, SPG1 =

1.024 while the minimum rate occurred at 0.02 dB/minute on subject Q, SPG1 = 1.017. After urination, the maximum rate of dehydration occurred at 0.40 dB/minute with subject L, SPG1 = 1.020 while the minimum rate was 0.11 dB/minute occurring in subject C, SPG1 = 1.025.

Fig.5.5 is the graph of the subject's BMI against time taken for individual metabolic process to complete and process urine. The figure shows that BMI is related to the time it takes to process urine, and also related with the rate of hydration and dehydration in accordance with previous findings [115]. Fig.5.6 depicts the empirical result of the sensitivity of a galvanic coupled signal to detect hydration due to body fluid intake, while Fig.5.7 is the simulation result for a 100 mL maximum fluid absorption with the proposed circuit model.
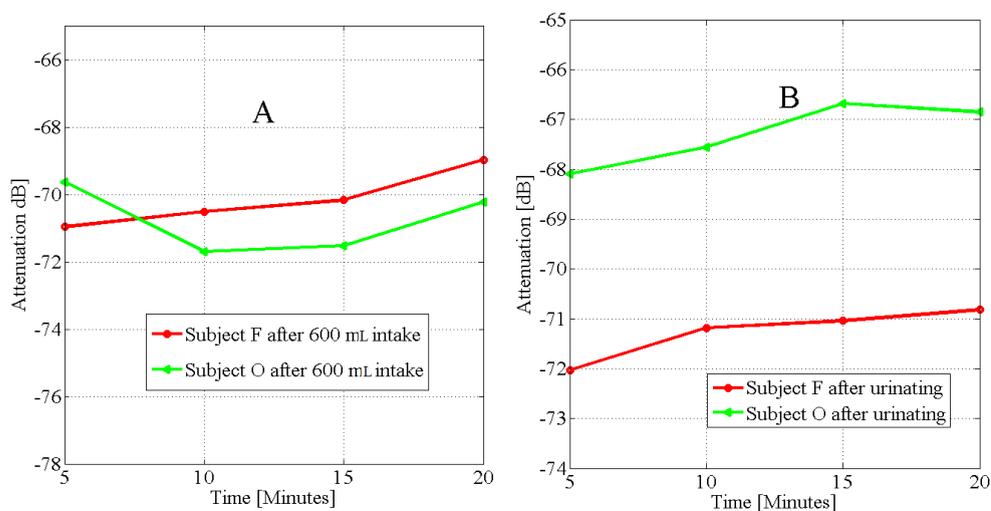
FIGURE 5.1: Graph of the rate of hydration A, and dehydration B, after 600 mL fluid intake on subjects F and O observed at 1.2 MHz, $W_2 < W_0$, subjects were hyper hydrated by the protocol

Subjects D, K, and L, height 166 cm, 182 cm and 176 cm respectively participated in the control and sensitivity tests.
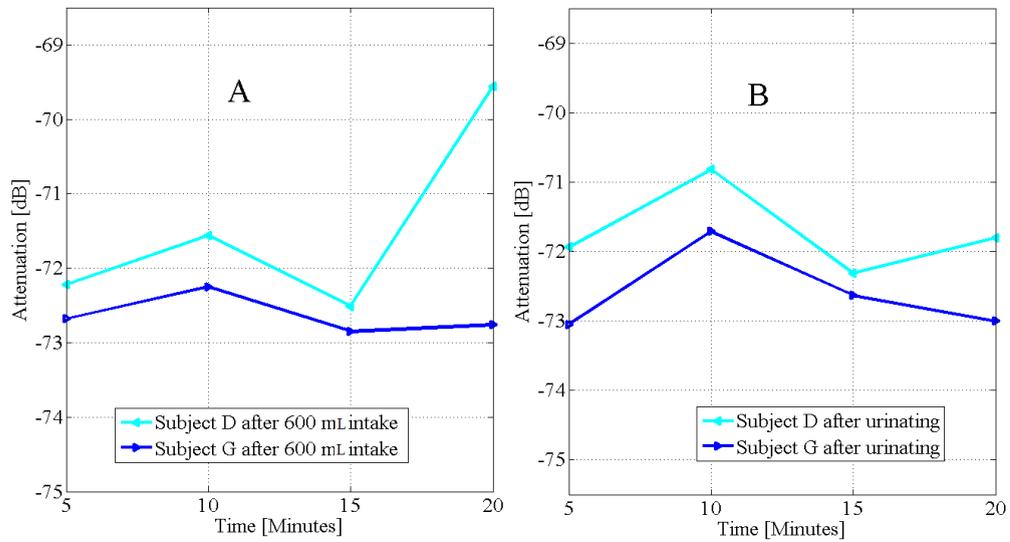
FIGURE 5.2: Graph of the rate of hydration A, and dehydration B, after 600 mL of fluid intake on subjects D and G at 900 kHz, $W_2 = W_0$. Subjects were normally hydrated by the protocol
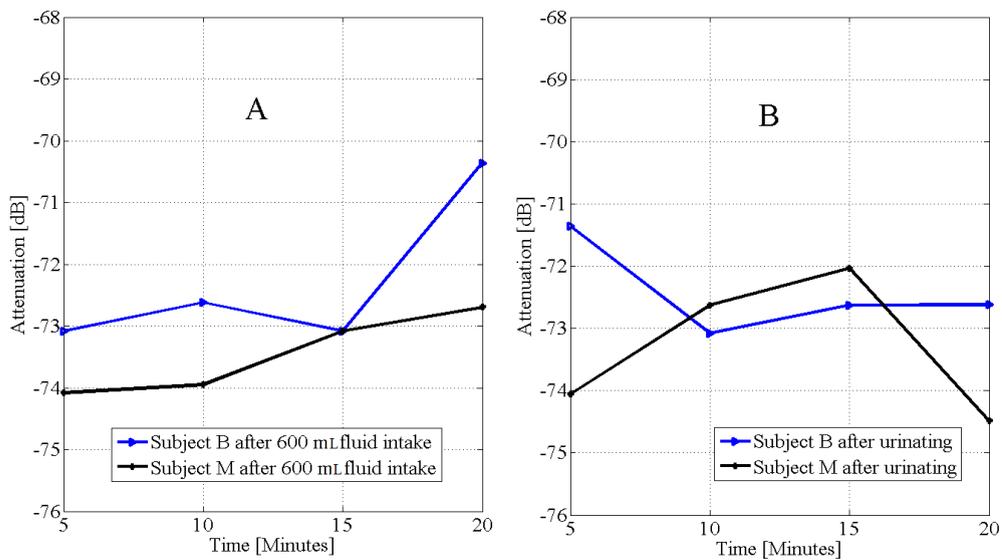
FIGURE 5.3: Graph of the rate of hydration A, and dehydration B, after 600 mL of fluid intake on subjects B and M observed at 900 kHz, $W_2 < W_0$. The protocol produced severe dehydration on subjects B and M. After urinating, subject B dehydrated and stopped after 10 minutes while subject M started dehydration after 15 minutes. Both showed longer period of re-absorption
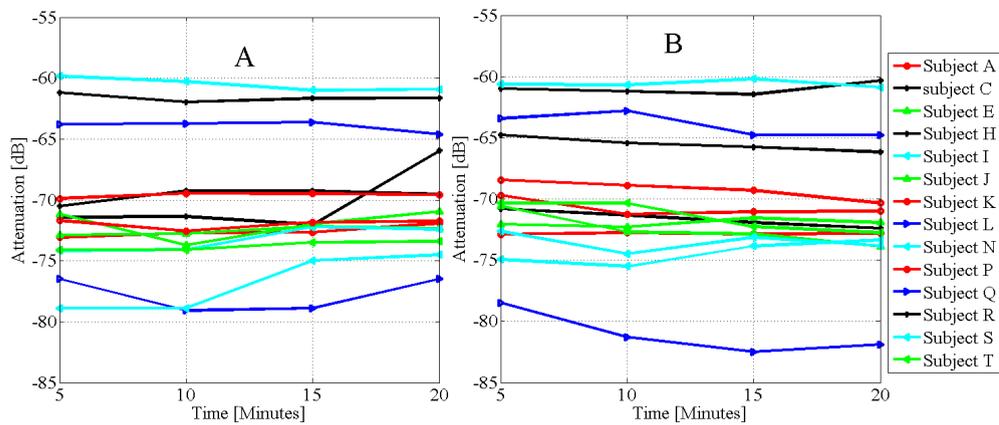
FIGURE 5.4: Graph of the rate of hydration A, and dehydration B, after 600 mL of fluid intake on subjects A,C,E,H,I,J,K,L,N,P,Q,R,S and T observed at 900 kHz. $W_2 < W_0$. The protocol produced mild dehydration on subjects
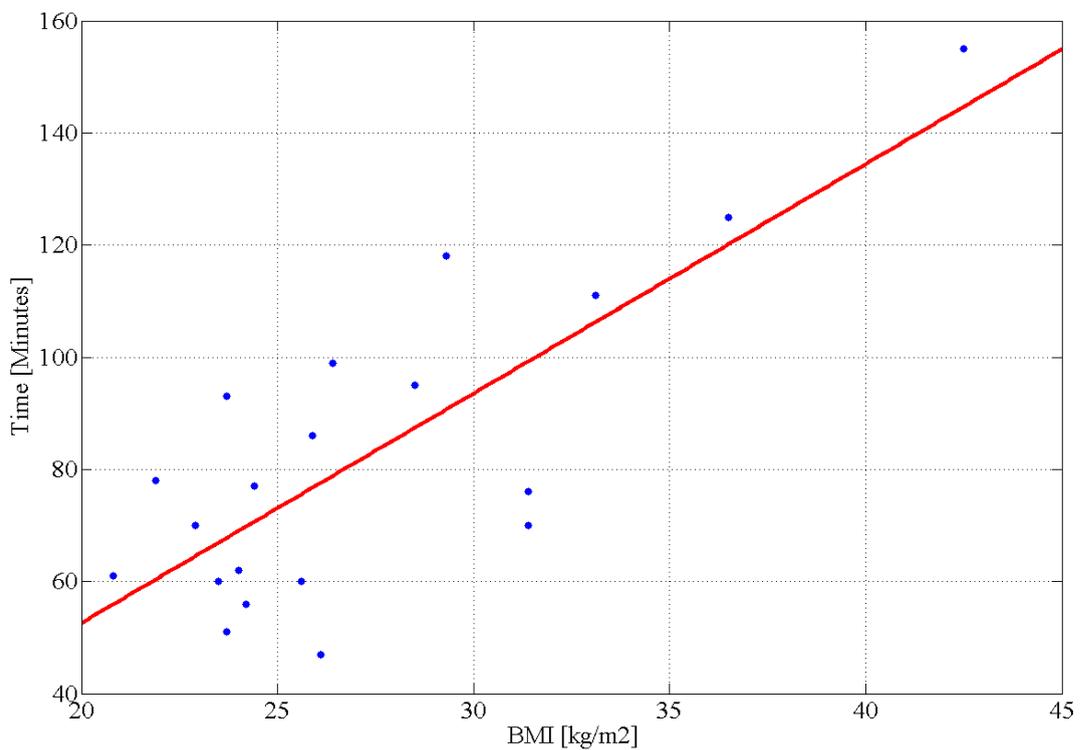
FIGURE 5.5: Graph of the relation between subject specific body mass index (BMI) and the time it took to urinate after consuming 600 mL of water

TABLE 5.2: Control and Sensitivity test, day I

Subject	BMI	W_0	W_1	W_2	SPG 1	SPG 2
	(kg/m^2)	(kg)	Fluid intake $= 100\ mL$ (kg)	(kg)	before drink	after drink
D	29.83	82.20	82.30	82.20	1.014	1.014
K	23.58	78.10	78.20	78.20	1.022	1.021
L	23.44	72.60	72.70	72.60	1.023	1.021

TABLE 5.3: Control and Sensitivity test, day II

Subject	BMI	W_0	W_1	W_2	SPG 1	SPG 2
	(kg/m^2)	(kg)	Fluid intake $= 250\ mL$ (kg)	(kg)	before drink	after drink
D	29.65	81.70	81.90	81.80	1.016	1.012
K	23.81	77.95	78.20	78.10	1.025	1.018
L	23.27	72.10	72.40	72.20	1.021	1.010

TABLE 5.4: Control and Sensitivity test, Day III

Subject	BMI	W_0	W_1	W_2	SPG 1	SPG 2
	(kg/m^2)	(kg)	Fluid intake $= 300\ mL$ (kg)	(kg)	before drink	after drink
D	29.90	82.40	82.70	82.55	1.014	1.014
K	23.81	78.00	78.20	78.10	1.023	1.021
L	23.34	72.30	72.60	72.35	1.018	1.007

Tables 5.2 - 5.4 represent the control and sensitivity results. The tables show that for the three random days tested, the variation in the subjects' body mass was below 2 kg and the change in body weight corresponded to the quantity of water consumed by the subjects on each day of the experiment. The weight also decreased after the subjects had urinated and the urine specific gravity dropped after water was consumed.

The control and sensitivity test Fig.5.6, show the variation between repeated measurements on 3 subjects at 3 random days for the
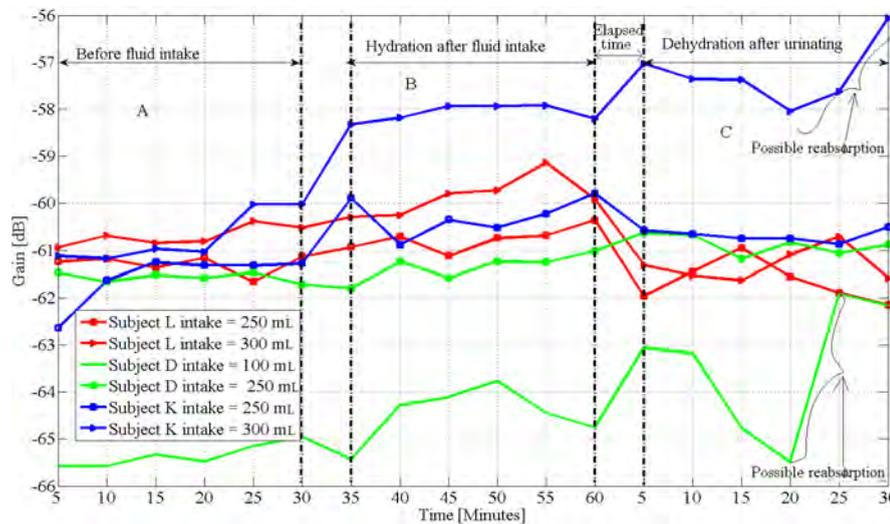
FIGURE 5.6: This graph represents the sensitivity test for an intrabody signal measured on 3 subjects for 3 random days at 900 kHz, before drink (A), after drinking 100 mL, 250 mL and 300 mL amounts of water (B), and after urinating (C). From 5 minutes - 30 minutes is the average attenuation measured before drink. After drink, the attenuation was measured from 35 - 60 minutes. The gap between measurement after drink and urination is a variable time that elapsed before each subject urinates. After urinating, the attenuation was again measured from 5 minutes to 30 minutes. Measurements were taken at 900 kHz and subject specific parameters are: Subject D height = 166 cm and BMI = 29.83 on day 1, Subject K height = 182 cm and BMI 23.81 on day 2, and subject L height = 176 cm and BMI 23.34 on day 3.

first 30 minutes and the hydration as the subjects consume different amounts of fluid. The standard deviation between average data points on the reported data for the three subjects used for control or base line values ranged from 0.08 - 0.18 dB for subject D, 0.47 - 0.58 dB for subject K and 0.21 - 0.22 dB for subject L. The deviation from the baseline on the subjects after 100 ml intake are, subject D increased to 1.31 dB while subjects K and L increased by 2.75 dB and 0.77 dB respectively after 250 mL. As the amount of water consumed increased, hydration increased, evidenced by the increase in signal gain. For example, subject D, increased by 4.4 dB when the amount consumed increased from 100 to 250 mL. After consuming
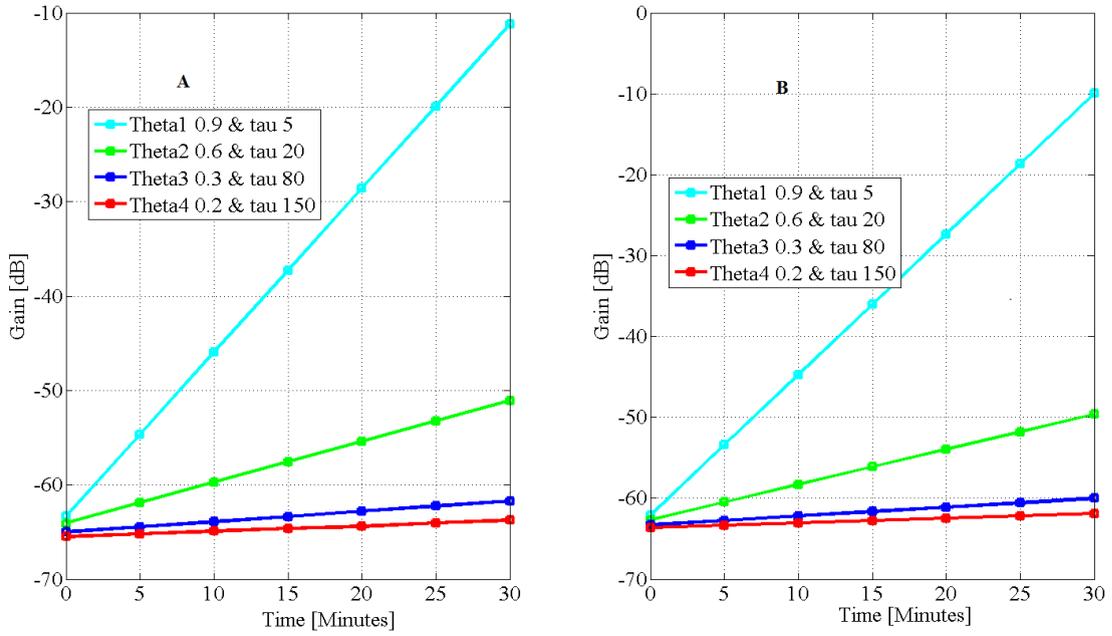
FIGURE 5.7: Simulated sensitivity of a galvanic coupled intrabody at 900 kHz at
different combinations of τ and θ. A is before 100 mL fluid intake and thickness
= 23 mm, while B is after 100 mL intake, assuming maximum concentration
of this amount within 20 cm inter-electrode distance, fluid thickness = 26 mm.
Predicted increase in attenuation are 1.5 dB for $\tau = 20$ and $\theta = 0.6$, and 1.70
dB for $\tau = 80$ and $\theta = 0.3$ and 1.91 dB for $\tau = 150$ and $\theta = 0.2$

300 ml, the change in signal gain from 250 mL to 300 mL on sub-
jects K and L were 1.57 dB and 0.64 dB respectively. The measured
attenuations after drink and after urination fall within base line val-
ues which were measured after fluid abstinence and before intake.
The variation in the degree of measured attenuation between the 3
subjects is a result of individual specific body composition, initial
hydration state and specific body metabolism.

The simulation results show that for maximum absorption of 100
mL within 20 cm channel length the gain for different combinations
of τ and θ are: $\tau = 20$ and $\theta = 0.6$ gain is 1.5 dB, and when $\tau = 80$ and $\theta = 0.3$ gain is 1.71 dB and for $\tau = 150$ and $\theta = 0.2$ gain
is 1.91 dB. The theoretical dependences of the sensitivity are the

individual metabolic function τ, muscle-fat ratio, an equivalent of body mass index represented as θ and initial fluid level. Empirically, it is suspected that a contributor to the sensitivity is height, which was not considered in the simulation. Others are subject specific endogenous processes or metabolism and initial body fluid state.

5.4 Discussion

Considering table 2.1, (summary of body fluid assessment techniques), it can be deduced that a good way to assess the performance of a new method is by comparison with known markers of hydration, especially methods that are most commonly used in clinical settings. The goal here is for a simple technique that can fit easily into wearable electronics for individual's day to day hydration measurement. Therefore it is of necessity to compare the new system with some of the hydration indices in table 2.1.

5.4.1 Urine Colour Indices

Urine colour is attributed to the level of concentration of soluble waste substances in the urine. Higher concentration of soluble wastes may indicate a level of dehydration because the human body, under healthy state, constantly tries to maintain homoeostatic water balance. Thus, with a loss of body water urine colour changes in proportion to the level of dehydration and darkens as dehydration increases

or as the concentration of soluble waste increases in the urine. Armstrong et al [48] found that urine colour can, in some, cases indicate a person's hydration state because the changes in urine colour coincides with other techniques for measuring human body hydration such as plasma osmolality and urine specific gravity. However, there is no standard urine colour index to match a given magnitude of an individual hydration or dehydration state especially when little changes occur that are not easily noticeable by observation. This research wants to overcome this by using the attenuation of a propagating electrical signal amplitude which changes as the body hydrates or dehydrates. The sensitivity test showed that up to 1.30 dB can be detected in the arm when 100 mL of water is consumed, an amount that would not be easy to observe as a significant change in the colour of a urine. Moreover, urine colour can change due to sickness, drugs and supplements.

5.4.2 Change in body mass

As stated previously human body mass contains 60-70% water [32] which dynamically changes with time. And short term changes in body mass are often used to quantify water gain or loss in clinical measurements, consequently, this study will use the differences in body mass to deduce the amount of water retained in the body and to relate it to changes in the intrabody signal passing through the body. However, it is obvious that as the body hydrates only a proportion of the amount consumed comes to the arm where the measurement

is occurring. The sensitivity test investigated the different amount of water required by each subject before it can be detected in the arm. Results show that the signal attenuation decreased as the body weight increased by the fluid consumed and increases as the body weight decreased due to loss of water, Fig.5.6.

5.4.3 Refractometry

With the loss of body water, urine specific gravity increases due to an increase in the concentration of urinary waste products [39]. The concentration is determined by the amount of urinary waste per unit volume of urine. Urine specific gravity measures the ratio of the density of urine relative to the density of pure water. A specific gravity greater than 1 means the fluid is denser than water [51]. Urine specific gravity measurements usually range from 1.002 to 1.030. This study shows that subjects with high SPG value usually had high hydration rates with the galvanic coupling method. However, SPG measurements are not reliable because, like urine colour changes, they are affected by sickness, drug and supplements.

5.4.4 Intrabody Signal Propagation Method

Chapter 4 has demonstrated that the proposed intrabody signal propagation method uses time varying changes in the galvanic coupled signal amplitude to predict hydration rates. In this experiment, the decrease in attenuation (hydration) or increase (dehydration)

during each observation matched the changes in the body weight recorded for all 20 subjects as well as the changes in the urine specific gravity and the visual observations of the urine colour.

Four distinct cases of human tissue hydration was observed. By defining W_2 as body mass after urination and W_0 as mass before drink, the observed cases are grouped as following:

Case 1: $W_2 < W_0$ = Hyper hydration

Case 2: $W_2 = W_0$ = Optimal hydration

Case 3: $W_2 > W_0$ = Severe dehydration

Case 4: $W_2 > W_0$ = Mild dehydration

The graphs show that hydration started and ceased at different times in each subject, 30% recorded hydration levels 10 minutes after drink while 25% recorded hydration levels at 5 minutes after the drink. Subjects with high SPG1 usually had higher rates of hydration while subjects with very low SPG1 had lower rates of hydration. Thus different individuals have different hydration rates and the specific gravity reading indicated an individual's initial dehydration state. Similarly, the amount of water consumed was too much for some subjects and just appropriate for others. These observations explain why the state of water balance is reached at different times and are dependent upon the initial body fluid level in each subject as shown in chapter 4, equation 4.12. Fig.5.5 shows that individuals with high BMI longer time-dependent metabolic processes, and lower rates of

hydration than persons with low BMI in line with the previous findings in chapter 4. The measured hydration rates lies within the range bounded by the mean value of the attenuation on an individual's baseline measurement. From Fig.5.6 the signal amplitude changed in proportion with the quantity of water absorbed by the tissues which was predicted theoretically in equation 5.2. Similarly, fluid consumption and losses caused changes in the body mass measurement in line with equations 5.2 and 5.3. The variations in the signal amplitude were caused by absorption of water by the tissues which caused an increase due to hydration or reduction in body weight due to loss of water by evaporation, metabolism and urination. The signal amplitude increased more prominently as the volume of fluid consumed increased. For instance, within the first 5 minutes, when the amount of water consumed by subject D increased from 100 mL to 250 mL, the signal attenuation decreased from -65.5 dB to -61.9 dB . The attenuation decreased as the amount of water consumed increased. This was reversed in the dehydration cycle measured after urination.

A review of bioimpedance and plasma osmolality methods (refer to table 2.1), indicates that intrabody methods, as shown in this experiment, have an improved sensitivity to detecting body fluid changes. Plasma osmolality measures the amount of osmoles (Osmol) of solute per kilogram of solvent (osmol/kg) and is regarded as one of the best methods of estimating dehydration level [27]. The osmolality of blood increases with dehydration and decreases with increasing

hydration. A problem with this method, however, is that it does not track body fluid changes below 3% of body mass [40, 117], table 2.1. This implies that for a 70 kg adult, plasma osmolality could only detect changes in body fluid level until the water loss causes up to 2.1 kg of body weight. The technique presented here is sensitive to 100 mL of fluid intake or 0.1 kg change in body weight due to hydration. Similarly, the bioimpedance method tracks total body water from estimates of extracellular and intracellular fluid volumes [118]. However, while there are valuable correlations between bioimpedance methods and isotope dilution [119], in 2007, Armstrong [27] argued that bioelectrical impedance methods may not be accurate when the amount of water loss is less than 800-1000 mL (table 2.1). The sensitivity test showed the intabody method is sensitive for up to 100 mL of fluid intake or water loss as observed in subject D. The sensitivity test suggests that sensitivity increases with decrease in height. Also the magnitude of the signal attenuation from theoretical simulation changed from -65.98 dB to -63.27 dB for $\tau = 80$ and $\theta = 0.3$, similar to empirical measurements Fig. 5.6. The simulation result, Fig.5.7, predicted a lowering of signal attenuation by 1.50 dB to as much as 1.91 dB depending on individual anthropometric ratio and body metabolism, when 100 mL is optimally absorbed in the arm. The empirical measurement detected 1.31 dB on subject D, BMI 29.83 kg/m^2 and height 166 cm. Thus the empirical measurement is evidenced by simulation results. However, a challenge to the

empirical measurements was that majority of the participants became uncomfortable remaining still during the 20 minutes period of the experiment, which was required to minimise movement artefacts and external effects. Thus only three subjects consented to participate in the control and sensitivity test when it was extended to 30 minutes of measurements. In addition, the initial hydration state of the subjects with SPG readings should not be the gold standard [27] for assessing human body hydration state.

5.5 Summary

This chapter demonstrates that galvanic coupled intrabody signal propagating through the body can measure the rate of hydration with sensitivity as low as 100 mL of fluid intake or loss. The system is non-invasive and hygienic. The study with 12 male and 8 female volunteers, shows that the rate of hydration does not depend on gender but on individual metabolic requirement, initial hydration level and body mass index. Hydration rates are not constant but are affected by the immediate body physiological state and metabolic equilibrium which in turn determines how long it takes to change from one fluid state to another. To use this technique, a baseline amplitude of the signal variations of an individual is required. This capacity makes it potentially applicable for monitoring changes in total body fluid level, targeted body fluid disorder and the response of tissues when monitored for targeted fluid level variations.

The next chapter will investigate a further use of galvanic intrabody coupling for detecting developments or evidence of fluid disorder using pathologically diagnosed lymphoedema patients as subjects.

Chapter 6

Application

6.1 Introduction: Assessment of Lymphoedema as an Example of Body Fluid Disorder

In this chapter, the research presents clinical experiments that test the application of a galvanic coupling technique for detecting lymphoedema. Lymphoedema is a disease associated with fluid stagnation caused by abnormal functioning of the lymph that leads to swelling of the body due to accumulation of tissue fluid on the affected area [120]. This thesis demonstrates that a galvanic coupled signal propagating along a lymphoedema affected limb could capture changes in the fluid level or fluid flow through the variance in attenuation of the propagating signal with time. The results show that signal attenuation on a unilateral lymphoedema affected limb changed in time by 0.16 dB/minute while the signal attenuation on a contralateral healthy limb varied by 1.83 dB/minute. The variance in attenuation with time could indicate flow rate. This would

imply that fluid accumulation would slow down the flow of body electrolytes up to half the rate on an unaffected contalateral part of the body. Monitoring these changes by observing the average rate of change of a galvanic coupled signal attenuation on the affected body part could potentially be used for diagnosing early developments of oedema in the body and for evaluating recovery in response to treatment procedures.

6.1.1 Characterising Lymphoedema as Body fluid Disorder

As stated earlier, lymphoedema is a chronic disorder of the lymphatic system whereby lymphatic vessels and/or nodes malfunction and accumulate fluid and other minerals in the surrounding tissue spaces [121]. The disorder results in imbalance between the interstitial fluid production and its transport leading to an unusual swelling of one or more limbs or the affected body part [120]. In lymphoedema disease, leaked fluids containing high molecular protein from lymphatic vessel remain stagnant under the skin, and, if undiagnosed early and left untreated can lead to progressive inflammation and damage to the affected body part [122, 123]. Lymphoedema is progressive in nature; early diagnosis is important because it helps timely intervention mostly because there is not yet a gold standard definition of treatment outcome [124, 125] and efforts are mainly focused on management, to minimize swelling, restore functionality of the affected area of the body, and prevent potential complications associated with

the disease [126]. It is now known that, early detection and appropriate management can alleviate the symptoms and slow its progression [127].

6.1.2 Diagnostic Methods

A 2003 report estimated a 0.13 - 2% increase in chronic lymphoedema over previous years with greater incidence among women [128]. Current estimates suggests about 8000 new cases of lymphoedema in Australia every year [121]. The indices draws attention to the diagnostic techniques since at present there in no complete cure, unless otherwise those diagnosed at the earliest stage of development which may be alleviated by good management techniques [16]. Some of the techniques for diagnosing lymphoedema include:

i Physical examination and investigation of the history of the affected area.

ii Limb volume measurement

iii Bioelectrical Impedance Spectroscopy method

iv Blood test and genetic test analysis

v Imaging techniques

Lymphoedema can co-exist with other medical conditions that causes swelling [129]; consequently a blood test is also used to examine the existential cause of oedema. The tests is to identify other infections

of the accumulated fluid, which makes it not an early diagnostic method but a pin-point validation of an existence of lymphoedema or other fluid disorder. For example, when infection is suspected on a swollen body part, a further blood test is performed to check the presence of a parasite [129]. Genetic testing is used for patients who have been diagnosed with primary lymphoedema [126]. The purpose of this test is to determine the presence of genes associated with diseases that causes lymphoedema and to be able to provide proper genetic counselling for the patient and to verify the probability of its re-occurrence along family lines. Some imaging techniques used for diagnosing fluid accumulation include, magnetic resonance imaging (MIR), computed tomography (CT) and ultrasound [16]. These techniques are more reliable although not available for day-to-day individual assessment. Moreover, they require real clinical training to operate whereas cancer treated patients and patients who have had axillary lymph dissection which are at higher risk of lymph dysfunction or blockage [129] need a system for out-of-hospital checks in order to determine early development of fluid disorder. A common practice among clinicians for patients at risk of lymphoedema is limb volume measurement [130]. Limb volume measurement at best would help to ascertain the severity of lymphoedema and to assess progress in treatment management. Treatment with multi-layer inelastic lymphoedema bandaging (MLLB), for instance is also monitored through limb volume measurement [130]. It is considered to

be present if the swollen limb is more than 10 % greater than contralateral unaffected limb and cannot be applied in a bilateral limb lymphoedema [127]. Therefore limb volume measurement has limited success and deviation from baseline are not easily determined. It is also prone to human error. A closely related practice for tracking sequential changes in circumference of an affected limb is the circumferential limb measurements which is criticised because it has no standard protocol [16]. Another frequently used method in practice is bioelectrical impedance assessment [127]. The bioimpedance analysis method relies on body impedance at 50 kHz. A 50 kHz current would not penetrate completely into cells due to high resistance of the outer layer of the skin, thereby limiting its reach on ICW compartments. Thus it can at best estimate ECW, and a prediction of total body water is usually better on a healthy person and not on persons with fluid disorder. Moreover, human tissue has both resistive and reactive components since cell membrane capacitance contributes significantly to the effective impedance of electrical signals across tissues [33]. Due to the capacitive behaviour of cell membranes, an appropriate frequency range is required for measuring ECW resistance and a higher frequency to penetrate into ICW. Jaffrin *et al* [65] has suggested <5 Mhz. Thus, bioimpedance spectroscopy (BIS) was proposed as improvement over bioimpedance analysis methods. BIS operates at multiple frequencies and assumes a 5 cylinder model of the human body, taking into account the effect of non-conducting tissues embedded in both the ECW and ICW

tissues that significantly contribute to the overall impedance of the body. And by calculating the extracelluar impedance separately from the intracellular impedance, the total body water can be estimated [131] and a comparison with a baseline can be used to estimate the presence of oedema. However, it uses the impedance of the body at a particular instant to estimate fluid level of which it has shown in chapter 4 that tissue impedance is variable. It is also difficult to be used correctly to target fluid changes on a specific part of the body. This means that a method that can detect the earliest accumulation body fluid is required to assist quick diagnosis and monitoring fluid levels on specific areas of the body. In laboratories, advanced technologies using imaging techniques are used to scan lymph vessels and nodes [132], but these require high laboratory skills. Because the tissue fluid in lymphoedema affected part of the body is stagnant, the objective in this chapter is to advance through testing the use of galvanic coupling intrabody signal propagation to detect very slow or stagnated movement of body fluid in a particular part of the body for the purpose of identifying the earliest development of oedema on tissues.

6.1.3   A New Diagnostic Method

The efficacy of this proposed system for diagnosing lymphoedema can be determined. First is to carry out preliminary measurements aimed at predicting the development of fluid accumulation. It has been discussed in chapter 2 how human tissue can be used as the

transmission medium in a galvanic coupling signal propagation. Electrodes are used as the communication interface to send a signal from the transmitter to receiver thereby reducing the chances of infection during use. The nature of the electrodes and the skin determine the contact impedance to the signal flow. For an individual, the electrode-skin contact impedance can be determined as shown in section 3.3.3. Therefore the propagating signal leaving the skin contact interface changes by the underlying tissue conditions. The proposed circuit model in chapter 4, Fig.4.1, models the propagation of the signal as a function of frequency, electrode-skin contact impedance [70], tissue dielectric properties [79], and the human body physiological parameters [72] as well as the dynamic changes in body fluid and internal metabolic function of an individual [37].

Tissue conductivity is related to the movement of the body electrolytes. Table 4.1 lists of some of the body electrolytes which stimulates the flow of electrical current. The impedance of the body, varies in proportion to changing body fluid resulting from hydration or dehydration. From equation (4.11), as the body fluid level rises, the tissue impedance increases by

$$Z_F(t) = Z_{f0} - Z_w(1 - e^{-\frac{t}{\tau}}) \qquad (6.1)$$

where t is the time for the change in impedance to occur, Z_{f0} is the impedance at time $t = 0$ just before hydration begins, t_f is the time to reach the state of water balance, Z_w is the impedance resulting

from the water flowing in into the tissues and the ratio $\frac{t}{\tau}$ is a characteristic that predicts the rate of flow. τ is the time constant that characterises a particular individual.

If the fluid level stops increasing or is relatively stagnant, the observed changes in attenuation (negative gain) would also be relatively invariable at that particular instant and in that part of the body.

Thus, after time interval $t(i)$

$$Z_F(t_1) \simeq Z_F(t_2) \simeq ... \simeq Z_F(t_m) \tag{6.2}$$

is the impedance for non-varying fluid level. Movement of body fluid due to hydration or dehydration causes tissue impedance to decrease or increase. Thus, if the body fluid flow is partial or insignificant over a period of time, the change in impedance $Z_F(t)$ would be partial and if the fluid flow stops, it would follow a static fluid model and tissue impedance $Z_F(t)$ would be constant.

Therefore, if $[X]$ is denoted as a set of the signal gains measured, from $t_1...t_m$ time intervals, and 5 measurements per $t(i)$ interval. The average gain measured per $t(i)$ interval is

$$\mu = \frac{\sum\limits_{i=1}^{n} X_n}{n} \tag{6.3}$$

where $n = 5$; and $E[\mu_m] = \rho$ average value of the mean across time $t_1...t_m$ at a particular frequency. If σ is modelled as the variation across time from $t_1...t_m$

$$\sigma = \sqrt{\frac{1}{m}[(\rho - \mu_1)^2 + (\rho - \mu_2)^2 + ... + (\rho - \mu_m)^2]} \qquad (6.4)$$

$$\sigma = \sqrt{\frac{1}{m}\sum_{i=1}^{m}(\rho - \mu_i)^2} \qquad (6.5)$$

Let the value of σ give a time value of the signal variation in attenuation due to fluid flow, then a high value of σ means a high deviation of the attenuation about the mean, which signifies normal fluid flow, while a low value of σ indicates a low movement of tissue fluid on the measured area of the body. This proposition shall be investigated on both healthy and lymphoedema affected subjects. Since the response of each tissue component to electrical stimulation depends on the tissue's dielectric properties, the conductivity would vary in accordance to the changes in ionic concentrations or movement at that frequency either by excess of body water relative to body solute, or deficiency of body water relative to body solute [133]. This is because conductivity is proportional to the movement of the body electrolytes. If body fluid is not circulating properly, for example, due to lymphatic damage, protenous substances accumulate under the skin. However, if the fluid is flowing, internal metabolic processes and physiological process would cause these substances to flow freely. The average change in time of the conductivity would vary partly due to intermittent hydration occurring or dehydration and or processes leading to body water homeostasis balance. Thus, theoretically, a stagnant body fluid would have relatively lower deviation

from the mean value of the attenuation observed in time, assuming other variables are also constant. Ideally, this implies that the average rate of change of signal attenuation can be used to diagnose, identify or monitor fluid accumulation or discharge in human body tissue inflammations, such as lymphoedema.

6.2 Experiments

6.2.1 Clinical Measurements on pathological lymphoedema participants

Subjects were recruited in collaboration with Lymphoedema Association of Victoria (LAV) with flyers advertised in LAV's news letter and placements at TSL clinic. Protocol 2 described in section 3.2 was used for this experiment. Two groups of people were required: unhealthy and healthy participants. Participants were given time to read and sign the ethics form prior to the commencement of the experiment. The lyphoedema affected participants are required to provide medical evidence of a pathologically diagnosed lymphoedema on the limb. Four subjects labelled L1–L4, who were pathologically diagnosed with unilateral lymphoedema, on the arm and one one on the leg participated in this study. Measurements were conducted at TSL clinic, a lymphoedema clinic specializing in compression garments. The healthy participants labelled H1–H3 had no previous diagnosis of lymphoedema and from observation had no swollen limb

and checked circumferential limb measurements (CLM). The circumferential limb measurements were measured at fixed intervals on 3 non-consecutive days selected randomly according to the availability of the subjects. The contralateral positions of the limbs of the affected subjects were also measured by marking both arms at 10 cm intervals from wrist to the head of humerus. Two major areas were classified, the mid point of the ulna as the lower arm and the upper arm as the mid point of the humerus on each participant. The subject with lympoedema on the leg was measured along the longus muscle. Participant's body mass, height and lymphoedema diagnosis as well as current medication were recorded.

6.2.2   Clinical Measurements : healthy participants

A similar protocol was adopted for healthy volunteers except the choice of the venue for the experiment. Participants were to choose between the university laboratory and their home. The condition for using the living room is to turn off all electronic appliances and any other potential sources of noise. The average room temperature was maintained at $25 \pm 0.1^{o}C$ throughout the experiment, as explained in section IV. Subjects H1–H3 participated in this test. The body mass and CLM were recorded on the first day, ensuring that the same position was measured on both arms similar to participants with lymphoedema.

6.2.3 Galvanic Coupling Measurements

The galvanic coupling measurement procedure was the same for both healthy and unhealthy participants. Measurements with the galvanic coupling were taken on the second day of contact. Measurements were taken first without fluid restriction on day 2 and after drink following fluid restriction on day 3. Only circumferential limb measurement and signing of ethics form was done at day 1. Measurement on a lymphoedema participant with the galvanic circuit is as shown in Fig.6.1. All the subjects followed the description given in sections 3.2 and 3.4. Again, body movements were strictly restricted to be as still as practically possible. The signal gain was measured 5 times at 3 minutes interval and the average was used. Subject L4 was excluded on the third test which required fluid restriction due to high blood pressure medication [134]. Fluid abstinence increases blood plasma concentration [47] which might affect blood pressure. On the third day, subjects were asked to abstain from fluid after supper till 10.00 am. Their limb circumference and weight were again measured and water was given them to drink. Five minutes was allowed for water to circulate into the body before measurement begun [34]. This time, because of the initial fluid restriction, measurements were recorded for 20 minutes only to encourage concentration and measurement of both arms were taken simultaneously.
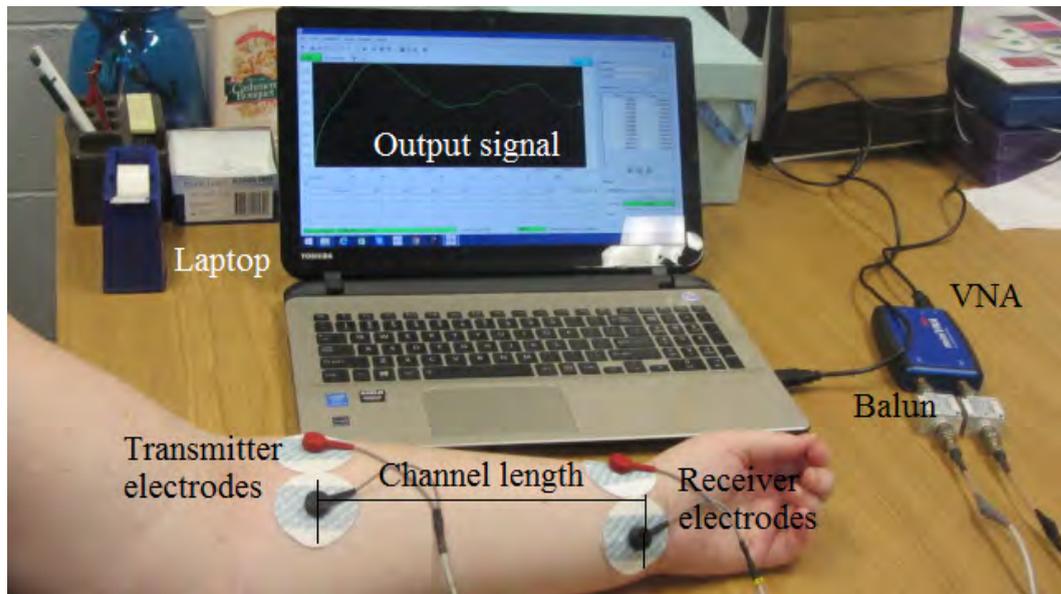
FIGURE 6.1: Measurement of galvanic coupled signal attenuation on the affected left arm of a lymphoedema subject

6.3 Results

Figure 6.2 is the result of the circumferential limb measurements on the lymphoedema affected participants measured within 6 weeks on three random days, while Fig.6.3 is a similar measurement on the healthy subjects. Subjects L1 and L4 have unilateral lymphoedema on the left arm, while L2 has unilateral lymphoedema on the right arm. Subject L3, however, has unilateral lymphoedema on the left leg. From the data in the figure, CLM on L1 (BMI = 31.7 kg/m^2) was 13.0% greater in limb size on the upper limb while the lower limb was larger by 29.6% on the first day of measurement. Repeated measurements on the second and third day showed little difference in circumferential measurements and BMI. The affected limb consistently had a more than 10% increase in limb size on the upper limb and 29% on the lower limb in comparison with measurements

Subject	Affected limb	Day	BMI (kg/m^2)	Affected (CLM)		Unaffected (CLM)		% Difference	
				upper (cm)	lower (cm)	upper (cm)	lower (cm)	upper (cm)	lower (cm)
L1	left arm	1	31.7	39.0	35.0	34.5	27.0	13.0	29.6
		2	31.5	39.2	35.0	34.5	27.0	13.6	29.6
		3	31.4	39.0	35.4	34.3	27.4	13.7	29.1
L2	Right arm	1	31.3	37.0	25.0	29.0	22.5	27.5	11.1
		2	30.5	36.8	25.3	29.0	22.7	26.8	11.4
		3	29.9	37.0	25.4	29.2	22.3	26.7	13.9
L3	Left leg	1	29.1	43.5	28.8	38.0	26.0	14.5	10.7
		2	29.2	43.6	29.2	38.1	26.3	14.4	11.0
		3	29.2	43.4	28.9	38.0	25.6	14.2	12.9
L4	Left arm	1	24.5	31.5	26.0	27.0	23.7	16.7	13.0
		2	24.4	31.5	26.0	27.0	23.2	16.7	12.0
		3	24.4	31.6	26.0	26.0	22.8	21.5	14.0

FIGURE 6.2: Circumferential limb measurements on lymphoedema affected participants

Subject	Day	BMI (kg/m^2)	Left limb		Right limb		% Difference	
			upper (cm)	lower (cm)	upper (cm)	lower (cm)	upper (cm)	lower (cm)
H1	1	29.2	31.5	27.4	29.6	26.0	6.4	5.3
	2	29.0	31.5	27.4	29.7	26.0	6.1	5.3
	3	29.1	31.6	27.5	29.6	26.0	6.7	5.7
H2	1	23.1	28.2	24.8	29.7	26.0	5.3	4.8
	2	23.6	28.6	25.0	30.2	26.3	5.6	5.2
	3	23.4	28.0	25.8	29.4	27.0	5.0	4.6
H3	1	24.1	30.4	25.5	29.5	25.0	3.1	2.0
	2	24.1	30.4	25.6	29.5	25.0	3.1	2.2
	3	24.2	30.5	25.2	29.5	25.0	3.4	2.0

FIGURE 6.3: Circumferential limb measurements on healthy participants

on the contralateral limb. This ratio agrees with the standard classification for lymphoedema diagnosis [16] (the presence of oedema on a swollen limb requires a reading more than 10% greater than contralateral unaffected limb).

Similar observations were made on all the other subjects as well as difference in their body mass indices. L2 with BMI 30.0 kg/m^2 has an affected upper limb greater than the contralateral limb by 27.5 % while the lower limb is greater by 11.1 %. L3, BMI 29.1 kg/m^2 has an affected left leg greater in size than the contralateral right leg by 22.3%. Circumferential measurement on subject L4, BMI 24.5 kg/m^2 was 16% greater than the upper limb, while the affected

lower limb was 13% more. Again, a repeat of the procedure on the healthy subjects, Fig. 6.3, provided a maximum ratio of 6.7 % on the upper limb and 5.3% on the lower limb of subject H1, BMI 29.0 kg/m^2 while on subject H2, BMI 23.4 kg/m^2, the upper right limb is greater than the left limb by 5.4% and the lower limb is greater by 4.8%. Both results reconfirm earlier pathological diagnosis of oedema on the lymphoedema participants and the absence of oedema on the healthy participants.

Fig.6.4 depicts the result of the galvanic measurement on lymphoedema affected subjects without fluid restriction and Fig.6.5 shows the result after fluid restriction from 10.0 pm to 10.0 am and ingestion of water. Similarly, Fig. 6.6 is the galvanic measurement on healthy subjects without fluid restriction. The result shows that limbs affected with oedema had higher signal gain or lower attenuation than the unaffected limbs without bias by fluid restriction and subjects with high BMI had higher signal attenuation on the unaffected limbs than the unaffected limbs of subjects with low BMI. Signal attenuation before fluid restriction on the pathologically diagnosed limbs of subjects L1–L4 is between -65.0 dB and -68.0 dB while the attenuation measured on the unaffected limbs are between -69.0 dB and -74.0 dB. Similar measurements on both arms of the healthy participants were between -71.0 dB and -76.0 dB.

Table 6.1 shows a comparison of the difference between the circumferential limb measurements between the affected and the unaffected

TABLE 6.1: Comparison of circumferential limb measurements (CLM) and average difference in galvanic signal amplitude between the affected and unaffected lower limbs

Subject	BMI kg/m^2	Percentage change in CLM	Difference in Gain dB
L1	31.5	29.6	8.0
L2	29.8	27.5	6.0
L3	29.2	14.5	1.2
L4	24.4	13.0	5.0

	Healthy participants		
	BMI kg/m^2	CLM left and right	Difference in Gain dB
H1	29.1	5.6	3.0
H2	23.5	3.8	4.0
H3	24.1	2.0	2.0

limbs and the average difference in the gain of a galvanic signal amplitude passing through the unaffected and the affected limbs. Subjects with high difference in CLM also had high difference in the magnitude of the signal and subjects with high BMI had higher difference in the amplitude of the signal between the affected and the unaffected limbs.

An observation on the rate at which the signal attenuation changes could be used to indicate flow rate. The attenuation varied at a near steady rate of 0.05 dB/minute in the first 25 minutes measured on L1, with maximum change occurring between 25–30 minutes at the rate of 0.26 dB/ minute on the lower limb of the lymphoedema affected arm. Similarly, the corresponding measurement on the healthy limb, of the same subject showed a higher change in the signal gain with rates doubling what was observed on the affected arm at 0.42
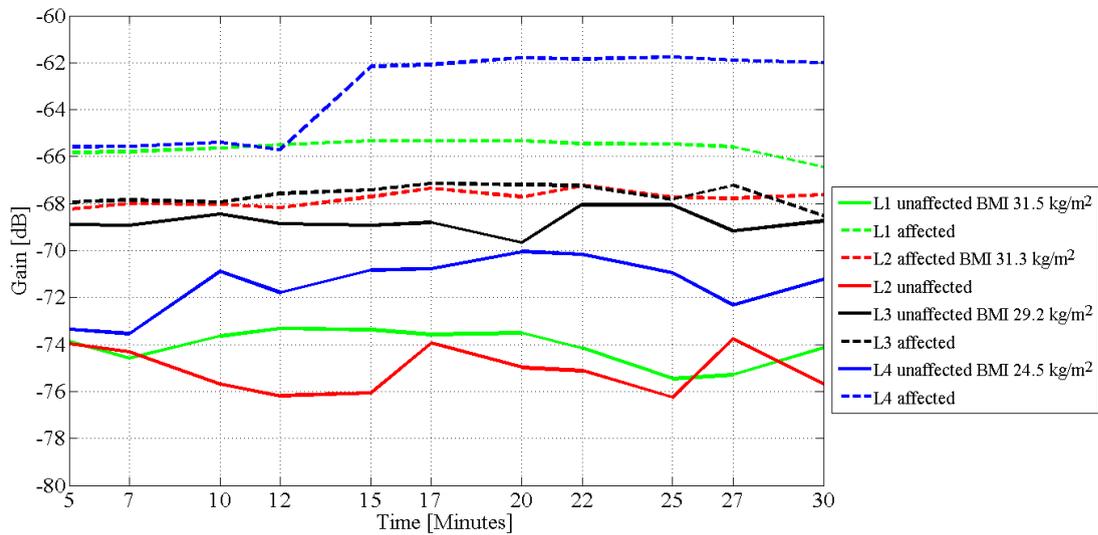
FIGURE 6.4: Graph of galvanic coupled signal attenuation at 900 kHz, on both arms of a lymphoedema affected subjects without fluid restriction

dB/minute. Similar observation was also made on subject L2. Measurements on the affected leg (subject L3) showed the signal attenuation changed slowly at the rate of 0.07 dB/minute on the affected leg while the rate on the unaffected leg is about 56% more than the rate on the affected leg similar to observations on the arm. The observation on the healthy subject shows constantly varying signal gain on both hands with an average rate of 0.27 dB/minute on both subjects. Subject L4 was not permitted to continue in further test because he was medically at risk. The result on subject L4 (Table 6.2) suggested possible effect of the medication on his measurement.

Fig.6.5 is the graph of the time varying changes in signal gain with the galvanic measurement recorded after fluid restriction and intake of water. The difference between the graphs of the affected and the unaffected limbs are clear and explainable. Measurements started 5 minutes after fluid intake and lasted for 20 minutes. Fluid restriction
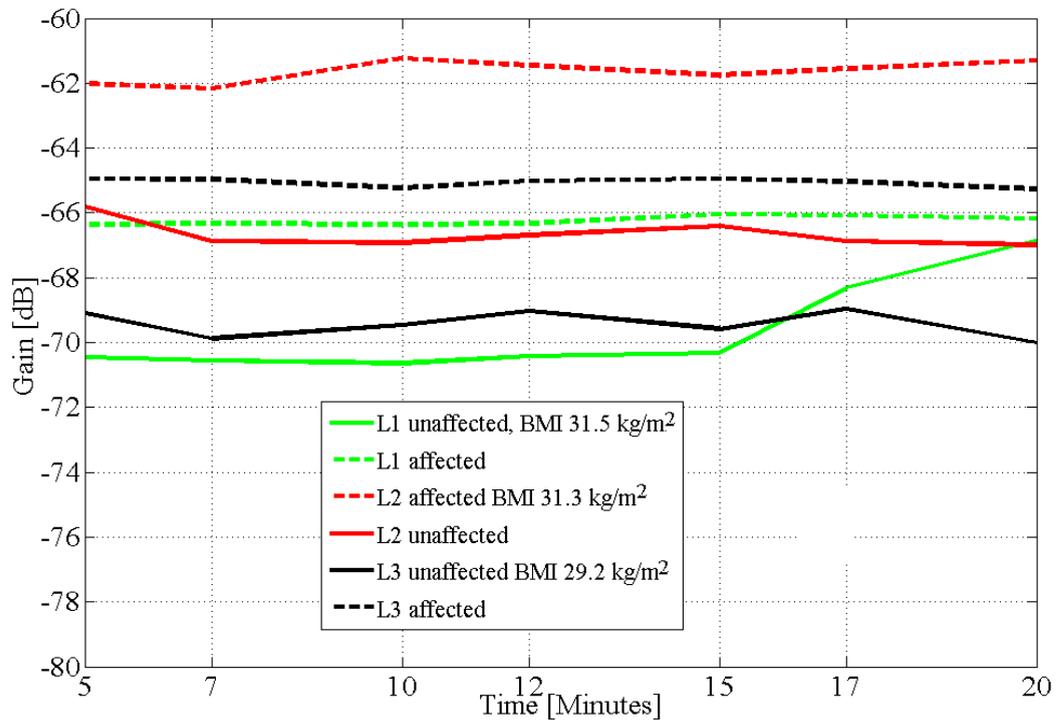
FIGURE 6.5: Graph of galvanic coupled signal attenuation at 900 kHz, after fluid restriction and intake of water, on both arms of lymphoedema affected subjects
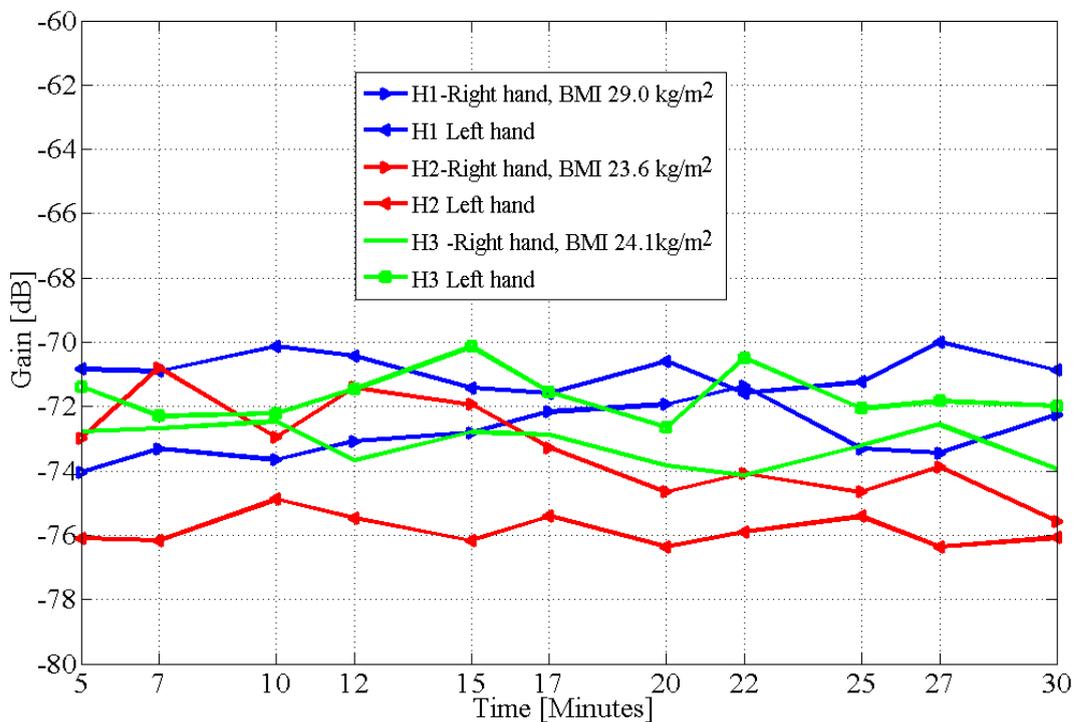
FIGURE 6.6: Graph of galvanic coupled signal attenuation at 900 kHz, on both arms of healthy subjects without fluid restriction
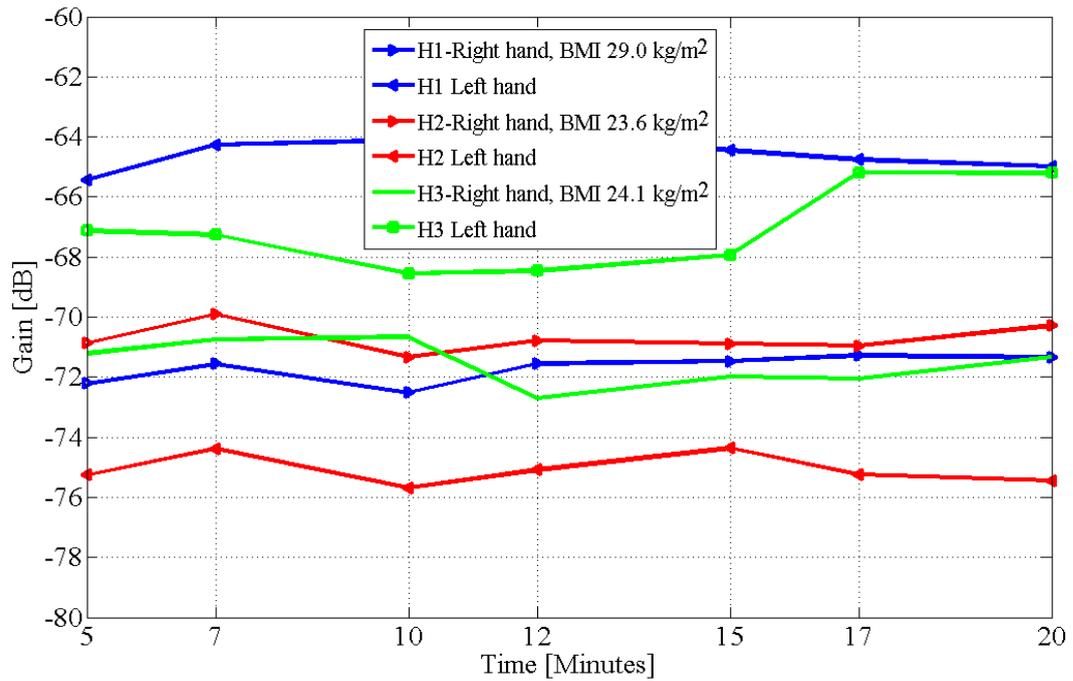
FIGURE 6.7: Graph of galvanic coupled signal attenuation at 900 kHz, after
fluid restriction and fluid intake, on both arms of healthy subjects

before consumption was to induce initial dehydration which would
accelerate absorption and possible flow after fluid intake. Again,
the result showed almost steady rate on the affected lower limb and
1.83 dB/minute on unaffected arm of subject L1. Subjects L2 and
L3 recorded 0.37 dB/minute and 0.15 dB/minute on the affected
limbs which increased to 0.82 dB/minute and 0.44 dB/minute on the
unaffected limbs respectively. Measurements on the healthy subjects,
(Table 6.3) was 1.22 dB/minute and 1.32 dB/minute on the left and
right limb of subject H1 and 0.59 dB/minute and 0.72 dB/minute
on subject H2 and 0.66 dB/minute and 0.87 dB on H3 respectively.
The hydration trends of healthy limbs follow previous findings in
chapters 4 and 6.

TABLE 6.2: Deviation in time of propagating galvanic signal on lymphoedema affected participants, day 2, without fluid restriction, and 3, after fluid restriction and ingestion of water

Subject	Day	BMI kg/m^2	Affected σ (dB/minute)	Unaffected σ (dB/minute)
L1	2	31.5	0.26	0.81
	3	31.4	0.16	1.83
L2	2	30.5	0.24	0.93
	3	29.9	0.37	0.82
L3	2	29.2	0.34	0.60
	3	29.2	0.15	0.44
L4	2	24.4	1.93	1.25*
	3	–	–	–

TABLE 6.3: Deviation in time of galvanic signal attenuation on healthy participants, day 2, without fluid restriction and day 3, after fluid restriction and ingestion of water

subject	Day	BMI kg/m^2	left limb σ (dB/minute)	Right limb σ (dB/minute)
H1	2	29.0	0.52	0.82
	3	29.1	1.22	1.32
H2	2	23.6	1.16	1.54
	3	23.4	0.59	0.72
H3	2	24.1	0.48	0.69
	3	24.2	0.66	0.87

Tables 6.2 and 6.3 depict the deviations in time. After fluid restriction and ingestion of water, the rate of change in the signal gain was still more than 100% slower than the unaffected arm. Contrarily, the rate of change in the attenuation of the signal on the healthy subject, H1 for example, was 1.22 dB/minute on the left limb and 1.32 dB/minute on the contralateral part, about 55% reduction in difference in comparison with the lymphoedema affected participants. Subject L4, beside lymphoedema, who was treated for high blood pressure with Amlodipine; a drug that widen blood vessels [134], was excluded from the remaining experiment. The gain on his affected

arm without fluid restriction was -65.59 dB while the unaffected arm was -73.36 dB as proposed. However, the change in attenuation at each point of measurement did not fit expectations and could have been altered by the Amlodipine medication.

6.4 Discussion

Galvanic coupled intrabody signal attenuation (negative gain) changes with human body fluid state as demonstrate in this work. However, in human body fluid disorder such as lymphoedema, there is a notable fluid retention caused by leakage or lymphatic vessel damage that leads to accumulation or stagnation of fluid on the affected body part [135]. This chapter demonstrates further that signal attenuation on a unilateral lymphoedema affected limb is low and the rate of change of the signal attenuation with respect to time is also small, indicating blocked or unnatural fluid flow. The circumferential limb volume measurements on both arms and legs of lymphoedema affected subjects showed more than 20% increase in volume of the swollen limb compared to the healthy contralateral limb. This phenomenon was pathologically diagnosed and characterised as unilateral lymphoedema four and a half years ago on subject L1, 3 years ago on subjects L2 and L4, and sixteen years ago on subject L3. Subjects' medical record showed that the difference in volume between the left and right limbs were a result of fluid retention on the upper and lower left limb. The accumulation implies that there is

an imbalance between fluid production and circulation [121] which was investigated on the affected arm and leg of subjects diagnosed with lymphoedema with the galvanic coupling circuit. The quantitative difference between the circumferential limb measurements and the difference in signal amplitude between the affected and the unaffected arms, table 6.1, shows that subjects with a high difference in circumferential limb measurement also had high difference in the average value of the measured signal amplitude. This implies that in a unilateral lymphoedema, the technology could also measure the severity of fluid accumulation. The mean deviation of the signal attenuation in time for the pathologically diagnosed subjects as given in table 6.2 shows 0.26 dB/minute and 0.16 dB/minute without and with fluid restriction, respectively, on subject L1. The deviation on the contralateral healthy right arm were 0.81 dB/minute and 1.83 dB/minute respectively. By defining σ as the time variation of the signal attenuation, it was theorized that a low value of σ means partial or stagnant fluid flow, while a high value of σ implies high deviation from the mean which suggests movement of body fluid. Results obtained with and without fluid restriction show low values of σ on the affected arm and high value of σ on the unaffected contralateral arm on the subjects with unilateral lymphoedema. Values between 0.15 dB/minute and 0.37 dB/minute are low and were measured on subjects that has lympoedema while values between 0.60 dB/minutes and 1.83 dB/minute are high and occurred on subjects who were not pathologically diagnosed with lymphoedema. Table

6.3 is the flow rate on the left and right arm of unhealthy subjects, which differed by more than 20%. Thus, both results could indicate partial fluid flow on the affected lower limb with flow rates half the unaffected arm (Figs.6.4 and 6.5). Low flow rates are associated with high BMI values and high flow rates with low BMI as discussed in chapters 4 and 5. It is generally known that lymphoedema disease is associated with inadequate flow of body fluid [124, 125]. The subjects in this study, use a compression garment as a treatment therapy to massage the affected tissue and discharge accumulated fluid on the affected limb [135, 136]. Responses to treatments such as this need to be monitored. The empirical measurements in this study detected evidence of fluid overload on the lower limb of each subject with attenuation rates half on the affected arm contrary to concomitant changes observed on healthy subjects without oedema on any of the limbs.

6.5 Summary

In this chapter, the use of galvanic coupled signal propagation to assess fluid accumulation on a unilateral lymphoedema affected limb was introduced. The results show that fluid accumulation can slow the rate of change of galvanic signal attenuation at least twice less than the rate on an unaffected arm of the same subject and can

increase if the subject dehydrates as was observed in the measurements on day 2. The theoretical predictions matched empirical measurements and show that body fluid flow can be monitored using galvanic coupled signal attenuation and the measured differences in attenuation over a period of 20 minutes can be used to observe body fluid flow which is essential for diagnosing early development of body fluid disorder such as lymphoedema and for monitoring responses to treatment. Future work will investigate larger group of pathological subjects.

Chapter 7

Conclusion and Future Work

7.1 Conclusion

Body composition assessment techniques are used to evaluate the proportions of human body tissue namely, fat and fat-free mass for appropriate determination of healthy and unhealthy body states. Human body tissue is non-homogeneous, multi-faceted and complex; therefore, different techniques are used to evaluate the different body compositions relative to another. Of the different tissue compositions, water is an important and major constituent of body cells, tissues and organs. Human brain and heart consists of 75% water, muscle 70% water, lungs 83% water, and skin 64% [137]. A loss of 10% of body water puts one at a considerable risk of death [9]. Without immediate compensation, a loss of more than 2% of body water causes reduction in brain performance, metabolic activities, thermoregulation, cardiovascular functions and body coordination

[9]. Current techniques for assessing human body hydration are either limited in accuracy and sensitivity or complex, expensive, high risk and bulky.

This thesis presents a simple, inexpensive and sensitive technique for monitoring hydration rates in real time which can be integrated into a wearable device. To this end, a circuit used for galvanic intrabody signal communication was adopted and modified to incorporate a time-dependent component which models fluid changes in real time to evaluate hydration using the attenuation of a signal coupled galvanically to the body as it propagates through tissues. The results obtained show that the method can be used for assessing not only human body hydration but could offer additional benefit in diagnosis of body fluid disorders.

This thesis will strengthen the significance of studies in body composition assessment and has provided a scientific response to the initial research question presented: "can signal attenuation of a galvanic coupled intrabody signal be used to indicate body fluid levels?"

This was substantially tested, first by examining in details important literature relating to the various techniques currently used for evaluating changes in body fluid levels. Current methods are either complex and expensive or simple with limited accuracy especially when the change in hydration is mild. This study also reviewed historically the evolution of galvanic intrabody signal communication and the circuit model used for communication through tissues which

had gaps arising from a common assumption that tissue impedances are static. This observation influenced this study and by correcting it helped to develop an electrical circuit model capable of assessing body fluid changes as an electrical signal propagates across human tissues when connected galvanically through the body.

In order to achieve the main objectives of this thesis, the search used materials and methods which were essential to design systematic protocols to determine if the proposed galvanic coupling circuit could be used to show that signal attenuation passing through the body indicates changes in body fluid levels and if similar coupling can be used to diagnose the progression of fluid accumulation in a unilateral lymphoedema.

In chapter 4, the thesis presented a new research outcome which showed a new method for measuring the rate of hydration in real time by the measuring the changes in the amplitude of a galvanically coupled signal passing through body tissues, designed, modelled and tested empirically on six subjects. The model proofed that real-time changes in signal attenuation can be predicted by incorporating measures such as τ which was defined as a time constant that characterises an individual's specific metabolic function of the body that affects the rate of hydration and θ as human body anthropometric ratio that is related to body mass index. The rate of hydration varied from 1.73 dB/minute, for high θ and low τ to 0.05 dB/minute for low θ and high τ which had comparable results with empirical measurements from different BMI, ranging from 0.6 dB/minute for

22.7 kg/m^2 down to 0.04 dB/minute for 41.2 kg/m^2. These results showed that the galvanic coupling circuit modelled in this research can predict changes in the volume of the body fluid with individuals with high BMI predicted to having higher time-dependent biological characteristics, lower metabolic rates and lower rates of hydration. The discoveries in this chapter led to further interest in searching for potential applications of this model to assist in various other areas involving body fluid monitoring and diagnosis of critical disease conditions associated with fluid accumulation.

Chapter 5 showed a sensitivity test of the model by simulation and empirical measurements and the potentials it has in response to different hydration states by comparison with other hydration measurement methods. The results from the experiments conducted showed that the galvanic coupled intrabody signal propagating through the body can measure the rate of hydration with sensitivity so low as to detect hydration occurring after 100 mL of fluid intake or loss while still retaining its non-invasive and hygienic characteristic. Studies with 12 male and 8 female volunteers in this section showed that the rate of hydration depended more on individual metabolic requirements, initial fluid level and body mass index and that hydration rates are not constant but are affected by the immediate body physiological state and metabolic equilibrium which in turn determines how long it takes to change from one fluid state to another. However, the chapter noted that the technique requires a measurement of a baseline value to be used as a reference for evaluating progression

or retrogression of hydration of an individual. Furthermore, because the circuit was adopted from an existing intrabody communication system, it can be easily integrated into existing wearable device in a cost effective way.

Finally, a study of a clinical application of the galvanic coupling technology for biomedical diagnosis was conducted which involved tests on patients who have been pathologically diagnosed with lymphoedema on either a hand or a leg. The results showed that firstly, fluid accumulation can slow flow rate to at least half the rate on an unaffected arm of the same subject and can increase highly if the subject dehydrates. Secondly, that body fluid accumulation can be monitored if a signal is propagated through galvanic coupling and that differences in the signal attenuation over a period of 20 minutes can be used to observe body fluid flow. This is essential for diagnosing early development of body fluid disorder such as lymphoedema and for monitoring responses to treatment procedures.

7.2   Challenges of Body Fluid Assessment

Body Composition assessment has been an on-going research for many decades. Investigation continues due to improvements in technology and the need for precise evaluation of tissue proportions for the purposes of health and medical care. Moreover the criteria for

choosing a particular method for evaluating body composition is usually tailored to a specific challenge. Therefore not one method addresses all. The complexity of the body and the inhomogeneity of tissues usually results in statistical assumptions often used in body composition estimation such as specific densities of each of the different tissues; whether they are identical from person to person and the way they are distributed in the body. Despite the existence of different methods of human body hydration assessment, empirical measurements do not usually conform to proposed models in all classes of people, and subject-specific anatomical parameters are difficult to account for. The majority of the proposed models do not fully address people by geography and race, nor by physiological structure and metabolism. Another important factor that has not been adequately emphasized in the literature, despite its role in body composition assessment, is the coupling mechanism by which instruments are connected to the body. The contact impedance between the assessing devices, usually electrodes and the human skin changes by body type, duration and weather; there is not yet sufficient research or models that thoroughly explained the electrode-skin impedance created which impacts on the measured output.

A primary aim of body composition assessment is to provide precise evaluation of the proportion of body tissues relative to another. Consequently, high precision device are required which are very expensive and difficult to use by ordinary citizens. Also, studies on

the optimal frequency for devices that use electric signal are inadequate, and with the standardization by IEEE of signal transmission through human body, the the integration of body composition assessment technologies into wearable electronic devices needs to be investigated further.

7.3 Future work

This study presents, in all probability, the first use of galvanic IBC signal propagation to investigate human body hydration. Therefore further theoretical and experimental models need to be developed to improve the representation of biological parameters, and electrode-skin impedances in a future model. With the circuit model presented in this work, future studies should seek to address the impacts of body movement on the signal if integrated to a wearable device. It has been shown that various postures and body movements encountered during the complex human body activities of daily living such as walking, talking, and so on, affects galvanic coupled signals. Therefore further research should try to make the circuit robust to body movements. Also the limitations of human body to electrical signal propagation need to be investigated further in order to draw a suitable baseline when coupling across joints, bones and hard skin surfaces. Therefore, further research should include larger number of people and also include an investigation into the effects of drugs and

supplements on future models. That said, the goal in a future research would include the development of a portable electronic device to track hydration in real time using the attenuation of a propagating signal and to integrate into a wearable electronic device. The technology will assist medical diagnosis and improve the cost effectiveness of health care through personal monitoring.

Appendix A

AppendixA

A.1 Transfer Function Equation

Considering the current flow diagram, using KVL:

$$V_i = 2I_1 Z_{ES} + I_2 \acute{Z}_T \tag{A.1}$$

$$I_4 \acute{Z}_L = I_2 \acute{Z}_T + I_5 \acute{Z}_b \tag{A.2}$$

$$I_2 \acute{Z}_T + I_6 \acute{Z}_L = I_4 \acute{Z}_L + I_7 \acute{Z}_T \tag{A.3}$$

$$I_6 \acute{Z}_L = I_5 \acute{Z}_b + I_7 \acute{Z}_T \tag{A.4}$$

$$I_4 \acute{Z}_L + I_7 \acute{Z}_T = I_3 \acute{Z}_b \tag{A.5}$$

$$I_7 \acute{Z}_T = I_8 (2Z_{ES} + \acute{Z}_L) \tag{A.6}$$

From KCL:

$$I_1 = I_2 + I_3 + I_4 \tag{A.7}$$

$$I_2 = I_1 + I_5 + I_6 \tag{A.8}$$

$$I_4 = -I_5 + I_7 + I_8 \tag{A.9}$$

$$-I_3 = I_7 + I_6 + I_8 \tag{A.10}$$

$$V_i = 2I_1 Z_{ES} + \acute{Z}_T I_2 + 0 + 0 + 0 + 0 + 0 + 0 \tag{A.11}$$

$$0 = 0 + I_2 \acute{Z}_T + 0 - \acute{Z}_L I_4 + I_5 \acute{Z}_b + 0 + 0 + 0 \tag{A.12}$$

$$0 = 0 + 0 + 0 + 0 + I_5 \acute{Z}_b - \acute{Z}_L I_6 + I_7 \acute{Z}_T + 0 \tag{A.13}$$

$$0 = 0 + 0 - I_3 \acute{Z}_b + I_4 \acute{Z}_L + 0 + 0 + I_7 \acute{Z}_T + 0 \tag{A.14}$$

$$0 = -I_1 + I_2 + I_3 + I_4 + 0 + 0 + 0 + 0 \tag{A.15}$$

$$0 = I_1 - I_2 + 0 + 0 + I_5 + I_6 + 0 + 0 \tag{A.16}$$

$$0 = 0 + 0 + 0 - I_4 - I_5 + 0 + I_7 + I_8 \tag{A.17}$$

$$0 = 0 + 0 + 0 + 0 + 0 + 0 + -I_7 \acute{Z}_T + (2Z_{ES} + \acute{Z}_L)I_8 \tag{A.18}$$

The corresponding matrix from the above equations is

$$
\begin{bmatrix} V_i \\ 0 \\ 0 \\ 0 \\ 0 \\ 0 \\ 0 \\ 0 \end{bmatrix}
=
\begin{bmatrix}
2Z_{ES} & \acute{Z}_T & 0 & 0 & 0 & 0 & 0 & 0 \\
0 & \acute{Z}_T & 0 & -\acute{Z}_L & \acute{Z}_b & 0 & 0 & 0 \\
0 & 0 & 0 & 0 & \acute{Z}_b & -\acute{Z}_L & -\acute{Z}_T & 0 \\
0 & 0 & -\acute{Z}_b & \acute{Z}_L & 0 & 0 & \acute{Z}_T & 0 \\
-1 & 1 & 1 & 1 & 0 & 0 & 0 & 0 \\
1 & -1 & 0 & 0 & 1 & 1 & 0 & 0 \\
0 & 0 & 0 & -1 & -1 & 0 & 1 & 1 \\
0 & 0 & 0 & 0 & 0 & 0 & -\acute{Z}_T & 2Z_{ES} + \acute{Z}_L
\end{bmatrix}
\begin{bmatrix} I_1 \\ I_2 \\ I_3 \\ I_4 \\ I_5 \\ I_6 \\ I_7 \\ I_8 \end{bmatrix}
$$
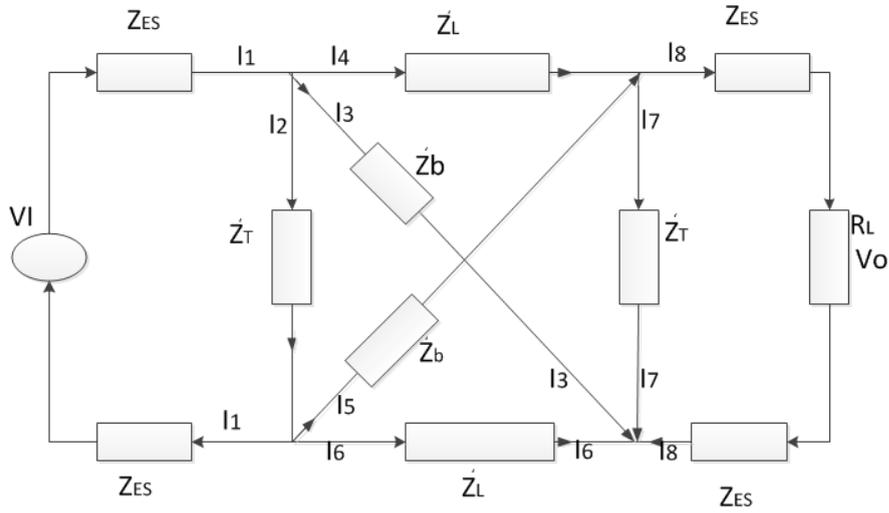
FIGURE A.1: The equivalent circuit showing directions of the current flow

Solving for I from the above equations

$$I = \begin{bmatrix} \dfrac{V_i(2\acute{Z}_b\acute{Z}_T\sigma_0)+2\acute{Z}_b\acute{Z}_L\acute{Z}_T\sigma_1}{4\acute{Z}_b\acute{Z}_T^3\sigma_4\sigma_3\sigma_2} \\[4mm] \dfrac{V_i(2\acute{Z}_b\acute{Z}_T\sigma_0)+2\acute{Z}_b\acute{Z}_L\acute{Z}_T\sigma_1}{4\acute{Z}_b\acute{Z}_T^3\sigma_4\sigma_3\sigma_2} \\[4mm] \dfrac{-V_i\sigma_1}{2\acute{Z}_T\sigma_4\sigma_3\sigma_2} \\[4mm] \dfrac{V_i\sigma_1}{2\acute{Z}_T\sigma_4\sigma_3\sigma_2} \\[2mm] \dfrac{-V_i\sigma_0}{2\acute{Z}_b\acute{Z}_T\sigma_4\sigma_3\sigma_2} \\[4mm] \dfrac{2V_i\acute{Z}_T^2(\sigma_4\sigma_2+\sigma_5(\sigma_6+\sigma_7+4\acute{Z}_bZ_{ES}\acute{Z}_L+2\acute{Z}_b\acute{Z}_L\acute{Z}_T)}{2\acute{Z}_T\sigma_4\sigma_3\sigma_2} \\[4mm] \dfrac{V_i(\acute{Z}_T\sigma_4\sigma_2+\sigma_5(\sigma_6+\sigma_7+4\acute{Z}_bZ_{ES}\acute{Z}_L+2\acute{Z}_b\acute{Z}_L\acute{Z}_T))}{\sigma_4\sigma_3\sigma_2} \\[4mm] \dfrac{V_i\sigma_5}{\sigma_2} \end{bmatrix}$$

$\sigma_0 =$

$2\acute{Z}_T^2(\sigma_4\sigma_2 + \sigma_5(\sigma_6 + \sigma_7 + 4\acute{Z}_bZ_{ES}\acute{Z}_L + 2\acute{Z}_b\acute{Z}_L\acute{Z}_T))\sigma_4$

$-4\acute{Z}_L\acute{Z}_T^3(\sigma_4\sigma_2 + \sigma_5(\sigma_6 + \sigma_7 + 4\acute{Z}_bZ_{ES}\acute{Z}_L + 2\acute{Z}_b\acute{Z}_L\acute{Z}_T));$

$$\sigma_1 =$$

$$(2\acute{Z}_T(\sigma_4\sigma_2 + \sigma_5(\sigma_6 + \sigma_7 + 4\acute{Z}_b Z_{ES}\acute{Z}_L + 2\acute{Z}_b\acute{Z}_L Z_T)) - 2\acute{Z}_T\sigma_5\sigma_3)\sigma_4$$
$$+ 4\acute{Z}_T^3(\sigma_4\sigma_2 + \sigma_5(\sigma_6 + \sigma_7 + 4\acute{Z}_b Z_{ES}\acute{Z}_L + 2\acute{Z}_b\acute{Z}_L\acute{Z}_T));$$

$$\sigma_2 =$$

$$8Z_{ES}^2(\acute{Z}_L^2 + \acute{Z}_L\acute{Z}_T + \acute{Z}_b\acute{Z}_L + \acute{Z}_b\acute{Z}_T) + 4Z_{ES}\acute{Z}_L^2(\acute{Z}_L + \acute{Z}_T + \acute{Z}_b) + 4Z_{ES}\acute{Z}_T(\acute{Z}_L\acute{Z}_T + \acute{Z}_b\acute{Z}_L +$$
$$\acute{Z}_b\acute{Z}_T) + 2\acute{Z}_l^2\acute{Z}_T(\acute{Z}_L + \acute{Z}_b);$$

$$\sigma_3 =$$

$$\sigma_6 + \acute{Z}^2 + 2\acute{Z}_L\acute{Z}_T^2 + \sigma_7 + 4\acute{Z}_b Z_{ES}\acute{Z}_L + 4\acute{Z}_b Z_{ES}\acute{Z}_T + 2\acute{Z}_b\acute{Z}_L Z_T + 4Z_{ES}\acute{Z}_L\acute{Z}_T;$$

$$\sigma_4 = 2\acute{Z}_b\acute{Z}_T + 2\acute{Z}_L\acute{Z}_T;$$

$$\sigma_6 = 4Z_{ES}\acute{Z}_L^2;$$

$$\sigma_7 = 2\acute{Z}_L^2\acute{Z}_T;$$

A.2   Approved Ethics Certificate

Elizabeth Hill

From:	Christine Near on behalf of Quest Ethics
Sent:	Wednesday, 2 September 2015 10:20 AM
To:	Research Ethics
Subject:	FW: Quest Ethics Notification - Application Process Finalised - Application Approved

```
-----Original Message-----
From: Quest NoReply
Sent: Wednesday, 2 September 2015 10:08 AM
To: Daniel Lai
Cc: Clement Asogwa; Patrick Mclaughlin; Stephen Collins
Subject: Quest Ethics Notification - Application Process Finalised - Application Approved
```

Dear DR TZE HUEI LAI,

Your ethics application has been formally reviewed and finalised.

» Application ID: HRE14-122
» Chief Investigator: DR TZE HUEI LAI
» Other Investigators: MR Clement Ogugua Asogwa, ASPR STEPHEN COLLINS, DR PATRICK MCLAUGHLIN
» Application Title: Intrabody signal propagation studies for human body composition » Form Version: 13-07

The application has been accepted and deemed to meet the requirements of the National Health and Medical Research Council (NHMRC) 'National Statement on Ethical Conduct in Human Research (2007)' by the Victoria University Human Research Ethics Committee. Approval has been granted for two (2) years from the approval date; 02/09/2015.

Continued approval of this research project by the Victoria University Human Research Ethics Committee (VUHREC) is conditional upon the provision of a report within 12 months of the above approval date or upon the completion of the project (if earlier). A report proforma may be downloaded from the Office for Research website at: http://research.vu.edu.au/hrec.php.

Please note that the Human Research Ethics Committee must be informed of the following: any changes to the approved research protocol, project timelines, any serious events or adverse and/or unforeseen events that may affect continued ethical acceptability of the project. In these unlikely events, researchers must immediately cease all data collection until the Committee has approved the changes. Researchers are also reminded of the need to notify the approving HREC of changes to personnel in research projects via a request for a minor amendment. It should also be noted that it is the Chief Investigators' responsibility to ensure the research project is conducted in line with the recommendations outlined in the National Health and Medical Research Council (NHMRC) 'National Statement on Ethical Conduct in Human Research (2007).'

On behalf of the Committee, I wish you all the best for the conduct of the project.

Secretary, Human Research Ethics Committee
Phone: 9919 4781 or 9919 4461
Email: researchethics@vu.edu.au

This is an automated email from an unattended email address. Do not reply to this address.

1

References

[1] Deloitte Touche Tohmatsu. *Global health care Outlook*, 2015. URL https://www2.deloitte.com/content/dam/Deloitte/global/Documents/Life-Sciences-Health-Care/gx-lshc-2015-health-care-outlook-global.pdf.

[2] Australian Institute of Health and Welfare. *Health expenditure Australia 2013–14. Australia's health series no. 54. Cat. no. AUS 63. Canberra: AIHW*, 2015. URL http://www.aihw.gov.au/.

[3] W. Katie. *The Future of Remote Patient Monitoring*, 2013. URL http://www.healthitoutcomes.com/doc/the-future-of-remote-patient-monitoring-0001/.

[4] C. Anthony. *Digital Health: Remote Monitoring, Smart Accessories and EHR Cost-Savings 2014-2019*, 2014. URL http://www.juniperresearch.com/researchstore/key-vertical-markets/digital-health/monitoring-smart-accessories-ehr/.

[5] W. H. Wu, A. A. T. Bui, M. A. Batalin, D. Liu, and W. J. Kaiser. Incremental diagnosis method for intelligent wearable sensor systems. *IEEE Trans. Inf. Technol. Biomed*, 11(5):553–562, 2007.

[6] J. Verghese, R. B. Lipton, C. B. Hall, G. Kuslansky, M. J. Katz, and H. Buschke. Abnormality of gait as a predictor of non-alzheimer's dementia. *N. Engl. J. Med.*, 347(22):1761–1768, 2002.

[7] G. B. Frisoni, N. C. Fox, C. R. Jack, P. Scheltens, and P. M. Thompson. The clinical use of structural mri in alzheimer disease. *Nat Rev Neurol*, 6(2):67–77, 2010.

[8] S. N Thornton. Thirst and hydration: physiology and consequences of dysfunction. *Physiol Behav*, 100(1):15–21, 2010.

[9] C.V Agostoni, J.L Bresson, and S Fairweather-Tait. Scientific opinion on dietary reference values for water. *EFSA J*, 8(3), 2010.

[10] B. David, M. Vicki, and H. Rob. Body composition measurement: a review of hydrodensitometry, anthropometry, and impedance methods. *Nutrition*, 14(3): 296–310, 1998.

[11] S. Heymsfield. *Human body composition*, volume 918. Human kinetics, 2005.

[12] W.J. Remme and K. Swedberg. Guidelines for the diagnosis and treatment of chronic heart failure. *European heart journal*, 22(17):1527–1560, 2001.

[13] K. Dickstein, A. Cohen-Solal, G. Filippatos, J. JV. McMurray, P. Ponikowski, P. A. Poole-Wilson, A. Stromberg, D. J. Veldhuisen, D. Atar, and A. W. Hoes. Esc guidelines for the diagnosis and treatment of acute and chronic heart failure 2008. *Eur J Heart Fail*, 10(10):933–989, 2008.

[14] C. Bingham, D. A. Hilton, and A. J. Nicholls. Diabetic muscle infarction: an unusual cause of leg swelling in a diabetic on continuous ambulatory peritoneal dialysis. *Nephrol. Dial. Transplant*, 13(9):2377–2379, 1998.

[15] M. Sagar, W. M. Bowerfind, and F. M. Wigley. A man with diabetes and a swollen leg. *The Lancet*, 353(9147):116, 1999.

[16] Lymphoedema Frame work. *Best Practice for the Management of Lymphoedema, International Consensus, London: MEP ltd, 2006*. URL http://www.woundsinternational.com/media/issues/210/files/content_175.pdf.

[17] M.l English, C. Waruiru, R. Mwakesi, and K. Marsh. Signs of dehydration in severe childhood malaria. *Trop Doct*, 27(4):235–236, 1997.

[18] M.C. English, C. Waruiru, C. Lightowler, S.A. Murphy, G. Kirigha, and K. Marsh. Hyponatraemia and dehydration in severe malaria. *Arch Dis Child*, 74(3):201–205, 1996.

[19] A. Boscoe, C. Paramore, and J. G. Verbalis. Cost of illness of hyponatremia in the united states. *Cost Eff Resour Alloc*, 4(1):1, 2006.

[20] J.R. Speakman, D. Booles, and R. Butterwick. Validation of dual energy x-ray absorptiometry (dxa) by comparison with chemical analysis of dogs and cats. *Int J Obes Relat Metab Disord*, 25(3), 2001.

[21] S. Y. Lee and D. Gallagher. Assessment methods in human body composition. *Current opinion in clinical nutrition and metabolic care*, 11(5):566, 2008.

[22] *Wireless Body Area Network.* URL http://www.allsyllabus.com/aj/seminar/Information_Science/Wireless%20Body%20Area%20Network.php#.V7-ZbVt9671.

[23] N. Pace and E. N. Rathbun. Studies on body composition. 3. the body water and chemically combined nitrogen content in relation to fat content. *J Biol Chem*, 158: 685–691, 1945.

[24] ZiMian Wang, P Deurenberg, W Wang, A Pietrobelli, R N Baumgartner, and S B Heymsfield. Hydration of fat-free body mass: review and critique of a classic body-composition constant. *Am. J. Clin. Nutr*, 69(5):833–841, 1999.

[25] F .D. Moore, K. H. Olesen, JD. McMurrey, HV. Parker, M. R. Ball, and C. M. Boyden. The body cell mass and its supporting environment: body composition in health and disease. 1963.

[26] H. C. Lukaski. Methods for the assessment of human body composition: traditional and new. *Am J Clin Nutr*, 46(4):537–556, 1987.

[27] L.E. Armstrong. Assessing hydration status: the elusive gold standard. *J. Am. Coll. Nutr.*, 26(5):575s–584s, 2007.

[28] S. Y. Lee and D. Gallagher. Assessment methods in human body composition. *Curr Opin Clin Nutr Metab Care*, 11(5):566, 2008.

[29] P.O. Astrand and K. Rodahl. *Textbook of work Physiology,Physiological Bases of Exercise.* 3rd ed. New York: McGraw-Hill Book Company, 1986.

[30] IEEE Standards Association. IEEE standard for local and metropolitan area networks part 15.6: Wireless body area networks. *IEEE std. 802.16.6*, Feb. 2012.

[31] C. O Asogwa, X Zhang, D Xiao, and A Hamed. Experimental analysis of aodv, dsr and dsdv protocols based on wireless body area network. In *Internet of Things*, pages 183–191. Springer, 2012.

[32] E. Jequier and F. Constant. Water as an essential nutrient: the physiological basis of hydration. *Eur J Clin Nut*, 64(2):115–123, 2010.

[33] O. G. Martinsen and S. Grimnes. London: Academic press.

[34] F. Peronnet, D. Mignault, P. Du Souich, S. Vergne, L. Le Bellego, L. Jimenez, and R. Rabasa-Lhoret. Pharmacokinetic analysis of absorption, distribution and disappearance of ingested water labeled with d2o in humans. *Eur J Appl Physiol*, 112(6):2213–2222, 2012.

[35] L. Rothlingshofer, M. Ulbrich, S. Hahne, and S. Leonhardt. Monitoring change of body fluid during physical exercise using bioimpedance spectroscopy and finite element simulations. *Journal of Electrical Bioimpedance*, 2(1):79–85, 2011.

[36] L Max, H David, Hardinsyah, D Jean-Francois, B Simon, and E. A. Lawrence. *Hydration for health*, 2016. URL http://www.h4hinitiative.com/.

[37] M.D. Mifflin, S.T. St Jeor, L.A. Hill, B.J. Scott, S.A. Daugherty, and Y. Koh. A new predictive equation for resting energy expenditure in healthy individuals. *Am. J. Clin. Nutr*, 51(2):241–247, 1990.

[38] M. Chaplin. Do we underestimate the importance of water in cell biology? *Nat. Rev. Mol. Cell Biol.*, 7(11):861–866, 2006.

[39] R. A. Oppliger and C. Bartok. Hydration testing of athletes. *Sports Med*, 32(15): 959–971, 2002.

[40] S.M. Shirreffs. Markers of hydration status. *Eur J Clin Nutr*, 57:S6–S9, 2003.

[41] L. E. Armstrong. Hydration assessment techniques. *Nutr. Rev*, 63(suppl 1):S40–S54, 2005.

[42] P.E. Watson, I.D. Watson, and R.D. Batt. Total body water volumes for adult males and females estimated from simple anthropometric measurements, 1980.

[43] A.R. Behnke, B.G. Feen, and W.C. Welham. The specific gravity of healthy men: body weight and volume as an index of obesity. *J Am Med Associ*, 118(7):495–498, 1942.

[44] P. Deurenberg, J.A. Weststrate, and K. Van Der Kooy. Is an adaptation of siri's formula for the calculation of body fat percentage from body density in the elderly necessary? *Eur J Clin Nutr*, 43(8):559–567, 1989.

[45] Z. Wang, R.N. Pierson, and S. B. Heymsfield. The five-level model: a new approach to organizing body-composition research. *Am J Clin Nutr*, 56(1):19–28, 1992.

[46] K. J. Ellis. Human body composition: in vivo methods. *Physiol. Rev*, 80(2): 649–680, 2000.

[47] J. M. Sands and H. E. Layton. The physiology of urinary concentration: An update. *Semi. Nephrol*, 29(3):178–195, 2009.

[48] L.E. Armstrong, J.A.H. Soto, and F.T. Hacker. Urinary indices during dehydration, exercise, and rehydration. *Occup Health Med*, 2(40):97, 1998.

[49] L. Graff. *A handbook of routine urinalysis*. Lippincott Williams & Wilkins, 1983.

[50] A.H Free and H. M Free. *Urinalysis in clinical laboratory practice*. Crc Press, 1975.

[51] L. E. Armstrong, C. M. Maresh, J. W. Castellani, M.F. Bergeron, R.W. Kenefick, K.E. LaGasse, and D. Riebe. Urinary indices of hydration status. *Int J Sport Nutr*, 4(3):265–279, 1994.

[52] R.P Francesconi, R.W Hubbard, P.C. Szlyk, D. Schnakenberg, D Carlson, N. Leva, I. Sils, L. Hubbard, V. Pease, and J. Young. Urinary and hematologic indexes of hypohydration. *J Appl Physiol*, 62(3):1271–1276, 1987.

[53] W.L.J.M. Deville, J.C. Yzermans, N. P. Van Duijn, P. D. Bezemer, D. A.W.M. Van Der Windt, and L. M. Bouter. The urine dipstick test useful to rule out infections. a meta-analysis of the accuracy. *BMC urology*, 4(1):1, 2004.

[54] C. Lentner, C. Lentner, and A. Wink. Units of measurement, body fluids, composition of the body, nutrition. geigy scientific tables. ciba-geigy ltd, basle, switzerland. 1981.

[55] D.S. Moran, Y. Heled, M. Margaliot, Y. Shani, A. Laor, S. Margaliot, E. E. Bickels, and Y. Shapiro. Hydration status measurement by radio frequency absorptiometry in young athletes—a new method and preliminary results, us and international patents pending. *Physiol Meas*, 25(1):51, 2003.

[56] H.P. Schwan. Electrical properties of tissue and cell suspensions. *Adv. Biol. Med. Phys*, 5:147–209, 1957.

[57] M-C. Asselin, S. Kriemler, D.R. Chettle, C.E. Webber, O. Bar-Or, and F.E. McNeill. Hydration status assessed by multi-frequency bioimpedance analysis. *Appl Radiat Isotopes*, 49(5):495–497, 1998.

[58] T. Hanai. Electrical properties of emulsions. *Emulsion science*, pages 354–477, 1968.

[59] J. Nyboer. Workable volume and flow concepts of bio-segments by electrical impedance plethysmography. *T.-I.-T. journal of life sciences*, 2(1):1–13, 1972.

[60] J. Nyboer, M. M. Kreider, and L. Hannapel. Electrical impedance plethysmography a physical and physiologic approach to peripheral vascular study. *Circulation*, 2(6):811–821, 1950.

[61] M. D. Van Loan, P. Withers, J. Matthie, and P. L. Mayclin. Use of bioimpedance spectroscopy to determine extracellular fluid, intracellular fluid, total body water, and fat-free mass. In *Human body composition*, pages 67–70. Springer, 1993.

[62] P. Wabel, P. Chamney, U. Moissl, and T. Jirka. Importance of whole-body bioimpedance spectroscopy for the management of fluid balance. *Blood Purif*, 27(1):75–80, 2009.

[63] K. Norman, N. Stobaus, M. Pirlich, and A. Bosy-Westphal. Bioelectrical phase angle and impedance vector analysis–clinical relevance and applicability of impedance parameters. *Clinical nutrition*, 31(6):854–861, 2012.

[64] A. Zouridakis, Y. V. Simos, I. I Verginadis, K. Charalabopoulos, V. Ragos, E. Dounousi, G. Boudouris, S. Karkabounas, A. Evangelou, and D. Peschos. Correlation of bioelectrical impedance analysis phase angle with changes in oxidative stress on end-stage renal disease patients, before, during, and after dialysis. *Ren Fail*, pages 1–6, 2016.

[65] M. Y. Jaffrin and H. Morel. Body fluid volumes measurements by impedance: A review of bioimpedance spectroscopy (bis) and bioimpedance analysis (bia) methods. *Med Eng Phys*, 30(10):1257–1269, 2008.

[66] A. De Lorenzo, P. Deurenberg, A. Andreoli, G.F. Sasso, M. Palestini, and R. Docimo. Multifrequency impedance in the assessment of body water losses during dialysis. *Kidney Blood Press Res*, 17(6):326–332, 1994.

[67] K.J. Ellis, S.J. Bell, G. M. Chertow, W. C. Chumlea, T. A. Knox, D. P. Kotler, H.C. Lukaski, and D.A Schoeller. Bioelectrical impedance methods in clinical research: a follow-up to the nih technology assessment conference. *Nutrition*, 15 (11):874–880, 1999.

[68] R. F. Kushner, R. Gudivaka, and D.A. Schoeller. Clinical characteristics influencing bioelectrical impedance analysis measurements. *Am J Clini Nutri*, 64(3): 423S–427S, 1996.

[69] Y. Song, Q. Hao, K. Zhang, Wang. M., Chu.Y., and Kang. B. The simulation method of the galvanic coupling intrabody communication with different signal transmission paths. *IEEE Trans. Instrum. Meas.*, 60(4):1257–1266, April 2011.

[70] B. Kibret, M. Seyedi, T.H.L. Daniel, and M. Faulkner. Investigation of galvanic coupled intrabody communication using human body circuit modell. *IEEE J. Health Inform.*, 18(4):1196–1206, 2014.

[71] R. Xu, H. Zhu, and J. Yuan. Electric-field intra-body communication channel modeling with finite-element method. *IEEE Trans.Biomed. Eng.*, 58(3):705–712, Mar. 2011.

[72] M. S. Wegmueller, A. Kuhn, J. Froehlich, M. Oberle, N. Felber, N. Kuster, and W. Fichtner. An attempt to model the human body as a communication channel. *IEEE Trans. Biomed. Eng.*, 54(10):1851–1857, Oct. 2007.

[73] K. Fujii, M. Takahashi, and K. Ito. Electric field distributions of wearable devices using the human body as a transmission channel. *IEEE Trans. Antennas Propag.*, 55(7):2080–2087, Jul. 2007.

[74] S.H. Pun, M.Y. Gao, Mak. P., M.I. Vai, and M. Du. Quasistatic modeling of human limb for intra-body communications with experiments. *IEEE Trans. Inf. Tehcnol. Biomed.*, 15(6):870–876, Nov. 2011.

[75] T. G. Zimmerman. Personal area networks: near-field intrabody communication. *IBM Syst.*, 35(3-4):609–617, Apr. 1996.

[76] S. Gabriel, R. Lau, and C. Gbirel. The dielectric properties of biological tissues: III. parametric models for the dielectric spectrum of tissues. *Phys. Med. Biol.*, 41 (11):2271–2293, 1996.

[77] D. Miklavcic, N. Pavselj, and F. Hart. Electric properties of tissues. In *Wiley Encyclopedia of Biomedical Engineering.* New York: Wiley Press, 2006.

[78] K. S. Cole and R. H. Cole. Dispersion and absorption in dielectrics part i: Alternating current characteristics. *J. Chem. Phys.*, 9(4):341–351, 1941.

[79] D. Andreuccetti and C. Fossi, R .and Petrucci. *Calculation of the Dielectric Properties of Body Tissues in the frequency range 10 Hz - 100 GHz.* [Online] Available: Url= http://niremf.ifac.cnr.it/tissprop/, 2013.

[80] World Health Organization. Guideline for drinking water quality. geneva. *World Health Organization*, 2011.

[81] U. G Kyle, I. Bosaeus, A. D De Lorenzo, P.l Deurenberg, M. Elia, J Gomez, B Heitmann, L Kent-Smith, J Melchior, and M Pirlich. Bioelectrical impedance analysis—part ii: utilization in clinical practice. *Clinical nutrition*, 23(6):1430–1453, 2004.

[82] Universities Australia NHMRC and, ARC and. *Australian code for the responsible conduct of research*, 2015. URL https://www.nhmrc.gov.au/guidelines-publications/e72.

[83] International Commission on Non-Ionizing Radiation Protection (ICNIRP). Guidelines for limiting exposure to time-varying electric, magnetic, and electromagnetic fields (up tp 300 ghz). *Health Physics.*, 74(4):494–522, Oct. 1998.

[84] S. Striefel. Ethical and legal electromyography. *Biofeedback*, 35(1):3–7, 2007.

[85] ANSI/AAMI/ISO 10993-1:2009/(R)2013 American National Standard Institute. *Biological evaluation of medical devices — Part 1: Evaluation and testing within a risk management process.* URL http://my.aami.org/aamiresources/previewfiles/1099301_1312_preview.pdf.

[86] A. Goldhamer, D. Lisle, B Parpia, S.V. Anderson, and T.C. Campbell. Medically supervised water-only fasting in the treatment of hypertension. *J. Manipulative Physiol. Ther.*, 24(5):335–339, 2001.

[87] NHMRC. *Guidelines approved under Section 95A of the Privacy Act 1988*, 2014. URL https://www.nhmrc.gov.au/guidelines-publications/pr2.

[88] S. C. Hayes. *Review of Research Evidence on Secondary Lymphoedema–Incidence, Prevention, Risk Factors and Treatment.* National Breast and Ovarian Cancer Centre Surry Hills, NSW.

[89] T. DiSipio, S. Rye, B. Newman, and S. Hayes. Incidence of unilateral arm lymphoedema after breast cancer: a systematic review and meta-analysis. *Lancet Oncol*, 14(6):500–515, 2013.

[90] C. WH. De Fijter, M. M. De Fijter, L. P. Oe, Ab. J.M. Donker, and P.M. De Vries. The impact of hydration status on the assessment of lean body mass by body electrical impedance in dialysis patients. *Adv Perit Dial*, 9:101–101, 1993.

[91] D. Pan, J. Han, P.l. Wilburn, and S. G. Rockson. Validation of a new technique for the quantitation of edema in the experimental setting. *Lymphat Res Biol*, 4 (3):153–158, 2006.

[92] National Instruments. *Introduction to Network Analyzer Measurements: Fundamentals and Background.* URL www.ni.com/rf-academy.

[93] J. Doug and M. Christopher. *A Tutorial on Baluns, Balun Transformers, Magic-Ts, and 180 degrees Hybrids.* URL https://www.markimicrowave.com/Assets/appnotes/balun_basics_primer.pdf.

[94] M. Seyedi, B. Kibret, D. TH. Lai, and M. Faulkner. A survey on intrabody communications for body area network applications. *IEEE Trans Biomed Eng*, 60 (8):2067–2079, 2013.

[95] National Fire Protection Asociation. *List of NFPA codes and standards.*

[96] World Health Organization. *Electromagnetic Fields (300 Hz to 300 GHz)*, 1993. URL http://www.inchem.org/documents/ehc/ehc/ehc184.htm.

[97] C Tonozzi, E Rudloff, and R Kirby. Perfusion versus hydration: impact on the fluid therapy plan. *Perfusion*, 31(12), 2009.

[98] Da Pan, Jennifer Han, Paul Wilburn, and Stanley G Rockson. Validation of a new technique for the quantitation of edema in the experimental setting. *Lymphat. Res. Biol*, 4(3):153–158, 2006.

[99] C. O'brien, A.J. Young, and M.N. Sawka. Bioelectrical impedance to estimate changes in hydration status. *Int. J. Sports Med*, 23(5):361–366, 2002.

[100] L. E. Armstrong, A. C. Pumerantz, K. A. Fiala, M. W. Roti, S. A. Kavouras, D. J. Casa, and C. M. Maresh. Human hydration indices: acute and longitudinal reference values. *Int J Sport Nutri*, 20(2):145, 2010.

[101] N. Vojavckova, J. Fialova, and J. Hercogova. Management of lymphedema. *Dermatol ther*, 25(4):352–357, 2012.

[102] M. S. Wegmueller. *Intra-body communication for biomedical sensor networks.* PhD thesis, Diss., Eidgenossische Technische Hochschule ETH Zurich, Nr. 17323, 2007, 2007.

[103] H. Skelton. The storage of water by various tissues of the body. *Arch. Intern. Med*, 40(2):140–152, 1927.

[104] A. Must and S.E. Anderson. Pediatric mini review. body mass index in children and adolescents: considerations for population-based applications. *Int J Obes*, 30: 590–594, 2006.

[105] P. Webb. Energy expenditure and fat-free mass in men and women. *Am. J. Clin. Nutr*, 34(9):1816–1826, 1981.

[106] P. Ritz, G. Berrut, I. Tack, M.J. Arnaud, and J. Tichet. Influence of gender and body composition on hydration and body water spaces. *Clin Nutri*, 27(5):740–746, 2008.

[107] L. F. Fried and P. M. Palevsky. Hyponatremia and hypernatremia. *Med. Clin. North Am*, 81(3):585–609, 1997.

[108] J. Gandy. Water intake: validity of population assessment and recommendations. *Eur. J. Nutri*, 54(2):11–16, 2015.

[109] F. Ibrahim, T. H.G. Thio, T. Faisal, and M. Neuman. The application of biomedical engineering techniques to the diagnosis and management of tropical diseases: a review. *Sensors*, 15(3):6947–6995, 2015.

[110] A. M. El-Sharkawy, P. Watson, K. R. Neal, O. Ljungqvist, R. J. Maughan, O. Sahota, and D. N. Lobo. Hydration and outcome in older patients admitted to hospital (the hoop prospective cohort study). *Age and ageing*, 44(6):943–947, 2015.

[111] J. C. Mentes, B. Wakefield, and K. Culp. Use of a urine color chart to monitor hydration status in nursing home residents. *Biol. Res. Nurs*, 7(3):197–203, 2006.

[112] R.P. Francesconi, R.W. Hubbard, P.C. Szlyk, D. Schnakenberg, D. Carlson, N. Leva, I. Sils, L. Hubbard, V. Pease, and J. Young. Urinary and hematologic indexes of hypohydration. *J.Appl. Physiol*, 62(3):1271–1276, 1987.

[113] M.B. Fortes, J. A Owen, P. Raymond-Barker, C. Bishop, S. Elghenzai, S. J Oliver, and N. P. Walsh. Is this elderly patient dehydrated? diagnostic accuracy of hydration assessment using physical signs, urine, and saliva markers. *J. Am. Med. Dir. Assoc*, 16(3):221–228, 2015.

[114] W. Gao, S. Emaminejad, H. Y. Y. Nyein, S. Challa, K. Chen, A. Peck, H. M. Fahad, H. Ota, H. Shiraki, and D. Kiriya. Fully integrated wearable sensor arrays for multiplexed in situ perspiration analysis. *Nature*, 529(7587):509–514, 2016.

[115] C.O Asogwa, A. Teshome, S. Collins, and D.TH. Lai. A circuit model of real time human body hydration. *IEEE Trans. Biomed.Eng*, 63, 2015.

[116] S. A. Kavouras. Assessing hydration status. *Curr. Opin. Clin. Nutr. Metab. Care*, 5(5):519–524, 2002.

[117] L. Bankir, N. Bouby, and M. Trinh-Trang-Tan. 2 the role of the kidney in the maintenance of water balance. *Bailliere Clin. Endoc*, 3(2):249–311, 1989.

[118] H.C. Lukaski. Applications of bioelectrical impedance analysis: a critical review. In *In Vivo Body Composition Studies*, pages 365–374. Springer, 1990.

[119] M. D. Van Loan, P. Withers, J. Matthie, and P. L Mayclin. Use of bioimpedance spectroscopy to determine extracellular fluid, intracellular fluid, total body water, and fat-free mass. In *Human body composition*, pages 67–70. Springer, 1993.

[120] S. C Hayes. *Review of Research Evidence on Secondary Lymphoedema–Incidence, Prevention, Risk Factors and Treatment.* National Breast and Ovarian Cancer Centre Surry Hills, NSW, 2008.

[121] S.G Rockson. Lymphedema. *Am. J. Med*, 110(4):288–295, 2001.

[122] J. MacLaren. Skin changes in lymphoedema: pathophysiology and management options. *Int J Palliat Nurs*, 7(8):381–388, 2001.

[123] E. Foldi, M. Junger, and H. Partsch. The science of lymphoedema bandaging. *EWMA Focus Document: Lymphoedema bandaging in practice*, 2005.

[124] N. Vojavckova, J. Fialova, and J. Hercogova. Management of lymphedema. *Dermatologic therapy*, 25(4):352–357, 2012.

[125] A. L. Cheville, C. L. McGarvey, J. A. Petrek, S. A. Russo, M. E. Taylor, and S. R.J. Thiadens. Lymphedema management. volume 13, pages 290–301. Elsevier, 2003.

[126] S. M. Ramos, L. S. O'Donnell, and G. Knight. Edema volume, not timing, is the key to success in lymphedema treatment. *Am J Surg*, 178(4):311–315, 1999.

[127] NLN Medical Advisory Committee. Position statement of the national lymphedema network. *National Lymphedema Network*, 2011.

[128] C.J. Moffatt, P.J. Franks, D.C. Doherty, A.F. Williams, C Badger, E. Jeffs, N. Bosanquet, and P. S Mortimer. Lymphoedema: an underestimated health problem. *Qjm*, 96(10):731–738, 2003.

[129] K. Kerchner, A. Fleischer, and G. Yosipovitch. Lower extremity lymphedema: Update: Pathophysiology, diagnosis, and treatment guidelines. *J Am Acad Dermatol*, 59(2):324–331, 2008.

[130] S.H. Ridner, L.D. Montgomery, J.T. Hepworth, B.R. Stewart, and J.M. Armer. Comparison of upper limb volume measurement techniques and arm symptoms between healthy volunteers and individuals with known lymphedema. *Lymphology*, 40(1):35–46, 2007.

[131] J. R. Matthie. Bioimpedance measurements of human body composition: critical analysis and outlook. *Expert review of medical devices*, 5(2):239–261, 2008.

[132] H. Ma and M. Iafrati. Diagnosis and management of lymphedema. *Haimovici's Vascular Surgery, 6th Edition*, pages 1221–1235, 2012.

[133] J. G. Verbalis. Disorders of body water homeostasis. *Best practice & research clinical endocrinology& metabolism*, 17(4):471–503, 2003.

[134] B. Dahlof, P. S. Sever, N. R. Poulter, H. Wedel, D. G. Beevers, M. Caulfield, R. Collins, S.E. Kjeldsen, A. Kristinsson, and G. T. McInnes. Prevention of cardio-vascular events with an antihypertensive regimen of amlodipine adding perindopril as required versus atenolol adding bendroflumethiazide as required, in the anglo-scandinavian cardiac outcomes trial-blood pressure lowering arm (ascot-bpla): a multicentre randomised controlled trial. *The Lancet*, 366(9489):895–906, 2005.

[135] R. J Kloecker. Compression garment for selective application for treatment of lymphedema and related illnesses manifested at various locations of the body, August 2002. US Patent 6,436,064.

[136] M. J Brennan and L.T. Miller. Overview of treatment options and review of the current role and use of compression garments, intermittent pumps, and exercise in the management of lymphedema. *Cancer*, 83(S12B):2821–2827, 1998.

[137] H.H. Mitchell, T.S. Hamilton, F.R. Steggerda, and H.W. Bean. The chemical composition of the adult human body and its bearing on the biochemistry of growth. *J. Biol. Chem*, 168:625–637, 1945.